

# **Isotopic Evolution of Groundwater Organic Contaminants: Experimental Investigation and Modeling Approaches**

## **Dissertation**

der Mathematisch-Naturwissenschaftlichen Fakultät  
der Eberhard Karls Universität Tübingen  
zur Erlangung des Grades eines  
Doktors der Naturwissenschaften  
(Dr. rer. nat.)

vorgelegt von  
M.Sc. Biao Jin  
aus Jilin/China

Tübingen  
2013

Tag der mündlichen Qualifikation:

18.12.2013

Dekan:

Prof. Dr. Wolfgang Rosenstiel

1. Berichterstatter:

Dr. Massimo Rolle

2. Berichterstatter:

Prof. Dr. Stefan Haderlein

3. Berichterstatter:

Prof. Dr. Christoph Schüth

*To my parents*

上善若水。水善利万物而不争，

处众人之所恶，故几于道。

—老子《道德经》

**The persons or things that have the highest excellence are just like water.**

**They benefit all things instead of contention.**

**They stay at the lowest place which all men dislike.**

**So this kind of persons and things are very close to 'Tao'.**

**—Laotse 《Tao Te King》**



# Contents

|  |           |
|--|-----------|
| <b>Contents</b> .....  | <b>5</b>  |
| <b>Abstract</b> .....  | <b>9</b>  |
| <b>Kurzfassung</b> .....   | <b>11</b> |
| <b>1. Introduction</b> .....   | <b>13</b> |
| 1.1 Background .....   | 13        |
| 1.2 Objectives.....  | 14        |
| 1.3 Structure of the thesis.....   | 15        |
| References .....   | 17        |
| <b>2. Chlorine Isotope Analysis of Organic Contaminants Using GC-qMS:<br/>Method Optimization and Comparison of Different Evaluation Schemes</b> ..... | <b>19</b> |
| Abstract .....   | 20        |
| 2.1 Introduction .....   | 21        |
| 2.2 Evaluation Schemes for Chlorine Isotope Ratios.....  | 23        |
| 2.2.1 Molecular Ion Method.....  | 24        |
| 2.2.2 Conventional and Modified Multiple Ion Methods.....  | 25        |
| 2.2.3 Complete Ion Method.....   | 26        |
| 2.3 Experimental Section.....  | 27        |
| 2.3.1 Materials and Methods .....  | 27        |
| 2.4 Results and Discussion.....  | 27        |
| 2.4.1 Comparison of Different Evaluation Schemes .....   | 28        |
| 2.4.2 Assessment of Instrumental Parameters .....  | 31        |
| 2.4.3 Effect of Standardization Procedure.....   | 34        |
| Outlook and Environmental Significance.....  | 37        |
| Supporting Information Available.....  | 38        |
| References .....   | 39        |
| <b>3. Integrated Carbon and Chlorine Isotope Modeling: Applications to<br/>Chlorinated Aliphatic Hydrocarbons Dechlorination</b> .....                 | <b>41</b> |
| Abstract .....   | 42        |
| 3.1 Introduction .....   | 43        |
| 3.2 Mathematical Description and Modeling Approach .....   | 44        |

|   |           |
|---|-----------|
| 3.2.1 Initial Relative Abundance of Carbon–Chlorine Isotopologues .....   | 44        |
| 3.2.2 Apparent Kinetic Isotope Effect during Cleavage of C-Cl Bonds .....   | 45        |
| 3.2.3 Modeling Contaminant Transformation and Carbon-Chlorine Isotopic Evolution .....  | 48        |
| 3.3 Results and Discussion .....  | 50        |
| 3.3.1 Biodegradation in Well-Mixed Systems .....  | 50        |
| 3.3.2 Biodegradation in Mass-Transfer Limited Systems .....   | 55        |
| Implications for Environmental Applications .....   | 59        |
| Supporting Information Available .....  | 59        |
| References .....  | 60        |
| <b>4. Mechanistic Approach to Multi-Element Isotope Modeling of Organic Contaminant Degradation.....</b>  | <b>63</b> |
| Abstract .....  | 63        |
| 4.1 Introduction.....   | 64        |
| 4.2 Modeling Approach .....   | 65        |
| 4.3 Results and Discussion .....  | 72        |
| 4.3.1. Toluene degradation.....   | 72        |
| 4.3.2 MTBE degradation.....   | 75        |
| 4.3.3. Nitrobenzene degradation .....   | 76        |
| 4.3.4. Comparison of mechanistic isotopologue approach and separate bulk isotope method in presence of position-specific isotopic signatures..... | 78        |
| Conclusions.....  | 80        |
| Supporting Information Available .....  | 81        |
| References.....   | 82        |
| <b>5. Diffusive Fractionation of Organic Contaminants in Aqueous Solution: Quantification of Spatial Isotope Gradients.....</b>                   | <b>87</b> |
| Abstract .....  | 88        |
| 5.1 Introduction.....   | 89        |
| 5.2 Materials and Methods.....  | 90        |
| 5.2.1 Diffusion Experiments .....   | 90        |
| 5.2.2 Chemicals.....  | 92        |
| 5.2.3 Analytical Methods .....  | 92        |
| 5.3 Results and Discussion .....  | 95        |
| 5.3.1 Diffusive isotope fractionation of isotopically-labeled petroleum hydrocarbons .....  | 95        |
| 5.3.2 Diffusive isotope fractionation of chlorinated compounds at natural abundance .....   | 99        |
| Environmental Significance .....  | 103       |

|  |            |
|--|------------|
| Supporting Information Available.....  | 105        |
| References .....   | 106        |
| <b>6. Conclusions and Outlook .....</b>  | <b>111</b> |
| 6.1 Conclusions .....  | 111        |
| 6.2 Outlook.....   | 112        |
| References .....   | 115        |
| <b>Acknowledgement .....</b>   | <b>117</b> |
| <b>Supporting Information.....</b>   | <b>119</b> |
| S1. Chlorine Isotope Analysis of Organic Contaminants Using GC-qMS: Method Optimization and Comparison of Different Evaluation Schemes ..... | 119        |
| S1. 3 Details on Chlorine Isotope Ratio Computations.....  | 119        |
| S1.2. List of Instrumental Parameters .....  | 125        |
| S1.3. Experimental dataset .....   | 126        |
| S1.4. Long-Time Monitoring of the Chlorine Isotope Ratios .....  | 127        |
| S1.5. Evaluation of <sup>13</sup> C Error.....   | 127        |
| Literature .....   | 129        |
| S2. Integrated Carbon and Chlorine Isotope Modeling: Applications to Chlorinated Aliphatic Hydrocarbons Dechlorination .....                 | 130        |
| S2.1 Initial abundances of carbon-chlorine isotopologues .....   | 130        |
| S2.2 Validation with Data from a Well-Mixed Experimental Setup.....  | 133        |
| S3.3 Governing equations and parameters used in the mass-transfer limited TCE biodegradation application .....                               | 134        |
| S3. Mechanistic Approach to Multi-Element Isotope Modeling of Organic Contaminant Degradation .....  | 138        |
| S3.1 Relative abundances of position-specific isotopologues.....   | 138        |
| S3.2 Model evaluation for nitrobenzene degradation.....  | 140        |
| Literature .....   | 143        |
| S4. Effects of Aqueous Diffusion on Spatial Isotopic Gradients of Organic Contaminants... 144  |            |
| S4.1 Experimental protocol.....  | 144        |
| S4.2 Modeling approach and parameter fitting .....   | 145        |
| S4.3 Comparison of Experimentally-Determined and Calculated Diffusion Coefficients..   | 146        |
| S4.4 Isotopologue-specific properties of cisDCE and TCE at natural isotopic abundance.   | 147        |
| Literature .....   | 149        |
| <b>Curriculum Vitae .....</b>  | <b>151</b> |





## Abstract

Groundwater pollution by organic contaminants such as chlorinated ethenes and petroleum hydrocarbons is a widespread environmental problem. Compound specific isotope analysis (CSIA) is a valuable tool to study microbial and abiotic transformation processes in environmental systems and has been increasingly applied in the past decade. This work focuses on experimental investigation and model interpretation of isotopic evolution during organic contaminants transformation and transport processes. The studies conducted in this dissertation include: i) Compound specific on-line chlorine isotope analysis of chlorinated hydrocarbons using gas chromatography coupled to a regular quadrupole mass spectrometer (GC-qMS). In this study we compared existing evaluation schemes to calculate chlorine isotope ratios with those that we modified or newly proposed. We also tested systematically important experimental procedures such as external vs. internal referencing schemes, and instrumental settings including split ratio, ionization energy and dwell times. ii) A self-consistent method was proposed to predict the evolution of carbon and chlorine isotope ratios during degradation of chlorinated hydrocarbons. The method treats explicitly the cleavage of isotopically different C-Cl bonds and thus considers, simultaneously, combined carbon-chlorine isotopologues. To illustrate the proposed modeling approach we focus on the reductive dehalogenation of chlorinated ethenes. We compare our method with the currently available approach, in which carbon and chlorine isotopologues are treated separately. The new approach provides an accurate description of dual-isotope effects regardless of the extent of the isotope fractionation and physical characteristics of the experimental system. iii) A multi-element isotope modeling approach was demonstrated to simultaneously predict the evolution of different isotopes during the transformation of organic contaminants. The isotopic trends of different elements are explicitly simulated by tracking position-specific isotopologues that contain the isotopes located at fractionating positions. Our approach provides a mechanistic description of different degradation pathways that accounts for the influence of both primary and secondary isotope effects during contaminant degradation. The method is particularly suited to quantitatively describe the isotopic evolution of relatively large organic contaminant molecules. We apply the proposed modeling approach to the degradation of toluene, methyl tert-butyl ether (MTBE) and nitrobenzene observed in previous experimental studies. Our model successfully predicts the multi-

element isotope data (both 2D and 3D), and accurately captures the distinct trends observed for different reaction pathways. iv) Laboratory experiments were performed to investigate and quantify the extent of diffusive isotope fractionation of organic contaminants in aqueous systems. As model compounds we selected petroleum hydrocarbons: toluene and ethylbenzene, in 1:2 mixtures of labeled (perdeuterated) and non-labeled isotopologues, as well as chlorinated solvents: trichloroethene (TCE) and cis-dichloroethene (cisDCE). The latter were studied at their natural isotopic abundance and the spatial-temporal change of chlorine isotope ratios was determined to assess the effect of diffusion on isotope fractionation. The proposed experimental approach allowed us to resolve concentration and isotopic gradients induced by isotopologue-specific diffusion, and to determine values of aqueous diffusion coefficients in agreement with published empirical correlations. The experiments were quantitatively interpreted with numerical simulations, used to determine the aqueous diffusion coefficients ( $D$ ) and the exponent ( $\beta$ ) of the inverse power-law relation between  $D$  and the molecular mass of the dissolved compounds:  $D \propto m^{-\beta}$ . The results show remarkable diffusive isotope fractionation for all the investigated organic compounds.

## Kurzfassung

Grundwasserverschmutzungen durch organische Schadstoffe wie chlorierte Ethene und Mineralölkohlenwasserstoffe sind ein verbreitetes ökologisches Problem. Die stoffspezifische Isotopenanalyse (CSIA) ist ein nützliches Hilfsmittel um mikrobielle und abiotische Umwandlungsprozesse in Umweltsystemen zu untersuchen und wurde im Laufe der letzten zehn Jahre immer häufiger angewendet. Diese Arbeit konzentriert sich auf die experimentelle Untersuchung und modellgestützte Interpretation der Isotopenfraktionierung organischer Schadstoffe durch Umwandlungs- und Transportprozesse. Folgende Untersuchungen wurden im Rahmen dieser Dissertation durchgeführt: i) eine Methode zur stoffspezifischen on-line Chlor-Isotopenanalyse chlorierter Kohlenwasserstoffe, mittels Gaschromatographie gekoppelt an ein Quadrupole Massenspektrometer (GC-qMS), wurde entwickelt, validiert und mit bereits existierenden Methoden verglichen. Weiterhin wurden wichtige experimentelle Vorgehensweisen, wie z.B. externe gegen interne Referenzsysteme, sowie Geräteeinstellungen, wie split ratio, Ionisierungsenergie und Verweilzeiten systematisch erprobt. ii) Ein konsistentes Verfahren zur Modellierung der Kohlenstoff- und Chlor-Isotopenfraktionierung während des Abbaus chlorierter Kohlenwasserstoffe wurde entwickelt. Das Verfahren berücksichtigt die Spaltung isotopisch unterschiedlicher C-Cl-Bindungen, und daher die unterschiedlichen Kohlenstoff-Chlor-Isotopologe, explizit. Zur Veranschaulichung wenden wir unseren Modellierungsansatz auf die reduktive Dehalogenierung chlorierter Ethene an. Wir vergleichen unser Verfahren mit dem momentan gängigen Ansatz, bei dem die Kohlenstoff- und Chlor-Isotopologe getrennt betrachtet werden. Das neue Verfahren ermöglicht die genaue Beschreibung von Doppel-Isotopen-Effekten unabhängig sowohl vom Ausmaß der Isotopenfraktionierung, als auch von den physikalischen Einflussgrößen des Versuchsaufbaus. iii) Für die gleichzeitige Vorhersage der Isotopenfraktionierung mehrerer Elemente in einem Molekül während der Umwandlung organischer Schadstoffe wurde ein mehrfache-Element-Isotopen-Modell-Ansatz entwickelt. Durch das Verfolgen derjenigen Isotopologe, welche die Isotope positionsspezifisch an den Fraktionierungsstellen aufweisen, werden die isotopischen Trends der verschiedenen Elemente während des Umwandlungsprozesses explizit simuliert. Unser Ansatz liefert eine mechanistische Beschreibung verschiedener Abbaupfade und berücksichtigt den Einfluss primärer, als auch sekundärer Isotopen-Effekte während des Schadstoffabbaus.

Die Methode ist vor allem für eine quantitative Beschreibung der Isotopenentwicklung relativ großer organischer Schadstoffmoleküle geeignet. Zur Validierung unseres Modells wenden wir dieses auf publizierte Daten aus Experimenten zum Abbau von Toluol, Methyl-tert-butylether (MTBE) und Nitrobenzol an. Mit Hilfe unseres Modells können wir die mehrfache-Element-Isotopen-Daten (sowohl 2D, als auch 3D) erfolgreich und die reaktionspfadspezifischen Trends exakt beschreiben. iv) Um das Ausmaß der Isotopenfraktionierung organischer Schadstoffe durch Diffusion in wässrigen Systemen zu untersuchen und zu quantifizieren wurden Laborexperimente durchgeführt. Als Modellsubstanzen verwendeten wir die Mineralölkohlenwasserstoffe Toluol und Ethylbenzol, im Verhältnis 1:2 als markierte (per-deutert) und nicht-markierte Isotopologe, und chlorierte Lösesmittel: Trichlorethen (TCE) und 1,2-Dichlorethen (cisDCE). Letztere wurden in ihrer natürlichen Isotopenhäufigkeit untersucht und die räumlich-zeitliche Veränderung der Chlor-Isotopenverhältnisse wurde erfasst, um den Effekt der Diffusion auf die Isotopenfraktionierung abzuschätzen. Der vorgestellte experimentelle Ansatz erlaubt die Auflösung von Konzentrations- und Isotopengradienten, welche durch isotopologspezifische Diffusion bedingt sind, und erlaubt die Bestimmung der Werte für Diffusionskoeffizienten in Wasser im Einklang mit publizierten empirischen Korrelationen. Die Experimente wurden quantitativ mithilfe numerischer Simulationen interpretiert und die Diffusionskoeffizienten in Wasser ( $D$ ) und der Exponent ( $\beta$ ) des inversen Potenzgesetzes zwischen  $D$  und der Molmasse der gelösten Stoffe genutzt:  $D \text{ am}^{-\beta}$ . Die Ergebnisse zeigen eine erhebliche Isotopenfraktionierung durch Diffusion bei allen untersuchten organischen Verbindungen.

# Chapter 1

---

## Introduction

### 1.1 Background

Groundwater contamination by organic contaminants such as chlorinated ethenes and petroleum hydrocarbons is a widespread environmental problem. These compounds can be dissolved in groundwater or can be present as non-aqueous-phase liquids (NAPLs), which act as long-term sources for contaminant plumes in the subsurface. The identification and quantification of the transformation pathways of these compounds in the environment are essential to understand their fate and transport in order to plan effective remediation strategies for contaminated sites (Wiedemeier et al., 1999).

Compound specific isotope analysis (CSIA) is a valuable tool to study microbial and abiotic transformation processes in environmental systems and has been increasingly applied in the past decade (Schmidt et al. 2004; Elsner et al., 2005). CSIA technique relies on the fact that light isotopes react faster than the heavy ones assuming a normal kinetic effect, therefore leading to enrichment of heavy isotopes in the remaining fraction. So far, stable carbon is the most popular element for CSIA applications to investigate degradation of various organic contaminants in both laboratory and field studies (e.g., Sherwood et al., 2001; Hunkeler et al., 2002). Recent advances in analytical techniques extended stable isotope techniques to other elements such as hydrogen, oxygen, nitrogen and chlorine. For instance, the new on-line GC-qMS approach for chlorine isotope analysis has significantly promoted implementation of chlorine CSIA in various environmental studies (Sakaguchi-Soder et al., 2007; Aeppli et al., 2010; Bernstein et al., 2011; Hitzfeld et al., 2011; Jin et al., 2011). This new on-line method avoids tedious off-line sample pretreatments and offers a fast determination of chlorine isotope ratios. However, the precision and accuracy of the method are influenced by both instrumental settings and mathematical evaluation schemes. Therefore, all these important parameters need to be systematically investigated and optimized in order to extend this approach to a wider range of halogenated organic compounds (Jin et al., 2011). The possibility to

analyze isotopic signatures of different isotope pairs facilitates applications of dual-element isotope approaches in numerous experimental studies to investigate the transformation of common groundwater organic contaminants (e.g., Morasch et al., 2001; Mancini et al., 2003; Zwank et al., 2005; Vogt et al., 2008; Abe et al., 2009). Despite the fact that mathematical modeling is a critical tool to transfer detailed and mechanistic laboratory observations to practical applications in complex environmental systems, isotope modeling approaches required for the interpretation of multi-element isotope data of environmentally-relevant transformation processes of organic contaminants are still rather limited (van Breukelen et al., 2005; Hunkeler et al., 2009; Jin et al., 2013). Therefore, it is of primary importance to provide accurate quantitative evaluation schemes capable of combining the isotopic evolution of different elements. Furthermore, the gap between the mechanistic understanding of contaminants transformation based on multi-element isotope analysis and the current state of the art of modeling approaches to quantitatively describe and interpret multi-element isotope evolution needs to be filled. Although isotope effects from physical processes are normally neglected, an increasing number of investigations have demonstrated the important role of physical processes on isotope fractionation of organic contaminants. Such processes include mass transfer limitations (Aeppli et al., 2009), sorption (Kopinke et al., 2005; Hohener et al., 2012), volatilization (Huang et al., 1999), aqueous diffusion and transverse dispersion (Rolle et al., 2010). In particular, diffusion is a major transport mechanism in saturated media and its importance is increasingly acknowledged in contaminant hydrology. However, research in diffusion-induced isotope fractionation mainly focused on isotope fractionation of dissolved trace gases (e.g., Schloemer et al., 2004; Bourg et al., 2008), and ionic species (e.g., Richter et al., 2006; Eggenkamp et al., 2009) in both laboratory and environmental systems. Diffusive isotope fractionation of uncharged polyatomic species, such as organic contaminants, have been far less understood and developed. This hinders a correct interpretation of isotopic data in groundwater systems and a quantitative assessment of contaminant transport and transformation using CSIA techniques.

## **1.2 Objectives**

This dissertation addresses the challenging questions in current environmental isotope research summarized above, and focuses on the investigation of isotopic evolution of

groundwater organic contaminants using experimental and modeling approaches. The specific goals of this work are:

- Systematically evaluate and optimize the instrumental settings, evaluation methods and reference schemes potentially affecting the precision and reproducibility of chlorine isotope analysis using the GC-qMS method.
- Illustrate a modeling approach which simultaneously and self-consistently integrates the carbon and chlorine isotope evolution, and compare the proposed method with the currently available isotopologue evaluation scheme.
- Apply the proposed modeling approach to correctly and accurately simulate carbon and chlorine isotopic data observed in biodegradation experiments performed both in well-mixed systems and in the presence of mass-transfer limitations.
- Propose a new multi-element modeling approach based on position-specific isotopologues which only considers isotopically-sensitive atoms (i.e., atoms directly located at reactive positions or at positions adjacent to a reactive bond).
- Illustrate and validate the proposed mechanistic modeling methodology, and apply the model to predict the multi-element isotopic evolution for different degradation pathways observed in previous experimental studies.
- Perform laboratory experiments to investigate and quantify the extent of diffusive isotope fractionation of organic contaminants in aqueous systems using petroleum hydrocarbons as well as chlorinated solvents as model compounds.

### **1.3 Structure of the thesis**

In general, the studies within this dissertation cover a wide range of topics in current environmental isotope research, including chlorine CSIA using GC-qMS, carbon-chlorine dual isotope modeling, multi-element (i.e. carbon, hydrogen and nitrogen) isotope modeling and diffusive isotope fractionation of organic contaminants. Specifically, these topics are introduced and organized in the following order:

- Chapter 2 presents detailed evaluation and optimization of the GC-qMS approach for chlorine isotope determination.

- Chapter 3 demonstrates an integrated carbon-chlorine dual isotope modeling approach.
- Chapter 4 proposes a mechanistic multi-element isotope modeling approach for relatively large organic contaminant molecules.
- Chapter 5 reports the experimental investigation of diffusion-induced isotope fractionation of organic contaminants in aqueous systems.



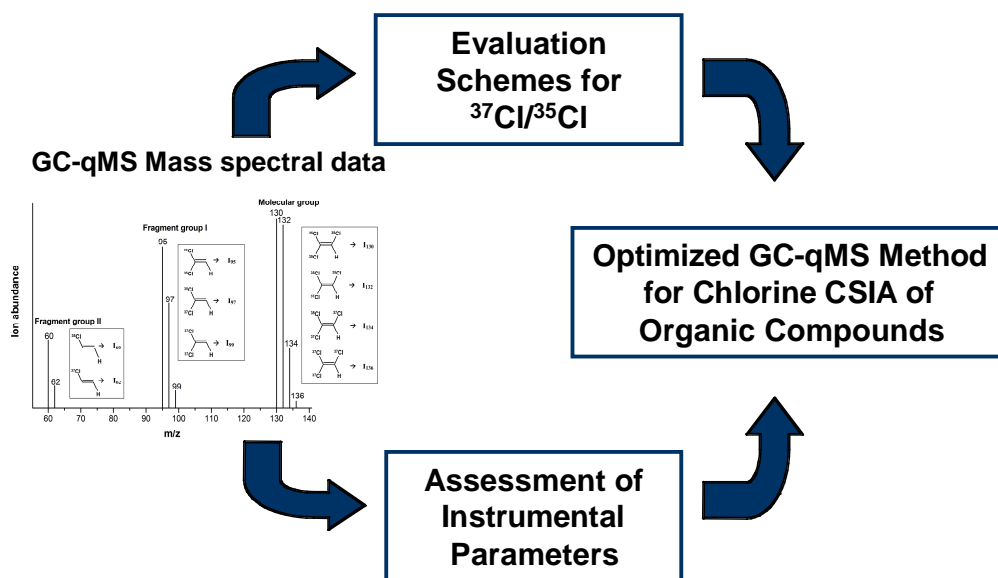
## References

- Aeppli, C., Holmstrand, H., Andersson, P., Gustafsson, O., 2010. Direct Compound-Specific Stable Chlorine Isotope Analysis of Organic Compounds with Quadrupole GC/MS Using Standard Isotope Bracketing. *Anal. Chem.* 82, 420-426.
- Aeppli, C., Berg, M., Cirpka, O.A., Holliger, C., Schwarzenbach, R.P., Hofstetter, T.B., 2009. Influence of Mass-Transfer Limitations on Carbon Isotope Fractionation during Microbial Dechlorination of Trichloroethene. *Environ. Sci. Technol.* 43, 8813-8820.
- Abe, Y., Aravena, R., Zopfi, J., Shouakar-Stash, O., Cox, E., Roberts, J.D., Hunkeler, D., 2009. Carbon and Chlorine Isotope Fractionation during Aerobic Oxidation and Reductive Dechlorination of Vinyl Chloride and cis-1,2-Dichloroethene. *Environmental Science & Technology* 43, 101-107.
- Bernstein, A., Shouakar-Stash, O., Ebert, K., Laskov, C., Hunkeler, D., Jeannotat, S., Sakaguchi-Soder, K., Laaks, J., Jochmann, M.A., Cretnik, S., Jager, J., Haderlein, S.B., Schmidt, T.C., Aravena, R., Elsner, M., 2011. Compound-Specific Chlorine Isotope Analysis: A Comparison of Gas Chromatography/Isotope Ratio Mass Spectrometry and Gas Chromatography/Quadrupole Mass Spectrometry Methods in an Interlaboratory Study. *Anal. Chem.* 83, 7624-7634.
- Bourg, I.C., Sposito, G., 2008. Isotopic fractionation of noble gases by diffusion in liquid water: Molecular dynamics simulations and hydrologic applications. *Geochimica Et Cosmochimica Acta* 72, 2237-2247.
- Elsner, M., Zwank, L., Hunkeler, D., Schwarzenbach, R.P., 2005. A new concept linking observable stable isotope fractionation to transformation pathways of organic pollutants. *Environ. Sci. Technol.* 39, 6896-6916.
- Eggenkamp, H.G.M., Coleman, M.L., 2009. The effect of aqueous diffusion on the fractionation of chlorine and bromine stable isotopes. *Geochimica Et Cosmochimica Acta* 73, 3539-3548.
- Hunkeler, D., Aravena, R., Cox, E., 2002. Carbon isotopes as a tool to evaluate the origin and fate of vinyl chloride: Laboratory experiments and modeling of isotope evolution. *Environ. Sci. Technol.* 36, 3378-3384.
- Hunkeler, D., Van Breukelen, B.M., Elsner, M., 2009. Modeling Chlorine Isotope Trends during Sequential Transformation of Chlorinated Ethenes. *Environmental Science & Technology* 43, 6750-6756.
- Hitzfeld, K.L., Gehre, M., Richnow, H.H., 2011. A novel online approach to the determination of isotopic ratios for organically bound chlorine, bromine and sulphur. *Rapid Commun. Mass Spectrom.* 25, 3114-3122.
- Huang, L., Sturchio, N.C., Abrajano, T., Heraty, L.J., Holt, B.D., 1999. Carbon and chlorine isotope fractionation of chlorinated aliphatic hydrocarbons by evaporation. *Organic Geochemistry* 30, 777-785.
- Hohener, P., Silvestre, V., Lefrancois, A., Loquet, D., Botosoa, E.P., Robins, R.J., Remaud, G.S., 2012. Analytical model for site-specific isotope fractionation in C-13 during sorption: Determination by
- Jin, B., Laskov, C., Rolle, M., Haderlein, S.B., 2011. Chlorine Isotope Analysis of Organic Contaminants Using GC-qMS: Method Optimization and Comparison of Different Evaluation Schemes. *Environ. Sci. Technol.* 45, 5279-5286.

- Jin, B., Haderlein, S.B., Rolle, M., 2013. Integrated carbon and chlorine isotope modeling: applications to chlorinated aliphatic hydrocarbons dechlorination. *Environmental Science & Technology* 47, 1443-1451.
- Kopinke, F.D., Georgi, A., Voskamp, M., Richnow, H.H., 2005. Carbon isotope fractionation of organic contaminants due to retardation on humic substances: Implications for natural attenuation studies in aquifers. *Environmental Science & Technology* 39, 6052-6062.
- Morasch, B., Richnow, H.H., Schink, B., Meckenstock, R.U., 2001. Stable hydrogen and carbon isotope fractionation during microbial toluene degradation: Mechanistic and environmental aspects. *Appl. Environ. Microbiol.* 67, 4842-4849.
- Mancini, S.A., Ulrich, A.C., Lacrampe-Couloume, G., Sleep, B., Edwards, E.A., Lollar, B.S., 2003. Carbon and hydrogen isotopic fractionation during anaerobic biodegradation of benzene. *Appl. Environ. Microbiol.* 69, 191-198.
- Rolle, M., Chiogna, G., Bauer, R., Griebler, C., Grathwohl, P., 2010. Isotopic Fractionation by Transverse Dispersion: Flow-through Microcosms and Reactive Transport Modeling Study. *Environmental Science & Technology* 44, 6167-6173.
- Richter, F.M., Mendybaev, R.A., Christensen, J.N., Hutcheon, I.D., Williams, R.W., Sturchio, N.C., Beloso, A.D., 2006. Kinetic isotopic fractionation during diffusion of ionic species in water. *Geochimica Et Cosmochimica Acta* 70, 277-289.
- Schmidt, T.C., Zwank, L., Elsner, M., Berg, M., Meckenstock, R.U., Haderlein, S.B., 2004. Compound-specific stable isotope analysis of organic contaminants in natural environments: a critical review of the state of the art, prospects, and future challenges. *Anal. Bioanal. Chem.* 378, 283-300.
- Sherwood Lollar, B., Slater, G.F., Sleep, B., Witt, M., Klecka, G.M., Harkness, M., Spivack, J., 2001. Stable carbon isotope evidence for intrinsic bioremediation of tetrachloroethene and trichloroethene at area 6, Dover Air Force Base. *Environmental Science and Technology* 35, 261-269.
- Sakaguchi-Soder, K., Jager, J., Grund, H., Matthaus, F., Schuth, C., 2007. Monitoring and evaluation of dechlorination processes using compound-specific chlorine isotope analysis. *Rapid Commun. Mass Spectrom.* 21, 3077-3084.
- Schloemer, S., Krooss, B.M., 2004. Molecular transport of methane, ethane and nitrogen and the influence of diffusion on the chemical and isotopic composition of natural gas accumulations. *Geofluids* 4, 81-108.
- Vogt, C., Cyrus, E., Herklotz, I., Schlosser, D., Bahr, A., Herrmann, S., Richnow, H.H., Fischer, A., 2008. Evaluation of Toluene Degradation Pathways by Two-Dimensional Stable Isotope Fractionation. *Environ. Sci. Technol.* 42, 7793-7800.
- van Breukelen, B.M., Hunkeler, D., Volkering, F., 2005. Quantification of sequential chlorinated ethene degradation by use of a reactive transport model incorporating isotope fractionation. *Environmental Science & Technology* 39, 4189-4197.
- Wiedemeier, T. H., Rifai H. S., Newell, C. J., Wilson, J. T.; *Natural Attenuation of Fuels and Chlorinated Solvents in the Subsurface*; John Wiley & Sons: NY, USA, 1999.
- Zwank, L., Berg, M., Elsner, M., Schmidt, T.C., Schwarzenbach, R.P., Haderlein, S.B., 2005. New evaluation scheme for two-dimensional isotope analysis to decipher biodegradation processes: Application to groundwater contamination by MTBE (vol 39, pg 1018, 2005). *Environ. Sci. Technol.* 39, 7344-7344.

## Chapter 2

# Chlorine Isotope Analysis of Organic Contaminants Using GC-qMS: Method Optimization and Comparison of Different Evaluation Schemes<sup>1</sup>



<sup>1</sup>Modified from Jin, B.; Laskov, C.; Rolle, M.; Haderlein, S. B., Chlorine Isotope Analysis of Organic Contaminants Using GC-qMS: Method Optimization and Comparison of Different Evaluation Schemes. *Environ. Sci. Technol.* **2011**, *45*, (12), 5279-5286. Copyright 2011 American Chemical Society.

## Abstract

Compound specific on-line chlorine isotope analysis of chlorinated hydrocarbons was evaluated and validated using gas chromatography coupled to a regular quadrupole mass spectrometer (GC-qMS). This technique avoids tedious off-line sample pretreatments, but requires mathematical data analysis to derive chlorine isotope ratios from mass spectra. We compared existing evaluation schemes to calculate chlorine isotope ratios with those that we modified or newly proposed. We also tested systematically important experimental procedures such as external vs. internal referencing schemes, and instrumental settings including split ratio, ionization energy and dwell times. To this end, headspace samples of tetrachloroethene (PCE), trichloroethene (TCE) and cis-dichloroethene (cDCE) at aqueous concentrations in the range of 20-500  $\mu\text{g/L}$  (mass on column range 3.2 to 115 pmol) were analyzed using GC-qMS. The results ( $^{37}\text{Cl}/^{35}\text{Cl}$  ratios) showed satisfying to good precisions with relative standard deviations (n=5) between 0.4 ‰ and 2.1 ‰. However, we found that the achievable precision considerably varies depending on the applied data evaluation scheme, the instrumental settings and the analyte. A systematic evaluation of these factors allowed us to optimize the GC-qMS technique to determine chlorine isotope ratios of chlorinated organic contaminants.

## 2.1 Introduction

Chlorinated organic compounds such as PCE, TCE and their transformation products are notorious groundwater pollutants (1). They occur in dissolved state and as non-aqueous-phase liquids (NAPLs), which act as long-term sources for contaminant plumes in the subsurface (1-2).

Compound specific isotope analysis (CSIA) has been successfully used in a variety of studies to quantify the fate of chlorinated organic pollutants, as well as to identify contaminant sources in groundwater (2-6). Recently, there has been increasing interest for dual element isotope analysis (7-12) as it improves the robustness and range of applications of CSIA approaches considerably. Chlorine CSIA provides a valuable tool to detect and quantify biodegradation processes and abiotic transformation of the chlorinated organic compounds in the subsurface. However, unlike the well-established and widely implemented stable carbon isotope analysis (2, 3), traditional analytical techniques used for stable chlorine isotopes require tedious off-line sample treatment and dedicated instrumentation. After chromatographic separation the chlorinated analytes have to be converted quantitatively into compounds containing only one chlorine atom (e.g. CsCl, CH<sub>3</sub>Cl). These pure compounds are then analyzed for their isotopic ratio using either a thermal ionization mass spectrometer (TIMS for solid CsCl) or a dual-inlet gas isotope ratio mass spectrometer (DI-IRMS for gaseous CH<sub>3</sub>Cl) (13-17). Using a gas chromatograph (GC) coupled to a continuous flow isotope ratio mass spectrometer (CF-IRMS) Shouakar-Stash et al. (14) established the first on-line method for chlorine CSIA of and reported a concept for deriving chlorine isotope ratios for PCE, TCE and cis-DCE. Sakaguchi-Soeder et al. (18) introduced an alternative instrumental approach for on-line compound specific chlorine isotope analysis using widely available gas chromatography-quadrupole mass spectrometry (GC-qMS). They determined chlorine isotope ratios for PCE and TCE, and referenced their data to an internal standard trichlorofluoromethane (CFCl<sub>3</sub>). Very recently, Aeppli et al. (20) determined chlorine isotope compositions of PCE, PCP and DDT with GC-qMS using on-column liquid injection and bracketing with external standards of known chlorine isotope composition.

In contrast to carbon, hydrogen, nitrogen and oxygen the two stable isotopes of chlorine are two-mass units apart and both occur at relatively similar abundances (<sup>35</sup>Cl at 75.78 %

and  $^{37}\text{Cl}$  at 24.22 %) (17). These characteristics may facilitate a scanning quadrupole MS to record mass spectral data sufficiently precise to calculate isotope ratios (19). However, unlike an IRMS, which allows detecting several masses simultaneously, a quadrupole MS has only one detector, which records selected masses consecutively. Therefore, instrument parameters of a quadrupole mass spectrometer including dwell time, number of selected masses, etc, are crucial factors for the reproducibility and precision of chlorine CSIA using GC-qMS.

Elsner and Hunkeler (19) provided a theoretical basis to calculate chlorine isotope ratios and quantify isotope fractionation using ion-current ratios of molecular/fragment ions. They showed that accurate chlorine isotope ratios can in principle be derived from ratios of any pair of two-mass apart isotopologue molecular or fragment ions, i.e. the result of data evaluation methods considering different molecular/fragment ions should be the same. This important concept, however, only holds if the mass spectrometer used is free of bias or drift with regard to any molecular or fragment ion. While the IRMS technology meets these requirements due to its simultaneous detection of analyte ions, the sequential recording of ions by a single detector in the qMS technology may be more prone to drift and discrimination between analyte ions. Thus, the type of computation scheme for deriving chlorine isotope ratios may be of significance and needs to be evaluated for quadrupole mass spectrometers. Previous experimental studies (18, 20) applied different evaluation schemes for chlorine isotope determination by GC-qMS. Sakaguchi-Soeder et al. (18) used a multiple ion method, considering the two most abundant ions in each ion group, Aeppli et al. (20) determined chlorine isotope ratios using solely molecular ions. One promising strategy to minimize potential bias or discrimination effects in the computation of chlorine isotope ratios from qMS spectra is to include all chlorine containing (fragment) ions in the computational scheme. This, however, as well as a comparison of existing evaluation schemes, referencing methods and instrumental settings in terms of precision and accuracy of chlorine CSIA using the qMS technology is not yet available.

Therefore, the major goals of this study are 1) to apply and compare existing evaluation schemes (i.e. molecular ion method, multiple ion methods) and propose alternative schemes (complete ion method) to determine chlorine isotope ratios from qMS spectra, 2) to systematically evaluate and optimize the instrument settings and reference schemes

potentially affecting the precision and reproducibility of the GC-qMS method. To this end, we applied the various instrumental settings, evaluation schemes, and referencing procedures at similar experimental conditions and instrumentation to a common data set of analytes including PCE, TCE and cis-DCE to identify optimized settings and procedures.

## 2.2 Evaluation Schemes for Chlorine Isotope Ratios

For a chlorinated organic compound, the relative abundance of an isotopologue containing “k”  $^{37}\text{Cl}$  atoms out of a total of “n” chlorine atoms can be expressed as (10):

$$I_{(n,k)} = \binom{n}{k} H^k L^{n-k} \quad (2.1)$$

$$\binom{n}{k} = \frac{(n-k+1) \cdot (n-k+2) \cdots (n-1) \cdot (n)}{k!} \quad (2.2)$$

where  $I$  is the relative abundance of a certain isotopologue of a chlorinated compound,  $H$  is the abundance of  $^{37}\text{Cl}$ ,  $L$  is the abundance of  $^{35}\text{Cl}$ ,  $n$  is the total number of chlorine atoms in a certain chlorinated compound and  $k$  is the number of  $^{37}\text{Cl}$  atoms in a specified isotopologue. The binomial coefficient (eq 2.2) represents the number of possible ways in which  $k$  atoms of  $^{37}\text{Cl}$  can be distributed over  $n$  positions of chlorine atoms in a molecule.

In principle, a chlorine isotope ratio can be computed from the ratio of any pair of neighboring isotopologue molecule or fragment ions with a difference of two mass units (19):

$$R = \frac{k}{(n-k+1)} \cdot \frac{I_{(n,k)}}{I_{(n,k-1)}} \quad (2.3)$$

where  $R$  is the  $^{37}\text{Cl}/^{35}\text{Cl}$  ratio,  $n$  is the total number of chlorine atoms in a certain chlorinated compound,  $k$  is the number of  $^{37}\text{Cl}$  atoms in a specified isotopologue,  $I$  is the measured ion abundance at different mass over charge ratios ( $m/z$ ) (see Fig. 2.1).

However, as mentioned above, limitations of GC-qMS require the use of evaluation schemes to determine  $^{37}\text{Cl}/^{35}\text{Cl}$  ratios. In the following we briefly describe existing and modified /newly-proposed evaluation schemes.

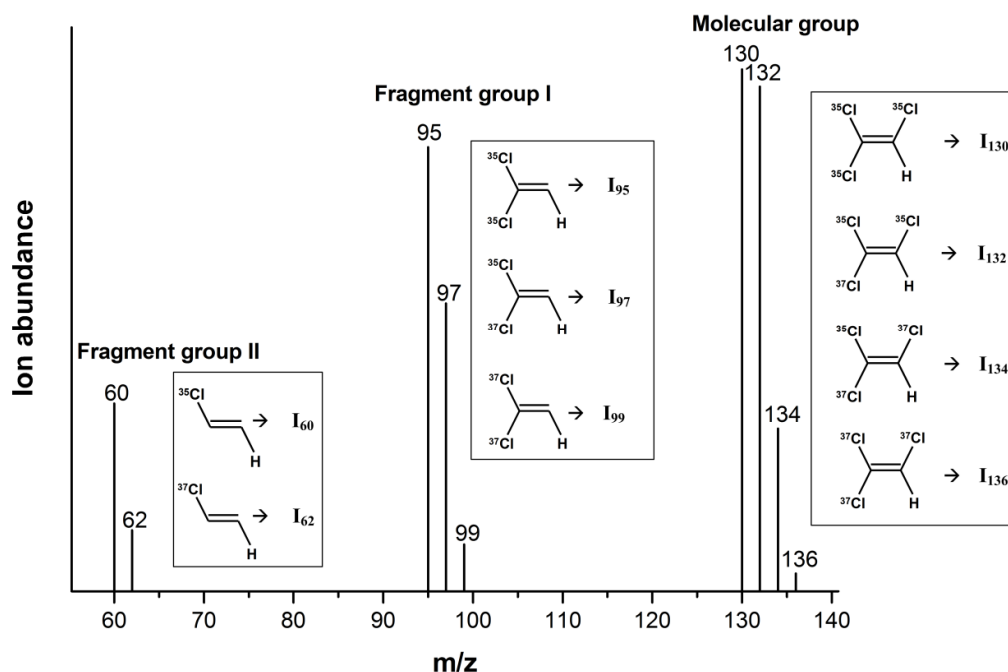


**Figure 2.1.** Mass spectra and isotopologues of trichloroethene (TCE) obtained from a quadrupole mass spectrometer.

### 2.2.1 Molecular Ion Method

The molecular ion method considers only the two most abundant molecular ions (e.g.  $I_{132}$  &  $I_{130}$  in Fig.2.1) of the analyte (20). Therefore, the chlorine isotopic ratios of chlorinated ethenes perchloroethene (PCE), trichloroethene (TCE), dichloroethene (DCE) and monochloroethene (i.e., vinyl chloride, VC) computed using eq 2.3 result in:

$$R_M^{PCE} = \frac{1}{4} \cdot \frac{I_{166}}{I_{164}} \quad (2.4)$$

$$R_M^{TCE} = \frac{1}{3} \cdot \frac{I_{132}}{I_{130}} \quad (2.5)$$



$$R_M^{DCE} = \frac{1}{2} \cdot \frac{I_{98}}{I_{96}} \quad (2.6)$$

$$R_M^{VC} = \frac{I_{64}}{I_{62}} \quad (2.7)$$

where  $I$  is the corresponding molecular/fragment ion abundance at different  $m/z$  values,  $R$  is the corresponding chlorine isotope ratio.

### 2.2.2 Conventional and Modified Multiple Ion Methods

The multiple ion method considers  $^{37}\text{Cl}/^{35}\text{Cl}$  ratios of the two most abundant ions of each ion group, which are calculated according to eq 2.3. Then, a weighted average of these partial  $^{37}\text{Cl}/^{35}\text{Cl}$  ratios is determined, which takes into account their overall chlorine isotopic composition (18). We modified this multiple ion method to incorporate more information of the quadrupole mass spectra for chlorine isotope determination. In contrast to Sakaguchi-Soeder et al. (18) who used only the most abundant ion to calculate the weight factors, we defined these weight factors taking into account the two major ions in each ion group. The equations are summarized as follows:

$$R_{PCE} = a \times R_M^{PCE} + b \times R_{F1}^{PCE} + c \times R_{F2}^{PCE} + d \times R_{F3}^{PCE} \quad (2.8)$$

$$a = \frac{I_{166} + I_{164}}{(I_{166} + I_{164}) + (I_{131} + I_{129}) + (I_{96} + I_{94}) + (I_{61} + I_{59})}$$

$$b = \frac{I_{131} + I_{129}}{(I_{166} + I_{164}) + (I_{131} + I_{129}) + (I_{96} + I_{94}) + (I_{61} + I_{59})}$$

$$c = \frac{I_{96} + I_{94}}{(I_{166} + I_{164}) + (I_{131} + I_{129}) + (I_{96} + I_{94}) + (I_{61} + I_{59})}$$

$$d = \frac{I_{61} + I_{59}}{(I_{166} + I_{164}) + (I_{131} + I_{129}) + (I_{96} + I_{94}) + (I_{61} + I_{59})} \quad (2.9)$$

where  $I$  is the corresponding molecular/fragment ion abundance at different  $m/z$  values. The weight factors  $a$ ,  $b$ ,  $c$  and  $d$  are determined as the relative ion intensities among the two major ions from each group.  $R_M$ ,  $R_{F1}$ ,  $R_{F2}$  and  $R_{F3}$  are the partial chlorine isotope ratios

obtained from two major ions of each group. Similar equations for TCE and DCE are available in Supporting Information (see eqs S1.13 –S1.17).

### 2.2.3 Complete Ion Method

We also propose an alternative and more comprehensive approach which considers all ions of the mass spectra that contain chlorine atoms, which we refer to as the complete ion method. Specifically, if a molecule or fragment ion has  $i$  isotopologues, and in a certain isotopologue  $m$  out of  $n$  (total chlorine atoms) are  $^{37}\text{Cl}$ , the chlorine isotope ratio can be determined using the following general equation:

$$R = \frac{\text{Tot}(^{37}\text{Cl})}{\text{Tot}(^{35}\text{Cl})} = \frac{\sum_{j=1}^i m_j \cdot I_j}{\sum_{j=1}^i (n - m_j) \cdot I_j} \quad (2.10)$$

where  $\text{Tot}(^{37}\text{Cl})$  and  $\text{Tot}(^{35}\text{Cl})$  are the total number of  $^{37}\text{Cl}$  and  $^{35}\text{Cl}$  atoms,  $I$  is the ion abundance of a certain isotopologue ( $j$ ). As an example, the corresponding equations for DCE are given as:

$$R_M = \frac{\text{Tot}(^{37}\text{Cl})}{\text{Tot}(^{35}\text{Cl})} = \frac{2 \cdot I_{100} + I_{98}}{I_{98} + 2 \cdot I_{96}} \quad (2.11)$$

$$R_F = \frac{\text{Tot}(^{37}\text{Cl})}{\text{Tot}(^{35}\text{Cl})} = \frac{I_{63}}{I_{61}} \quad (2.12)$$

$$R_{\text{DCE}} = a \cdot R_M + b \cdot R_F \quad (2.13)$$

$$a = \frac{I_{100} + I_{98} + I_{96}}{I_{100} + I_{98} + I_{96} + I_{63} + I_{61}}$$

$$b = \frac{I_{63} + I_{61}}{I_{100} + I_{98} + I_{96} + I_{63} + I_{61}} \quad (2.14)$$

where  $R_M$  and  $R_F$  are partial chlorine isotope ratios of the molecular and fragment ion groups of DCE,  $a$  and  $b$  are the weight factors. Similarly, the equations for TCE and PCE are derived according to eq 2.10, and are available in the Supporting Information (S1).

## 2.3 Experimental Section

### 2.3.1 Materials and Methods

Methanol (>99.9%) from Merck (Darmstadt, Germany) was used to prepare the stock solutions of the following chlorinated ethenes (acronym; purity; manufacturer) used for chlorine isotope analysis: Cis-1,2-dichloroethene (cis-DCE; >97%; Aldrich (Steinheim, Germany)), trichloroethene (TCE; >99.5%; Merck (Darmstadt, Germany)) and PPG (California, U.S.A.), tetrachloroethene (PCE, >99.9%; Merck (Darmstadt, Germany)) and PPG (California, U.S.A.). Headspace samples at different aqueous concentrations were prepared by adding various amounts of the PCE/TCE stock solutions into 20 mL glass vials containing 15 mL Millipore water. The vials were then immediately sealed with Teflon-crimp caps (Fisher, Germany). To reach headspace equilibrium, samples were kept at 25 °C for one hour before GC-qMS analysis.

A 7890A gas chromatograph (GC) connected to a 5975C quadrupole mass selective detector (MSD) (both from Agilent, Santa Clara, CA, USA) was used. Automated headspace sample injection (500 µL) was facilitated by a COMBIPAL multipurpose auto-sampler (Gerstel, Australia) at 25 °C. The GC was equipped with a split/splitless injector and a capillary column (60 m × 250 µm, 1.4 µm film thickness; Restek, USA). Helium at 1 ml/min was used as carrier gas. The oven program was set as follows: 40 °C (2 min) → 110 °C @ 25 °C /min → 200 °C @ 15 °C /min (5min).

The quadrupole mass spectrometry was operated in the selected ion mode (SIM). Most of the experiments were conducted considering the following ions of the target analytes: PCE: 164, 166, 129, 131, 94, 96, 59, 61 m/z; TCE: 130, 132, 95, 97, 60, 62 m/z; cis-DCE (96, 98, 100, 61, 63 m/z). Thus, at least the two most abundant ions from each ion group were considered. After optimization, a dwell time of 30 ms and a positive electron impact ionization energy of 70 eV was applied.

## 2.4 Results and Discussion

Precision and reproducibility of compound specific chlorine isotope analysis using GC-qMS are affected by various factors including the computation and referencing methods

for data evaluation, instrumental settings and amounts of analyte applied as well as the number of chlorine atoms present in the analyte. We carefully evaluated these factors and present the results below.

#### 2.4.1 Comparison of Different Evaluation Schemes

In previous experimental studies (18, 20), the multiple ion method and the molecular ion method were applied to calculate chlorine isotope ratios. We compared the results of these evaluation schemes with the modified multiple ion and the complete ion method using the same GC-qMS system, analytical parameters and analytes in order to identify the most appropriate computation scheme for different chlorinated organic compounds.

Cis-DCE headspace samples (50 to 1500  $\mu\text{g/L}$  aqueous concentrations, 5 replicates at each concentration) were measured under the same instrumental conditions using a split ratio of 1:10. Chlorine isotope ratios obtained from the mass spectral data were calculated using the four different methods presented above.

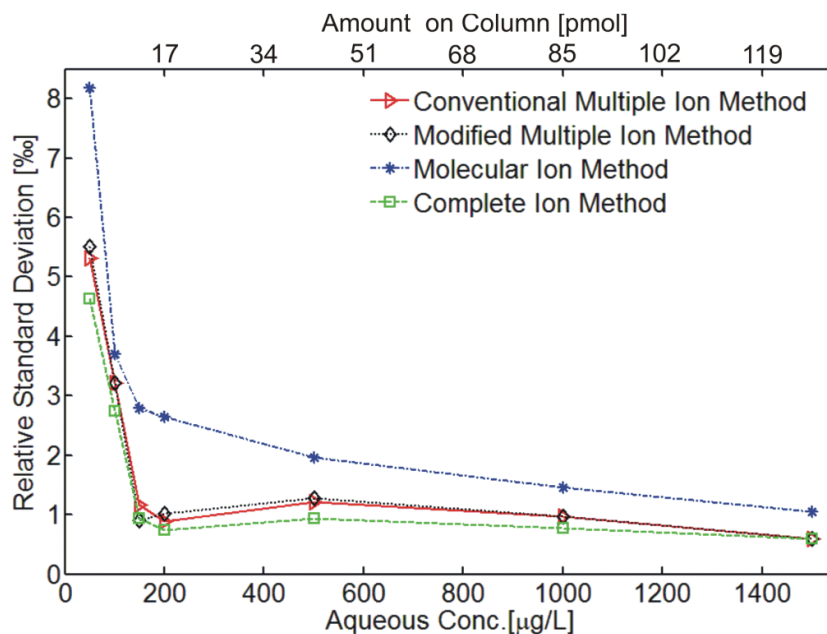


**Figure 2.2.** Relative standard deviation (RSD,  $n=5$ ) of cis-DCE chlorine isotope ratios using different evaluation schemes. The upper horizontal axis indicates the amount of analyte reaching the column.

As shown in Fig. 2.2, the amount of analyte reaching the column affects the precision of

GC-qMS method. The RSD values varied from 1.1 to 8.2‰ (molecular ion method), 0.6 to 5.3‰ (conventional multiple ion method), 0.6 to 5.5‰ (modified multiple ion method), and 0.6 to 4.6‰ (complete ion method) within the concentration range studied. Generally, the conventional multiple ion method and the modified multiple ion method did not differ significantly with regard to precision. The complete ion method showed the highest precision at all concentrations, while the molecular ion method resulted in the by far lowest precision among the four evaluation schemes. Particularly, at low concentrations ( $\leq 500 \mu\text{g/L}$ ) the complete ion method showed a higher precision than the multiple ion methods. To evaluate the performance of the complete ion method for analytes with more than two chlorine atoms, the full spectral data of PCE (14 ions) and TCE (9 ions) were considered in the SIM. Here, a lower precision of the complete ion method was obtained compared with the other three methods (see data in Table S1.2). This is due to the fact that including a high number of target ions in the SIM mode of a qMS conflicts with maintaining a sufficient dwell time (i.e. sampling time on each ion) and a reasonable scan rate (21-22). This tradeoff lowers the precision of the complete ion method for analytes containing more than two chlorine atoms. Thus, the complete ion method is particularly suited for analytes containing two chlorine atoms. To further compare the performances of the three other computational schemes, headspace samples of PCE and TCE mixtures at a series of aqueous concentrations (20 to 500  $\mu\text{g/L}$ ) were measured (5 replicates; split ratio 10:1). In Fig. 2.3, the results using the modified multiple ion method and the molecular ion method are plotted. As the conventional multiple ion method resulted in the same precision as the modified ion method (see Table S1 in Supporting Information) the data of the former are omitted for clarity in Fig. 2.3.

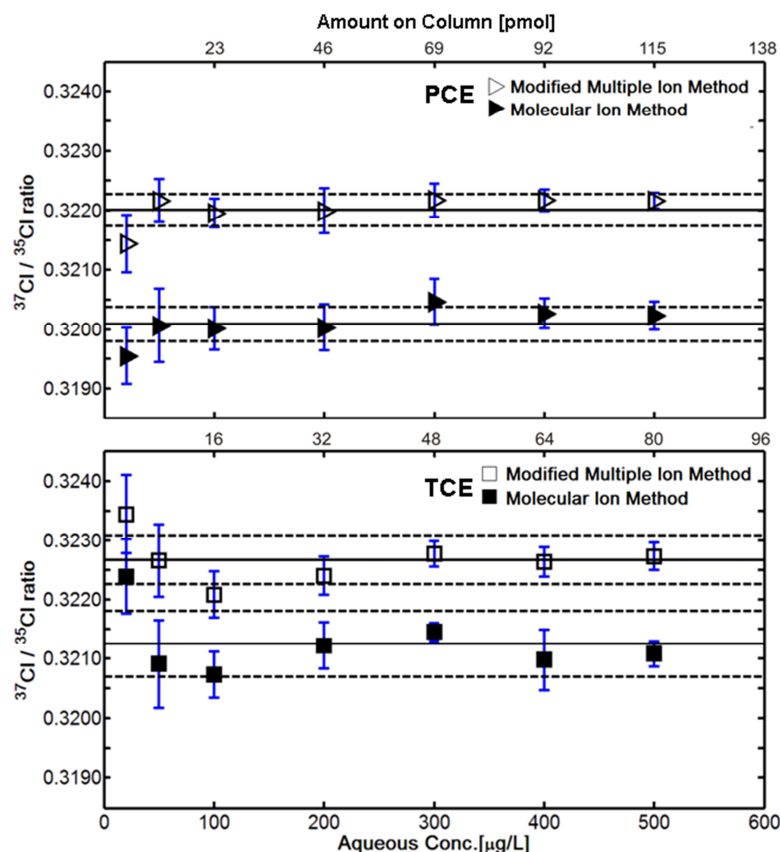


**Figure 2.3.** Chlorine isotope ratios of PCE and TCE (Merck) in headspace samples of various aqueous concentrations (20  $\mu\text{g/L}$  to 500  $\mu\text{g/L}$ ). The upper horizontal axes indicate the corresponding amount reaching the column. Solid horizontal lines are the average values; dotted lines are average standard deviations ( $1\sigma$ ,  $n=5$ ). Open symbols represent the modified multiple ion method, full symbols represent the molecular ion method.

As depicted in Fig. 2.3, the amount of analyte reaching the column affects both precision and accuracy. For the multiple ion method, average chlorine isotope values varied from 0.32144 ( $\pm 4.8 \times 10^{-4}$ , RSD: 1.5%) to 0.32216 ( $\pm 1.3 \times 10^{-4}$ , RSD: 0.4%) for PCE and from 0.32344 ( $\pm 6.6 \times 10^{-4}$ , RSD: 2.0%) to 0.32273 ( $\pm 2.3 \times 10^{-4}$ , RSD: 0.7%) for TCE. The results for the molecular ion method varied from 0.31955 ( $\pm 4.8 \times 10^{-4}$ , RSD: 1.5%) to 0.32023 ( $\pm 2.4 \times 10^{-4}$ , RSD: 0.8%) for PCE, and from 0.32239 ( $\pm 6.3 \times 10^{-4}$ , RSD: 2.0%) to 0.32108 ( $\pm 2.2 \times 10^{-4}$ , RSD: 0.7%) for TCE. Thus, the molecular ion method resulted in a lower precision than the multiple ion method that turns out to be the most precise computational scheme for analytes with three and four chlorine atoms such as PCE and TCE. Interestingly, a significant difference (approximately  $1.5 \times 10^{-3}$ ) of the average chlorine isotope ratios (solid horizontal lines in Fig. 3) was observed between the two

different evaluation schemes. In our study, the minimum amounts of compounds on column were 4.5 pmol (PCE) or 3.2 pmol (TCE) and the corresponding precisions are  $4.8 \times 10^{-4}$  ( $1\sigma$ ,  $n=5$ ,  $RSD=1.5\%$ , PCE) and  $6.6 \times 10^{-4}$  ( $1\sigma$ ,  $n=5$ ,  $RSD=2.0\%$ , TCE). Sakaguchi-Soeder et al. (18) obtained a standard deviation of  $7.2 \times 10^{-4}$  ( $1\sigma$ ,  $n=6$ ,  $RSD=2.2\%$ ) using 7 pmol on column PCE and  $5.8 \times 10^{-4}$  ( $1\sigma$ ,  $n=6$ ,  $RSD=1.8\%$ ) at 8 pmol on column TCE.

#### 2.4.2 Assessment of Instrumental Parameters

GC-qMS settings determine to a large extent the quality of mass spectral data, therefore affecting the precision and the accuracy of the method. Dwell time, an important MS parameter, specifies the individual data acquisition time for each selected set of ions (in our study 8 ions for PCE, 6 for TCE, and 5 for cis-DCE in the SIM mode). Headspace samples of cis-DCE, TCE and PCE mixtures at 200  $\mu\text{g/L}$  were measured at the dwell time values of 10, 20, 30, 50, 100 ms, respectively (Fig.2.4A-C).

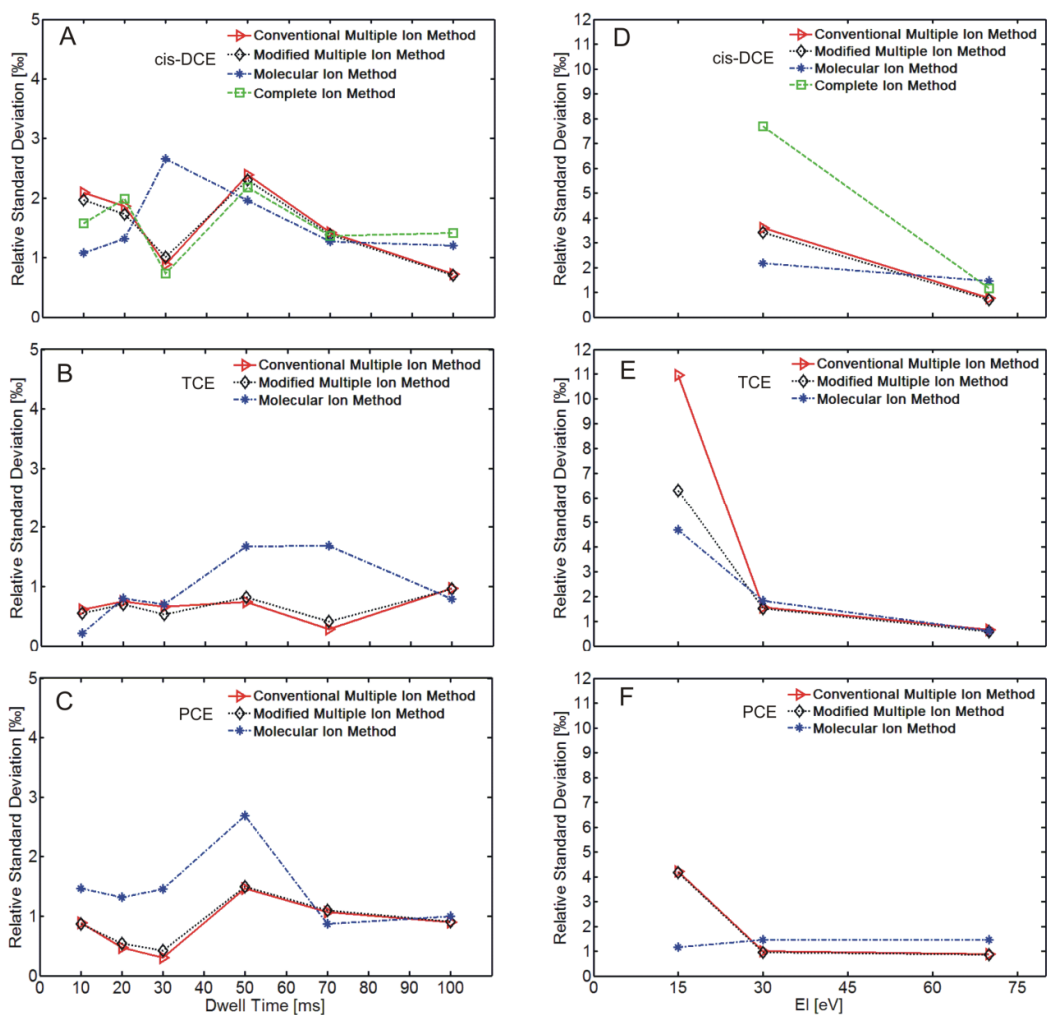


**Figure 2.4.** Effects of the qMS instrument parameters dwell time (A-C) and electron impact (EI) energy (D-F) on the precision of different evaluation schemes for chlorine isotope ratios. (D): At 15eV, chlorine isotope ratios of cis-DCE could not be determined due to the fact that several low-abundance ions were not detectable.

Our results reveal that the dwell time had a strong effect on the methods performances as the RSD values varied from 0.9 to 2.7‰ for cis-DCE, 0.21 to 1.0‰ for TCE and 0.3 to 2.7‰ for PCE, respectively. At a dwell time of 30 ms, the conventional and modified multiple ion methods showed the highest precision for cis-DCE and PCE, for TCE the highest precision of those two methods was observed within the range of 10 to 50 ms. For the molecular ion method, however, a higher precision was obtained either at a lower dwell time (10 to 20 ms) or at a higher dwell time (70 to 100 ms). Generally, a longer dwell time reduces the scan rate, therefore obtaining less data points over a certain



compound peak of the chromatogram and a shorter dwell time increases the data points, but inevitably lowers the precision of the data. At given chromatographic conditions an optimized value of the dwell time value depends on the target compound (i.e., the numbers of ions to be included in the SIM mode) and also on the characteristics of the specific qMS instrument.

To increase the fraction of molecular ions compared to fragment ions, the energy level in electron impact (EI) source of the mass spectrometer was lowered from the standard value of 70 eV down to 30 and 15 eV, respectively (Fig.2.4 D-F). Generally, lowering EI energy level did not result in a higher precision. The range of RSD values obtained at the different EI conditions varied from 0.7 to 7.7 ‰ for cis-DCE, 0.6 to 11.0 ‰ for TCE, and 0.9 to 4.2 ‰ for PCE. For all compounds and evaluation schemes, the most precise data were obtained at higher EI conditions. Only for the molecular ion method a higher precision for all compounds was obtained also at low EI values of 15 and 30 eV, suggesting that at a lower EI energy level, molecular ions have lower signal to noise ratios compared with those of fragment ions.

To evaluate the potential influence of the split ratio of the injector, headspace samples of 1, 5 and 10 mg/L aqueous mixtures of PCE and TCE were analyzed at split ratios of 1:10, 1:50 and 1:100, respectively. This setup ensures similar amounts of analytes reaching the column at the selected split ratios. The results are summarized in Table 2.1.

Generally, consistent chlorine isotope ratios and similar relative standard deviations were obtained at different split ratios. Thus, at comparable signal amplitudes the split ratio is not a controlling factor for the performance of chlorine isotope GC-qMS measurements when applying headspace injections, Note that also in this set of experiments the conventional and the modified multiple ion methods showed a higher precision than the molecular ion method.

**Table 2.1.**  $^{37}\text{Cl}/^{35}\text{Cl}$  ratios at different split ratio values but similar on column amounts of analytes

| Compound | Split Ratio <sup>a</sup> | n <sup>b</sup> | Conventional multiple ion method      |                    |         | Modified multiple ion method          |                    |         | Molecular ion method                  |                    |         |
|----------|--------------------------|----------------|---------------------------------------|--------------------|---------|---------------------------------------|--------------------|---------|---------------------------------------|--------------------|---------|
|          |                          |                | $^{37}\text{Cl}/^{35}\text{Cl}$ Ratio | STDV (1 $\sigma$ ) | RSD [%] | $^{37}\text{Cl}/^{35}\text{Cl}$ Ratio | STDV (1 $\sigma$ ) | RSD [%] | $^{37}\text{Cl}/^{35}\text{Cl}$ Ratio | STDV (1 $\sigma$ ) | RSD [%] |
| TCE      | 10:1                     | 5              | 0.32380                               | 0.00016            | 0.5     | 0.32346                               | 0.00018            | 0.6     | 0.32150                               | 0.00041            | 1.3     |
|          | 50:1                     | 5              | 0.32374                               | 0.00020            | 0.6     | 0.32337                               | 0.00018            | 0.6     | 0.32127                               | 0.00028            | 0.9     |
|          | 100:1                    | 5              | 0.32394                               | 0.00017            | 0.5     | 0.32359                               | 0.00015            | 0.5     | 0.32152                               | 0.00026            | 0.8     |
| PCE      | 10:1                     | 5              | 0.32246                               | 0.00021            | 0.7     | 0.32232                               | 0.00021            | 0.7     | 0.31930                               | 0.00051            | 1.6     |
|          | 50:1                     | 5              | 0.32248                               | 0.00019            | 0.6     | 0.32232                               | 0.00019            | 0.6     | 0.31935                               | 0.00024            | 0.8     |
|          | 100:1                    | 5              | 0.32249                               | 0.00010            | 0.3     | 0.32233                               | 0.00010            | 0.3     | 0.31932                               | 0.00015            | 0.5     |

a: corresponds to 160 pmol TCE and 230 pmol PCE reaching the column

b: number of replicates

### 2.4.3 Effect of Standardization Procedure

Using an internal isotope standard (i.e., a substance different from the target compound) is desirable as it reduces analysis time since samples and standards can be measured in the same chromatographic run. However, different compounds may have a different ionization chemistry, which might affect the accuracy and the precision of referencing isotope values with internal standards. For this reason, the external standardization is usually recommended and applied for CSIA. In order to test the performances of the two reference strategies for the GC-qMS method, internal and external standardization protocols were compared. To this end the target analyte PCE (Merck) was referenced either to TCE (Merck) as the internal standard or to the external standards of PCE (PPG) and TCE (Merck), respectively. Both, samples and external standards were at 1000  $\mu\text{g/L}$  aqueous concentrations, and they were injected in alternation (i.e. one sample followed by one standard). Chlorine isotope ratios of standard and sample analyses were determined using both, the multiple ion and the molecular ion methods. Finally,  $\delta^{37}\text{Cl}$  values of PCE (Merck) were reported by referencing the chlorine isotope ratios of PCE (Merck) to the ones of the standard compounds (i.e. TCE-Merck; PCE-PPG).

**Table 2.2.**  $\delta^{37}\text{Cl}$  values of PCE (Merck) referenced to different internal and external standards

| Method                    | $^{37}\text{Cl}/^{35}\text{Cl}$ Ratio * | RSD <sup>§</sup><br>[‰] | Referenced $\delta^{37}\text{Cl}$ of PCE-Merck [‰] <sup>#</sup> |                   |                   |
|---------------------------|---|-------------------------|---|-------------------|-------------------|
|                           |   |                         | Internal Standard   | External Standard | External Standard |
|                           |   |                         | TCE-Merck   | TCE-Merck         | PCE-PPG           |
| Conventional Multiple Ion | 0.32196 ± 0.000036                      | 0.1                     | -2.7 ± 0.5  | -2.8 ± 0.6        | 1.8 ± 0.6         |
| Modified Multiple Ion     | 0.32178 ± 0.000034                      | 0.1                     | -2.1 ± 0.4  | -2.2 ± 0.6        | 1.8 ± 0.6         |
| Molecular Ion             | 0.31955 ± 0.000079                      | 0.2                     | -3.0 ± 0.6  | -3.5 ± 0.8        | 2.2 ± 0.6         |

\*: standard deviation (1 $\sigma$ , n=5), §: relative standard deviation (1 $\sigma$ , n=5)

#:  $\delta^{37}\text{Cl}$  was calculated by referencing to the indicated standards and error propagation was applied

The data in Table 2.2 demonstrates that the conventional and modified multiple ion methods display a higher precision of both  $\delta^{37}\text{Cl}$  values and  $^{37}\text{Cl}/^{35}\text{Cl}$  ratios than the molecular ion method. Consistent  $\delta^{37}\text{Cl}$  values were observed using external and internal TCE (Merck) standards. Since PCE (PPG) is isotopically lighter than TCE (Merck) (8) more positive  $\delta^{37}\text{Cl}$  values are expected when referencing PCE (Merck) to PCE-PPG. Notably, the  $\delta^{37}\text{Cl}$  values using PCE (PPG) as an external standard showed the same precision as those using an external standard of TCE (Merck). This result is remarkable because even though PCE and TCE belong to the same compound class, not only their mass spectra differ but also the ionization efficiencies may vary due to the differences in symmetry of their structures. Thus, our data shows that at optimized instrumental conditions both internal and external referencing can give equally precise results using the GC-qMS method.

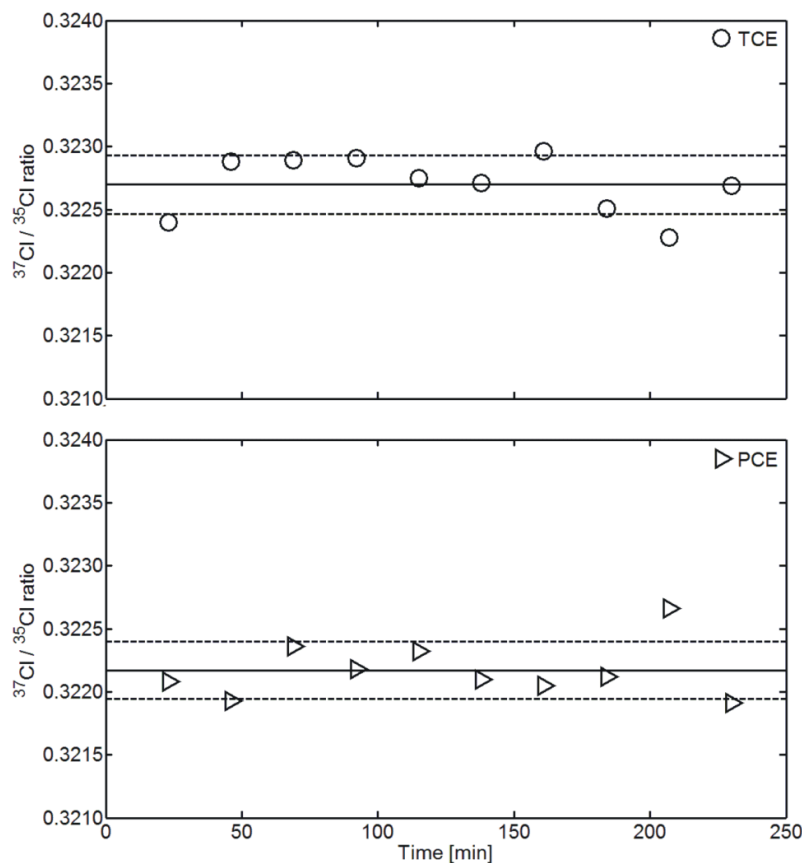


**Figure 2.5.** Temporal monitoring of measured chlorine isotope ratios of TCE and PCE. Solid horizontal lines are the average values and the dotted lines represent  $\pm$  standard deviations ( $1\sigma$ ,  $n=10$ ) of TCE ( $2.32 \times 10^{-4}$ ) and PCE ( $2.25 \times 10^{-4}$ ), or the corresponding relative standard deviations of TCE ( $\pm 0.7\%$ ) and PCE ( $\pm 0.8\%$ ).

Samples that already contain the compound that has been evaluated as internal standard require an external standardization procedure. Here, standard bracketing is normally applied to account for temporal drifts of the instrument. To explore the occurrence of such drifts we monitored chlorine isotope ratios over time spans that are typical for bracketing with external standards. Fig.2.5 reports the results over a period of 250 minutes. We observed some random fluctuations around the average but no systematic drift. It is important to note that regardless of the reference strategy applied, the quality of the raw data is the key factor that controls the performance of the GC-qMS method.

Furthermore, we also compared the chlorine isotope ratios that were obtained under somewhat different analytical conditions over time periods of several months. Also here

very consistent results were observed (see Supporting Information (S1)) which further indicates that the GC-qMS methodology developed and applied in this study is quite robust.

## Outlook and Environmental Significance

In this study we evaluated and optimized a GC-qMS method for online chlorine CSIA of chlorinated contaminants. Existing and proposed chlorine isotope ratio evaluation schemes were tested and compared. The choice of a suitable computational scheme is of importance since different schemes affect both the  $^{37}\text{Cl}/^{35}\text{Cl}$  ratios and the precision of the analysis. The methods considering more ions (i.e. complete ion method) are characterized by significantly higher precision for cis-DCE. For compounds with three or more chlorine atoms such as PCE and TCE, however, the complete ion method is no longer advantageous. The potential influences from the GC-qMS parameters, such as dwell time, ionization energy, split ratios, etc., were systematically tested and optimized together with the different evaluation schemes.

For practical applications and especially due to the suitability of the GC-qMS technique for the analysis of a wide variety of chlorinated hydrocarbons it is important to note that the chlorine isotope ratios tend to be overestimated in the presence of an increasing number of  $^{13}\text{C}$  atoms in the analyte. Aeppli et al. (20) presented an equation to quantify this error that can be safely ignored for chlorinated ethenes, but becomes significant for chlorinated compounds containing a higher number of carbon atoms such as chlorinated benzenes (Fig.2.6) or  $^{13}\text{C}$  isotopically-labeled analytes. Therefore, a correction on the chlorine isotope ratio is necessary in these cases.

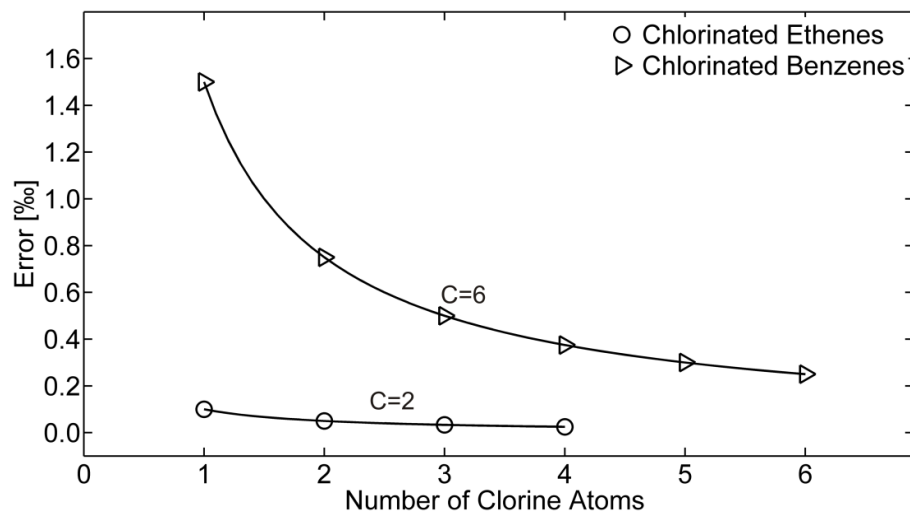


**Figure 2.6.** Overestimation (i.e.  $R_{\text{chlorine}} - R'_{\text{chlorine}}$ ) of raw  $^{37}\text{Cl}/^{35}\text{Cl}$  ratios caused by  $^{13}\text{C}$  exemplified by chlorinated ethenes and chlorinated benzenes. C is the number of carbon atoms. Assuming  $R_{\text{carbon}}$  equals 1% (approximate natural abundance of  $^{13}\text{C}$ ), the differences between apparent and theoretical partial  $^{37}\text{Cl}/^{35}\text{Cl}$  values were quantified using the equations derived by Aeppli et al. (20) for both chlorinated ethenes and chlorinated benzenes (Supporting Information, Eqn. S28).

The instrumental approach developed in this study is quite robust, universal with regard to the target analytes, sensitive, and does not require specialized instrumentation. Thus, it can contribute to widespread application of compound specific chlorine isotope analyses to further improve our understanding of chlorinated contaminants' transport and fate in the environment. However, our results demonstrate that the GC-qMS method needs proper validation as its performance depends on the applied computation scheme, the selected instrumental parameters and the compound analyzed. All these factors need to be considered and optimized in order to obtain high quality GC-qMS measurements.

### Supporting Information Available

Additional material including the description of the details on chlorine isotope computation, a list of instrumental parameters, additional data for figures and tables, long time monitoring of the chlorine isotope ratios and computation of  $^{13}\text{C}$  error is available in the Supporting Information (S1).

## References

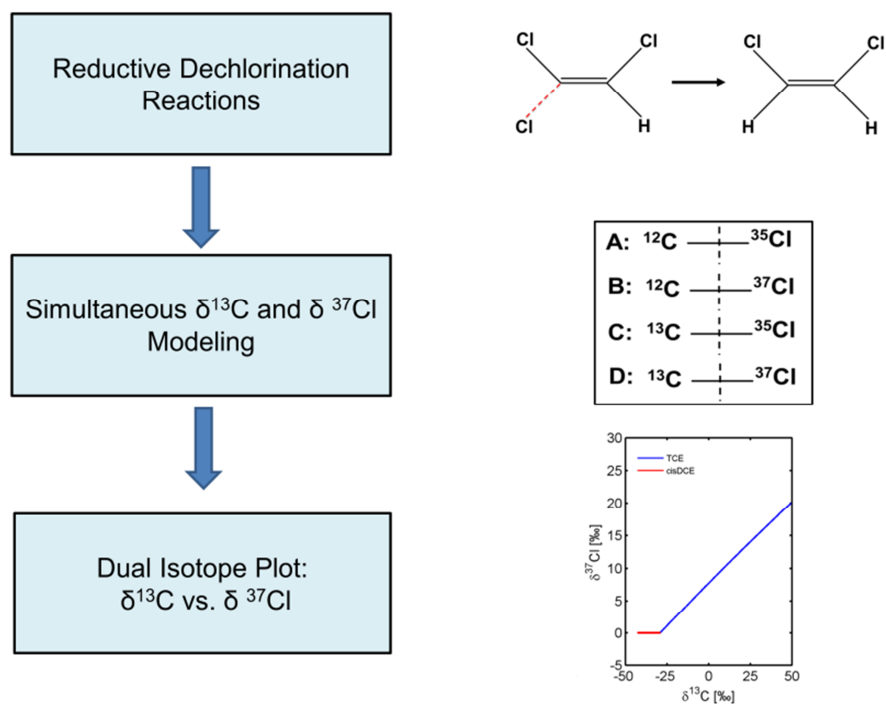
- (1) Wiedemeier, T. H.; Rifai H. S.; Newell, C. J.; Wilson, J. T.; Natural Attenuation of Fuels and Chlorinated Solvents in the Subsurface; John Wiley & Sons: NY, USA, **1999**.
- (2) Hunkeler, D., Meckenstock, R.U., Sherwood-Lollar, B., Schmidt, T., Wilson, J.T.; A Guide for Assessing Biodegradation and Source Identification of Organic Groundwater Contaminants using Compound Specific Isotope Analysis (CSIA). US Environmental Protection Agency (EPA) EPA 600/R-08/148, **2008**.
- (3) Blessing, M.; Schmidt, T. C.; Dinkel, R.; Haderlein, S. B., Delineation of multiple chlorinated ethene sources in an industrialized area - A forensic field study using compound-specific isotope analysis. *Environ. Sci. Technol.* **2009**, *43*, (8), 2701-2707.
- (4) Schmidt, T. C.; Zwank, L.; Elsner, M.; Berg, M.; Meckenstock, R. U.; Haderlein, S. B., Compound-specific stable isotope analysis of organic contaminants in natural environments: a critical review of the state of the art, prospects, and future challenges. *Analytical and Bioanalytical Chemistry* **2004**, *378*, (2), 283-300.
- (5) Meckenstock, R. U.; Morasch, B.; Griebler, C.; Richnow, H. H., Stable isotope fractionation analysis as a tool to monitor biodegradation in contaminated aquifers. *J. Contam. Hydrol.* **2004**, *75*, (3-4), 215-255.
- (6) Hofstetter, T. B.; Schwarzenbach, R. P.; Bernasconi, S. M., Assessing transformation processes of organic compounds using stable isotope fractionation. *Environ. Sci. Technol.* **2008**, *42*, (21), 7737-7743.
- (7) Morasch, B.; Richnow, H. H.; Schink, B.; Meckenstock, R. U., Stable hydrogen and carbon isotope fractionation during microbial toluene degradation: Mechanistic and environmental aspects. *App. Environ. Microbiol.* **2001**, *67*, (10), 4842-4849.
- (8) van Warmerdam, E. M.; Frappe, S. K.; Aravena, R.; Drimmie, R. J.; Flatt, H.; Cherry, J. A., Stable chlorine and carbon isotope measurements of selected chlorinated organic solvents. *Appl. Geochem.* **1995**, *10*, (5), 547-552.
- (9) Zwank, L.; Berg, M.; Elsner, M.; Schmidt, T. C.; Schwarzenbach, R. P.; Haderlein, S. B., New evaluation scheme for two-dimensional isotope analysis to decipher biodegradation processes: Application to groundwater contamination by MTBE. *Environ. Sci. Technol.* **2005**, *39*, (18), 7344-7344.
- (10) Hofstetter, T. B.; Reddy, C. M.; Heraty, L. J.; Berg, M.; Sturchio, N. C., Carbon and chlorine isotope effects during abiotic reductive dechlorination of polychlorinated ethanes. *Environ. Sci. Technol.* **2007**, *41*, (13), 4662-4668.
- (11) Shouakar-Stash, O.; Frappe, S. K.; Drimmie, R. J., Stable hydrogen, carbon and chlorine isotope measurements of selected chlorinated organic solvents. *J. Contam. Hydrol.* **2003**, *60*, (3-4), 211-228.
- (12) Abe, Y.; Aravena, R.; Zopfi, J.; Shouakar-Stash, O.; Cox, E.; Roberts, J. D.; Hunkeler, D., Carbon and chlorine isotope fractionation during aerobic oxidation and reductive dechlorination of vinyl chloride and cis-1,2-dichloroethene. *Environ. Sci. Technol.* **2009**, *43*, (1), 101-107.
- (13) Vogt, C.; Cyrus, E.; Herklotz, I.; Schlosser, D.; Bahr, A.; Herrmann, S.; Richnow, H. H.; Fischer, A., Evaluation of toluene degradation pathways by two-dimensional stable isotope fractionation. *Environ. Sci. Technol.* **2008**, *42*, (21), 7793-7800.
- (14) Shouakar-Stash, O.; Drimmie, R. J.; Zhang, M.; Frappe, S. K. Compound-specific chlorine isotope ratios of TCE, PCE and DCE isomers by direct injection using CF-IRMS. *Appl. Geochem.* **2006**, *21*, 766-781.
- (15) Halas, S.; Pelc, A., New isotope ratio mass spectrometric method of precise  $\delta(37)\text{Cl}$  determinations. *Rapid Commun Mass Spectrom* **2009**, *23*, (7), 1061-4.
- (16) Holt, B. D.; Heraty, L. J.; Sturchio, N. C., Extraction of chlorinated aliphatic hydrocarbons from groundwater at micromolar concentrations for isotopic analysis of chlorine. *Environ. Pollution* **2001**, *113*, (3), 263-269.
- (17) Hoefs J.; Stable Isotope Geochemistry, 6th ed.; Springer: Berlin, Germany, **2009**.

- (18) Sakaguchi-Soder, K.; Jager, J.; Grund, H.; Matthaus, F.; Schuth, C., Monitoring and evaluation of dechlorination processes using compound-specific chlorine isotope analysis. *Rapid Commun. Mass Spectrom.* **2007**, *21*, (18), 3077-3084.
- (19) Elsner, M.; Hunkeler, D., Evaluating chlorine isotope effects from isotope ratios and mass spectra of polychlorinated molecules. *Anal. Chem.* **2008**, *80*, (12), 4731-4740.
- (20) Aeppli, C.; Holmstrand, H.; Adersson, P.; Gustafsson, Ö., Direct compound-specific stable chlorine isotope analysis of organic compounds with quadrupole GC/MS using standard isotope bracketing. *Anal. Chem.* **2010**, *82*, (1), 420-426 .
- (21) Eveleigh, L. J.; Ducauze, C. J., Optimization of the dwell-time for the quantitative analysis by gas chromatography mass spectrometry. *J. Chromatogr. A* **1997**, *765*, (2), 241-245.
- (22) Matthews, D. E.; Hayes, J. M., Systematic-errors in gas chromatography mass spectrometry isotope ratio measurement. *Anal. Chem.* **1976**, *48*, (9), 1375-1382.



## Chapter 3

### Integrated Carbon and Chlorine Isotope Modeling: Applications to Chlorinated Aliphatic Hydrocarbons Dechlorination<sup>2</sup>



<sup>2</sup> Modified from Jin, B., Haderlein, S.B., Rolle, M., 2013. Integrated carbon and chlorine isotope modeling: applications to chlorinated aliphatic hydrocarbons dechlorination. Environ. Sci. Technol. 47, 1443-1451. Copyright 2013 American Chemical Society.

## Abstract

We propose a self-consistent method to predict the evolution of carbon and chlorine isotope ratios during degradation of chlorinated hydrocarbons. The method treats explicitly the cleavage of isotopically different C-Cl bonds and thus considers, simultaneously, combined carbon-chlorine isotopologues. To illustrate the proposed modeling approach we focus on the reductive dehalogenation of chlorinated ethenes. We compare our method with the currently available approach, in which carbon and chlorine isotopologues are treated separately. The new approach provides an accurate description of dual-isotope effects regardless of the extent of the isotope fractionation and physical characteristics of the experimental system. We successfully applied the new approach to published experimental results on dehalogenation of chlorinated ethenes both in well-mixed systems and in situations where mass-transfer limitations control the overall rate of biodegradation. The advantages of our self-consistent dual isotope modeling approach proved to be most evident when isotope fractionation factors of carbon and chlorine differed significantly and for systems with mass-transfer limitations, where both physical and (bio)chemical transformation processes affect the observed isotopic values.

### 3.1 Introduction

Chlorinated aliphatic hydrocarbons (CAHs), such as chlorinated ethenes, are widespread organic contaminants of environmental concern due to their high toxicity [1, 2]. The identification and quantification of the transformation pathways of these compounds in the environment are essential to understand their fate and transport and to design effective management or remediation strategies of contaminated sites. Compound specific isotope analysis (CSIA) is a valuable tool to study microbial and abiotic transformation processes in environmental systems and has been increasingly applied over the past years [2-6]. CSIA relies on the fact that a normal kinetic isotope effect (i.e. light isotope reacts faster than the heavy one) typically occurs during transformation of organic contaminants, leading to enrichment of heavy isotopes in the remaining fraction [7]. Reductive dechlorination is the predominant transformation process of CAHs in anoxic environments, where these contaminants are dehalogenated sequentially into less chlorinated compounds. Carbon CSIA has been widely used to monitor dechlorination of CAHs in both laboratory systems and at contaminated sites [8-11]. Recent advances on on-line chlorine isotope analysis have facilitated an increasing number of applications of chlorine CSIA for CAHs [12-15]. A carbon–chlorine dual isotope approach is of great advantage for the study of CAHs degradation since it allows identifying different reaction mechanisms leading to contaminant transformation. The dual isotope approach focuses on the relationship between the carbon and chlorine isotope evolution and considerably advances a quantitative application of CSIA [16-18].

In many studies investigating the carbon isotopic behavior of chlorinated hydrocarbons in environmental systems [e.g., 8, 19, 20], the carbon isotopologue containing exclusively  $^{13}\text{C}$  is often neglected due to the low natural abundance of  $^{13}\text{C}$  (1.11%). Thus, for chlorinated ethenes, the analysis typically considers only a light ( $^{12}\text{C}$ - $^{12}\text{C}$ ) and a heavy ( $^{12}\text{C}$ - $^{13}\text{C}$ ) isotopologue. Instead, monitoring chlorine isotope ratios requires a more complex evaluation scheme due to the comparable natural abundances of both  $^{35}\text{Cl}$  (75.78%) and  $^{37}\text{Cl}$  (24.22%) [21]. Hofstetter et al. [17] proposed an evaluation method linking kinetic isotope effect (KIE) to the observed chlorine isotope signatures of CAHs. Elsner and Hunkeler [22] provided a theoretical basis to compute chlorine isotope ratios

according to the abundances of chlorine isotopologues of polychlorinated hydrocarbons, offering a new possibility to monitor chlorine isotope ratio shifts by tracking various chlorine isotopologues. Hunkeler et al. [23] developed a conceptual and mathematical framework to predict chlorine isotope fractionation of chlorinated organic compounds during reductive dechlorination processes. They proposed two approaches based on the evolution of chlorine isotopes and chlorine isotopologues, respectively. Recent contributions have further explored the practical application of CAHs dual carbon-chlorine isotope analysis in laboratory experiments [18], field investigations [24] and reactive transport simulations [25].

Since the additional diagnostic value of a dual isotope approach is increasingly recognized, it is of primary importance to provide accurate quantitative evaluation schemes capable of combining the isotopic evolution of different elements. To this end, the objective of this contribution is to propose a novel approach for a combined multi-element isotopic modeling. We focus on reductive dechlorination of CAHs with the specific goals of: i) illustrating a modeling approach which simultaneously and self-consistently integrates the carbon and chlorine isotope evolution, ii) comparing and validating the proposed method with the currently available isotopologue evaluation scheme [23], and iii) applying the proposed modeling approach to correctly and accurately simulate carbon and chlorine isotopic data observed in biodegradation experiments performed both in well-mixed systems and in the presence of mass-transfer limitations.

## **3.2 Mathematical Description and Modeling Approach**

### **3.2.1 Initial Relative Abundance of Carbon–Chlorine Isotopologues.**

We consider the simultaneous occurrence of stable carbon and chlorine isotopes and monitor the evolution of isotopic ratios of combined carbon–chlorine isotopologues during transformation processes. The initial relative abundances of the isotopologues are computed using a binomial distribution combining the occurrence of both C and Cl isotopes:

$$A_j = \binom{u}{v} \cdot P_{^{13}\text{C}}^v \cdot P_{^{12}\text{C}}^{u-v} \cdot \binom{h}{i} \cdot P_{^{37}\text{Cl}}^i \cdot P_{^{35}\text{Cl}}^{h-i} \quad (3.1)$$

where  $A_j$  is the relative abundance of an isotopologue  $j$  containing  $v$   $^{13}\text{C}$  out of total  $u$  carbon atoms and  $i$   $^{37}\text{Cl}$  out of total  $h$  chlorine atoms and  $P$  is the abundance of corresponding carbon and chlorine isotopes.

The number of isotopologues for a certain chlorinated compound depends on the composition of carbon and chlorine isotopes as well as on the number of chemically equivalent C-Cl bonds. For the compounds considered in this study, trichloroethene (TCE), cis-dichloroethene (cis-DCE) and vinyl chloride (VC), the isotopologues considered and their computed abundances are listed in the Supporting Information. For instance, the isotopic composition of cis-DCE requires the specification of nine carbon–chlorine isotopologues, whose relative abundance can be computed using eq 3.1 (Supporting Information (S2), Table S2.2). More complex is the C-Cl isotopic description of TCE in which not all C-Cl bonds are chemically equivalent (i.e, the cleavage of different bonds leads to the formation of different products). In this case the isotopologue abundance can be calculated considering all possible combinations of C and Cl isotopic composition for each reacting C-Cl bond:

$$A_j = P_{^{13}\text{C}}^v \cdot P_{^{12}\text{C}}^{u-v} \cdot P_{^{37}\text{Cl}}^i \cdot P_{^{35}\text{Cl}}^{h-i} \quad (3.2)$$

A number of 32 isotopologues are, therefore, necessary to completely describe the C and Cl isotopic composition of TCE (see Supporting Information for further details and the isotopologues list provided in Table S2.3).

### 3.2.2 Apparent Kinetic Isotope Effect during Cleavage of C-Cl Bonds

Isotopologues of a certain chlorinated hydrocarbon, R-C-Cl, may include four isotopic different C-Cl bonds:  $^{12}\text{C}-^{35}\text{Cl}$ ,  $^{13}\text{C}-^{35}\text{Cl}$ ,  $^{12}\text{C}-^{37}\text{Cl}$ , and  $^{13}\text{C}-^{37}\text{Cl}$ , respectively. Assuming first-order kinetics, the reaction rate during cleavage of a specific isotopic C-Cl bond are:

$$r_{^{12}\text{C}-^{35}\text{Cl}} = k_{^{12}\text{C}-^{35}\text{Cl}} \cdot C_j \cdot \frac{a-b}{a} \cdot \frac{c-d}{c} \quad (3.3)$$

$$r_{^{13}\text{C}-^{35}\text{Cl}} = k_{^{13}\text{C}-^{35}\text{Cl}} \cdot C_j \cdot \frac{b}{a} \cdot \frac{c-d}{c} \quad (3.4)$$

$$r_{^{12}\text{C}-^{37}\text{Cl}} = k_{^{12}\text{C}-^{37}\text{Cl}} \cdot C_j \cdot \frac{a-b}{a} \cdot \frac{d}{c} \quad (3.5)$$

$$r_{^{13}\text{C}-^{37}\text{Cl}} = k_{^{13}\text{C}-^{37}\text{Cl}} \cdot C_j \cdot \frac{b}{a} \cdot \frac{d}{c} \quad (3.6)$$

where  $r$  is the bond-specific reaction rate during cleavage of a certain isotopic C-Cl bond of an isotopologue  $j$ ,  $k$  is C-Cl bond-specific reaction rate constant,  $C_j$  is the concentration of the  $j^{\text{th}}$  isotopologue,  $a$  is the number of carbon atoms at reactive position,  $b$  is the number of  $^{13}\text{C}$  in reactive position;  $c$  is the number of chlorine atoms at reactive position and  $d$  is the number of  $^{37}\text{Cl}$  at reactive position.

According to the rule of the geometric mean [5, 7], the carbon isotope discrimination between  $^{13}\text{C}$  and  $^{12}\text{C}$  is the same for a C- $^{35}\text{Cl}$  and a C- $^{37}\text{Cl}$  bond and this also holds for  $^{35}\text{Cl}$  and  $^{37}\text{Cl}$  considering the bonds  $^{12}\text{C}-\text{Cl}$  and  $^{13}\text{C}-\text{Cl}$ . Therefore, neglecting secondary isotope effects, apparent kinetic isotope effects (AKIEs) during the cleavage of the different C-Cl bonds can be described as:

$$\frac{k_{^{13}\text{C}-^{35}\text{Cl}}}{k_{^{12}\text{C}-^{35}\text{Cl}}} = \frac{\frac{d[R-^{13}\text{C}-^{35}\text{Cl}]}{dt}}{\frac{d[R-^{12}\text{C}-^{35}\text{Cl}]}{dt}} \cdot \frac{[R-^{12}\text{C}-^{35}\text{Cl}]}{[R-^{13}\text{C}-^{35}\text{Cl}]} = \frac{1}{AKIE_C} = \alpha_{C,rp} \quad (3.7)$$

$$\frac{k_{^{13}\text{C}-^{37}\text{Cl}}}{k_{^{12}\text{C}-^{37}\text{Cl}}} = \frac{\frac{d[R-^{13}\text{C}-^{37}\text{Cl}]}{dt}}{\frac{d[R-^{12}\text{C}-^{37}\text{Cl}]}{dt}} \cdot \frac{[R-^{12}\text{C}-^{37}\text{Cl}]}{[R-^{13}\text{C}-^{37}\text{Cl}]} = \frac{1}{AKIE_C} = \alpha_{C,rp} \quad (3.8)$$

Similarly, we can derive:

$$\frac{k_{12\text{C-}^{37}\text{Cl}}}{k_{12\text{C-}^{35}\text{Cl}}} = \frac{k_{13\text{C-}^{37}\text{Cl}}}{k_{13\text{C-}^{35}\text{Cl}}} = \frac{1}{AKIE_{Cl}} = \alpha_{Cl,rp} \quad (3.9)$$

Combining eq 3.7 and eq 3.9 leads to:

$$\frac{k_{13\text{C-}^{37}\text{Cl}}}{k_{12\text{C-}^{35}\text{Cl}}} = \frac{1}{AKIE_C} \cdot \frac{1}{AKIE_{Cl}} = \alpha_{C,rp} \cdot \alpha_{Cl,rp} \quad (3.10)$$

$AKIE_C$  and  $AKIE_{Cl}$  are the kinetic isotope effects, and  $\alpha_{C,rp}$  and  $\alpha_{Cl,rp}$  are fractionation factors on reactive position. They are related to the bulk isotope enrichment factors by [5]:

$$AKIE \approx \frac{1}{1 + n/x \cdot \varepsilon_{bulk}} \quad (3.11)$$

$$\alpha_{rp} = \frac{1}{AKIE} \quad (3.12)$$

where  $n$  is the number of atoms of the element considered,  $x$  is the number of the atoms of the element located at the reactive position,  $\varepsilon_{bulk}$  is the bulk enrichment factor,  $\alpha_{rp}$  is the fractionation factor on the reactive position. Our approach directly tracks the breaking of carbon and chlorine bonds and considers combined carbon-chlorine isotopologues. Therefore, only one rate constant is required which can be derived from the specific rate constants of various isotopically different C-Cl bonds:

$$k_i = k_{12\text{C-}^{35}\text{Cl}} \cdot F_{12\text{C-}^{35}\text{Cl}} + k_{12\text{C-}^{37}\text{Cl}} \cdot F_{12\text{C-}^{37}\text{Cl}} + k_{13\text{C-}^{35}\text{Cl}} \cdot F_{13\text{C-}^{35}\text{Cl}} + k_{13\text{C-}^{37}\text{Cl}} \cdot F_{13\text{C-}^{37}\text{Cl}} \quad (3.13)$$

where  $k_i$  is the overall rate constant,  $k_{C-Cl}$  is the bond specific rate constant (see eqs 3.3-3.6), and  $F$  is the probability that a certain C-Cl bond is at a reactive position.

In the following we briefly illustrate the differences between our integrated method (IM) and the currently available method (CM) for interpretation of C and Cl dual isotope data described in [23]. In the latter, carbon and chlorine isotopologues are described separately and the two element-specific rate constants are expressed as:

$${}^C k_i = {}^{12C}k \cdot {}^{12Cl}F + {}^{13C}k \cdot {}^{13Cl}F \quad (3.14)$$

$${}^{Cl} k_i = {}^{35Cl}k \cdot {}^{35Cl}F + {}^{37Cl}k \cdot {}^{37Cl}F \quad (3.15)$$

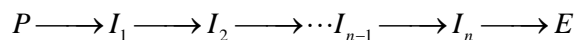
where  ${}^C k_i$  is the overall constant for carbon isotopologues,  ${}^{Cl} k_i$  is the overall rate constant for chlorine isotopologues,  ${}^{12C}k$ ,  ${}^{13C}k$ ,  ${}^{35Cl}k$  and  ${}^{37Cl}k$ , are the isotope specific rate constants,  $F$  is the probability that a certain carbon or chlorine isotope is at a reactive position. During the course of the reaction, the overall rate constants for the carbon and chlorine systems tend to differ implying an independent evolution of the two systems. We quantify the discrepancy with the ratio,  $\eta$  [-], between the remaining fractions of total carbon and chlorine isotopologues:

$$\eta = \frac{f_{C,t}}{f_{Cl,t}} \quad (3.16)$$

where  $f_{C,t}$  and  $f_{Cl,t}$  [-] are the remaining fraction of chlorinated compound's carbon and chlorine isotopologues at time  $t$ , respectively. The overall rate constants  ${}^C k_i$  and  ${}^{Cl} k_i$  do not change correspondingly as the reaction progresses and result in different extent of degradation. Therefore, deviations of  $\eta$  from unity are obtained using different  $\varepsilon_C$  and  $\varepsilon_{Cl}$  values.

### 3.2.3 Modeling Contaminant Transformation and Carbon-Chlorine Isotopic Evolution

The evolution of carbon and chlorine isotope ratios during CAHs transformation are simulated by tracking the transformation of all the carbon–chlorine isotopologues, using bond-specific reaction rates as defined in the previous section. Considering a sequential degradation pathway, such as reductive dechlorination, the reaction proceeds from the parent compound to the final end product through a series of intermediate species:





Concentration changes of a certain isotopologue  $j$  of the precursor (P), the intermediate compounds (I), or the end product (E) can be described by a coupled system of ordinary differential equations:

$$\frac{d[{}^j\text{P}]}{dt} = -\sum_{k=1}^m r_k^j \quad (3.17)$$

$$\frac{d[{}^j\text{I}_n]}{dt} = +\sum_{k=1}^m l_{n-1} r_k^j - \sum_{k=1}^m l_n r_k^j \quad (3.18)$$

$$\frac{d[{}^j\text{E}]}{dt} = +\sum_{k=1}^m l_n r_k^j \quad (3.19)$$

where  $r$  is the bond specific reaction rate (see eqs 3.3-3.6),  $m$  ( $1 \leq m \leq 4$ ) is the total number of possible different isotopic bonds on the reactive position of an isotopologue  $j$ .

Focusing on reductive dechlorination of chlorinated ethenes, we solved the system of differential equations using Matlab. The calculated isotopologues' concentrations can be used to compute carbon and chlorine isotope ratios following the procedure we have recently proposed to determine chlorine isotope ratios using all fragment ions in GC-qMS measurements ("Complete Ion Method" in Jin et al. [14]). Thus, the carbon and chlorine isotope ratios can be expressed as:

$$R_C = \frac{\text{Tot}({}^{13}\text{C})}{\text{Tot}({}^{12}\text{C})} = \frac{\sum_{j=1}^t v \cdot C_j}{\sum_{j=1}^t (u - v) \cdot C_j} \quad (3.20)$$

$$R_{Cl} = \frac{\text{Tot}({}^{37}\text{Cl})}{\text{Tot}({}^{35}\text{Cl})} = \frac{\sum_{j=1}^t i \cdot C_j}{\sum_{j=1}^t (h - i) \cdot C_j} \quad (3.21)$$

where  $R_C$  and  $R_{Cl}$  are the carbon and chlorine isotope ratios,  $Tot(^{12}C, ^{13}C, ^{35}Cl, \text{ or } ^{37}Cl)$  is the total concentration of a certain isotope,  $C_j$  is the concentration of the  $j^{\text{th}}$  isotopologue, and  $u, v, h$  and  $i$  are the number of C and Cl isotopes as defined in eq 3.1.

To illustrate our modeling approach we select different examples of CAHs degradation and we simulate the evolution of C and Cl isotope ratios in both well-mixed systems and in the presence of mass-transfer limitations.

### 3.3 Results and Discussion

#### 3.3.1 Biodegradation in Well-Mixed Systems

As first application of our modeling framework we consider a hypothetical batch system where reductive dechlorination of TCE occurs either as one-step process (TCE  $\rightarrow$  cis-DCE) or as multi-step sequential reaction to the final product ethene. These examples are selected to compare our integrated modeling approach (IM), allowing simultaneous simulation of C and Cl isotope ratios, with the current method (CM), in which carbon and chlorine isotopologues are simulated separately [23].

The reactions take place in anaerobic, well-mixed batch reactors ( $V=250$  mL) where TCE with an initial concentration of  $380 \mu\text{M}$  is degraded following a first-order kinetics ( $k=0.07 \text{ day}^{-1}$ ). A typical bulk enrichment factor for carbon,  $\varepsilon_{C,TCE}=-20\%$  (from reference [5]) was selected from a range of reported values, whereas for chlorine experimental values are scarce, and we adopted  $\varepsilon_{Cl,TCE}=-4\%$ , which is within the range observed in [26]. The results of the simulations of the one-step reaction system are reported in the dual isotope plot of Fig. 3.1, panel A1. Both  $\delta^{37}Cl$  and  $\delta^{13}C$  values of the reactant (TCE) increase during the course of the reaction (i.e, cleavage of C-Cl bonds) since light carbon isotopes preferentially react and are transferred to the dehalogenated product and light chlorine isotopes are released preferentially from TCE. The line representing cis-DCE is horizontal since in this one-step reaction the  $\delta^{13}C$  starts from the initial value of  $\varepsilon_{C,DCE}$  ( $-18.5\%$ , from [18]) and approaches a value of  $0\%$  (i.e., complete conversion of the parent compound), whereas the  $\delta^{37}Cl$  value remains the same as the original chlorine isotope signature of TCE. At early reaction times the slope of the TCE line in the dual isotope

plot can be approximated as the ratio between bulk chlorine and carbon enrichment factors [23]:

$$\frac{\Delta\delta^{37}\text{Cl}}{\Delta\delta^{13}\text{C}} = \frac{\varepsilon_{\text{Cl}} \times (\delta^{37}\text{Cl} + 1)}{\varepsilon_{\text{C}} \times (\delta^{13}\text{C} + 1)} \approx \frac{\varepsilon_{\text{Cl}}}{\varepsilon_{\text{C}}} \quad (3.22)$$

where  $\Delta\delta^{13}\text{C}$  and  $\Delta\delta^{37}\text{Cl}$  are the incremental changes in carbon and chlorine isotope values,  $\varepsilon_{\text{Cl}}$  and  $\varepsilon_{\text{C}}$  are the bulk carbon and chlorine enrichment factors, respectively.

At late reaction times the slope deviates from the constant value (blue dotted line) because of the increasing difference between the  $\delta^{13}\text{C}$  and  $\delta^{37}\text{Cl}$  values. Both modeling approaches (IM and CM) produce a linear relation at early times and predict the deviation from the linear behavior as the degradation reaction proceeds. However, the extent of the deviation from a linear trend is different for IM and CM. This is caused by the different approaches and formulations of the two dual-isotope models. CM simulates the variation of concentration of carbon and chlorine isotopologues separately, which means solving twice the governing differential equations, independently for the C and Cl systems. In such a way, independent changes of the reaction rate constants (eqs 3.14 and 3.15) are introduced which cause the TCE carbon isotopologues to be consumed more rapidly than the TCE chlorine isotopologues. Thus, the  $\delta^{37}\text{Cl}$  and  $\delta^{13}\text{C}$  are not correspondingly computed at each time step. This can be avoided applying the IM presented in this study since all carbon-chlorine isotopologues are tracked simultaneously. The two different methods (i.e., CM and IM) result in differences in the slopes for TCE in the dual isotope plot. The differences increase as the reaction progresses. In the base case scenario (Fig. 3.1, plot A1) the discrepancies for both C and Cl at the end of the simulation (~90% of the initial mass degraded) are  $\delta^{13}\text{C}=10.4\text{‰}$  and  $\delta^{37}\text{Cl}=1.7\text{‰}$ , respectively. Such differences are significant and well above the analytical precision for both C and Cl isotope ratios. The one-step reaction simulations were repeated varying the ratio between bulk C and Cl TCE enrichment factors by one order of magnitude. The results for the increased ( $\varepsilon_{\text{C},\text{TCE}}=-20\text{‰}$  and  $\varepsilon_{\text{Cl},\text{TCE}}=-0.4\text{‰}$ ) and the decreased ratios ( $\varepsilon_{\text{C},\text{TCE}}=-2\text{‰}$  and  $\varepsilon_{\text{Cl},\text{TCE}}=-4\text{‰}$ ) are reported in Fig. 3.1, A2 and A3, respectively. An increased difference between C and Cl enrichment factors resulted in a larger deviation from a linear relation in the TCE dual isotope plot. Conversely, linear trends and insignificant difference (<

0.1‰) between the two modeling approaches are obtained when selecting similar enrichment factors for C and Cl.

The same procedure with three different scenarios has been applied for the multi-step sequential reaction. The results for the base-case scenario are reported in Fig. 3.1, panel B1. It can be noticed that the cis-DCE and VC lines start at the initial values of  $\epsilon_{C,cisDCE} = -18.5\text{‰}$ ,  $\epsilon_{Cl,cisDCE} = -1.5\text{‰}$  [18] and show a positive slope since these intermediate products undergo further degradation with successive cleavage of C-Cl bonds. The trend of TCE is the same as observed for the one-step reaction with deviation from a linear relation at later reaction times. The simulations have been repeated changing the ratio of carbon and chlorine enrichment factors (Fig. 3.1, B2 and B3) as for the one-step case.

These scenario simulations for the one-step and sequential TCE degradation show an overall good agreement between the CM and IM modeling approaches. The match becomes nearly perfect at early reaction times and when similar C and Cl bulk enrichment factors are considered. The IM method proposed in this study allows improving the dual isotope description at late reaction time and for large differences in the  $\epsilon_C$  and  $\epsilon_{Cl}$  values.

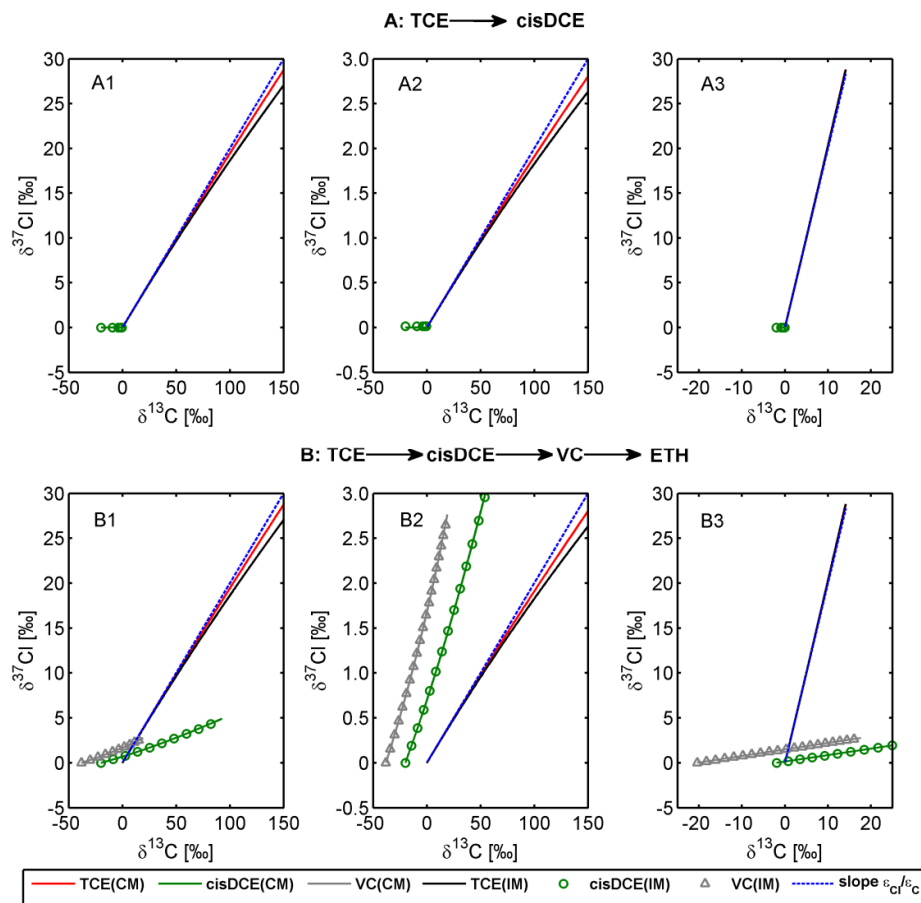


**Figure 3.1.** Carbon-chlorine dual isotope plots during one-step (A) and sequential (B) dechlorination reactions. A1 and B1:  $\epsilon_{C,TCE}=-20\text{‰}$ ,  $\epsilon_{Cl,TCE}=-4\text{‰}$ ; A2 and B2:  $\epsilon_{C,TCE}=-20\text{‰}$ ,  $\epsilon_{Cl,TCE}=-0.4\text{‰}$ ; A3 and B3:  $\epsilon_{C,TCE}=-2\text{‰}$ ,  $\epsilon_{Cl,TCE}=-4\text{‰}$ ;  $\epsilon_{C,cisDCE}=-18.5\text{‰}$ ,  $\epsilon_{Cl,cisDCE}=-1.5\text{‰}$ ;  $\epsilon_{C,VC}=-25.2\text{‰}$ ,  $\epsilon_{Cl,VC}=-1.8\text{‰}$  (the values for cis-DCE and VC are the same as reported in [18]).

A further quantitative comparison of the approaches can be obtained by computing and plotting the discrepancy ratio  $\eta$  (eq 3.16) between the remaining fractions of total carbon and total chlorine isotopologues computed using CM. As described above, with the CM approach the  $\delta^{37}Cl$  and  $\delta^{13}C$  are not computed correspondingly at each time step, thus introducing a systematic bias which increases during the course of the reaction. Fig. 3.2 shows the computed  $\eta$  values with the CM for the three sets of enrichment factors considered previously in the TCE degradation scenarios (Fig. 3.1, A1-A3). The results show that the inconsistency (i.e., deviation from unity) is more significant for larger differences between  $\epsilon_C$  and  $\epsilon_{Cl}$ . Such discrepancy is not a concern using the proposed integrated method. In fact, the IM approach directly tracks the breaking of C-Cl bonds

and remains unbiased also at late reaction times, thus allowing a more accurate description of degradation processes.

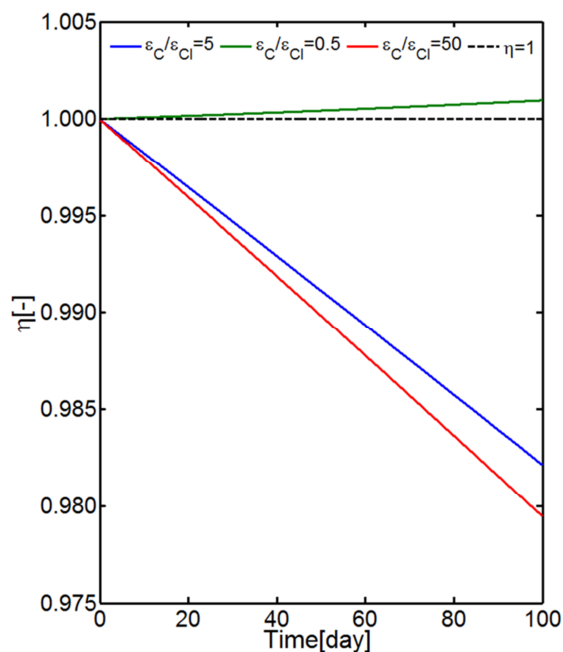


**Figure 3.2.** Discrepancy in the computation of the remaining fractions of TCE carbon and chlorine isotopologues using CM.

To validate our modeling approach with experimental data, we refer to the work of Abe et al. [18]. In that study, aerobic and anaerobic degradation of cis-DCE and VC were investigated in laboratory microcosms. The evolution of both carbon and chlorine isotope ratios was followed by measuring C and Cl stable isotopes of cis-DCE and VC. Details on the approach are provided in the Supporting Information, where Fig. S2.2 shows the comparison between the experimental data and the simulations using CM and IM. Both methods can capture the observed dual isotope behavior for cis-DCE and VC, since the measured C and Cl isotope ratios are mostly in the range where the dual isotope relation can be well approximated with a constant slope given by the ratio of the bulk chlorine and carbon enrichment factors. As observed in the scenarios described above (Fig. 3.1), the discrepancies between the two methods become significant at late reaction times. At the end of the simulation the differences are  $\delta^{13}C=9.8\text{‰}$  and  $\delta^{37}Cl=1.0\text{‰}$  for VC and  $\delta^{13}C=7.2\text{‰}$  and  $\delta^{37}Cl=0.2\text{‰}$  for cis-DCE.

### 3.3.2 Biodegradation in Mass-Transfer Limited Systems

An increasing number of recent experimental and modeling studies have pointed out the influence of mass-transfer effects on the observed isotope fractionation of organic contaminants (20, 28-34). Therefore, it is important to provide modeling tools allowing the interpretation of observed isotopic signatures when both physical mass-transfer processes and (bio)chemical transformations occur. To this end, we illustrate the capability of the proposed integrated C-Cl modeling approach to correctly simulate the dual isotope evolution when biodegradation is limited by mass-transfer processes. We consider the experimental setup investigated by Aeppli et al. [20], where reductive dechlorination of TCE was limited by the kinetics of interphase mass transfer. The authors performed microcosm experiments in both a three-phase system (tetradecane containing 50 mM TCE + aqueous phase + gas phase containing the electron donor H<sub>2</sub>) and a two-phase system (gas and aqueous phases). In our modeling study we focus the attention on the three-phase system in which TCE mass transfer between the organic and the aqueous phase limited the biodegradation activity and caused a masking of the observed kinetic isotope effects. In the experiments only carbon isotopes were measured, whereas in our simulations we consider both C and Cl to evaluate the potential of dual isotope monitoring in such a complex, mass-transfer limited system. We perform the simulations using both the current method (CM) and our newly proposed integrated method (IM). The governing equations describing the evolution of the species concentrations are the same as reported by Aeppli et al. (eqs 3.2-3.8 in [20]) and include a double-Monod reaction kinetics for the degradation of the chlorinated compounds using H<sub>2</sub> as electron donor and linear driving force terms to represent the interphase mass-transfer. However, the implementation and solution of the system of equations is different since we use an isotopologue-based approach and we track simultaneously the evolution of each isotopologue. For instance, using the IM method, the governing equation describing TCE degradation in the aqueous phase and the mass-transfer from the organic phase can be written as:

$$\frac{d [{}^jTCE]_{aq}}{dt} = - \sum_{k=1}^m r_k^j + \kappa_{TCE}^{org-aq} \cdot a_0^{aq} \cdot ([{}^jTCE]_{aq}^{eq} - [{}^jTCE]_{aq}) \quad (3.23)$$

where  $j$  indicates each of the 32 carbon-chlorine TCE isotopologues (Table S2.3 Supporting Information (S2)),  $r_k^j$  is the bond-specific reaction rate,  $\kappa_{TCE}^{org-aq}$  is the mass-transfer coefficient which is considered the same for each isotopologue, and  $a_0^{aq}$  is the interface area per unit volume of the aqueous phase. The detailed system of equations solved and the list of the kinetic parameters given in [20] and used in our simulations are provided in the Supporting Information (eqs S2.2-S2.12 and Table S2.4).

The results of the simulations are shown in Fig. 3.3 for both the current method (CM) and the integrated method (IM). Both approaches give satisfying results in reproducing the evolution of TCE and cis-DCE concentrations observed in the aqueous phase (panels A1 and B1), whereas remarkable differences can be noticed in the simulation of the isotopic behavior. In particular concerning the carbon signature, a lower final  $\delta^{13}C$  value of TCE ( $\sim 0\text{‰}$ ) was achieved using CM (panel A2) compared to about  $40\text{‰}$  using IM (panel B2). The results using the IM approach allow capturing the observed  $\delta^{13}C$  values of TCE, while the CM method underestimates the experimental observations. Nearly identical results for the two modeling approaches were obtained when considering the chlorine isotopic signature. This different behavior causes the major differences between the two simulation methods that can be observed in the dual isotope plots (panels A4 and B4). The results of CM show that the slope changes considerably, whereas a linear trend is obtained when using the integrated method. These differences stem from the fact that using CM the carbon isotopologues of TCE are consumed more rapidly than the chlorine isotopologues. This effect was already observed in a well-mixed system (Fig. 3.1), but here it is magnified by the mass-transfer limitation. In fact, when mass-transfer limits the overall degradation, the observable isotope fractionation is masked since the reactive process results in less discrimination between light and heavy isotopes. As a consequence, an increase in the amount of heavy isotopes consumed by the reaction causes the overall rate constant to change (see Fig. 3.2). Due to the substantial difference in the natural abundances of C and Cl heavy isotopes, the masking effect is more pronounced for the  $\delta^{13}C$  values. Therefore, applying an isotopologue modeling approach separating between C and Cl results in a distinct evolution of the C and Cl systems and, ultimately, in non-linear dual isotope plots. This shortcoming can be avoided using the integrated method (IM) which does not produce artificial differences on the overall rate constants and results in linear  $\delta^{37}Cl$  vs.  $\delta^{13}C$  plots such as the one shown in Fig. 3.3, panel B4. Therefore, this



method yields a correct description of the expected behavior in a dual isotope plot and is ideally suited to quantitatively reproduce the results of dual C and Cl isotope analysis even in the presence of mass-transfer limitations.

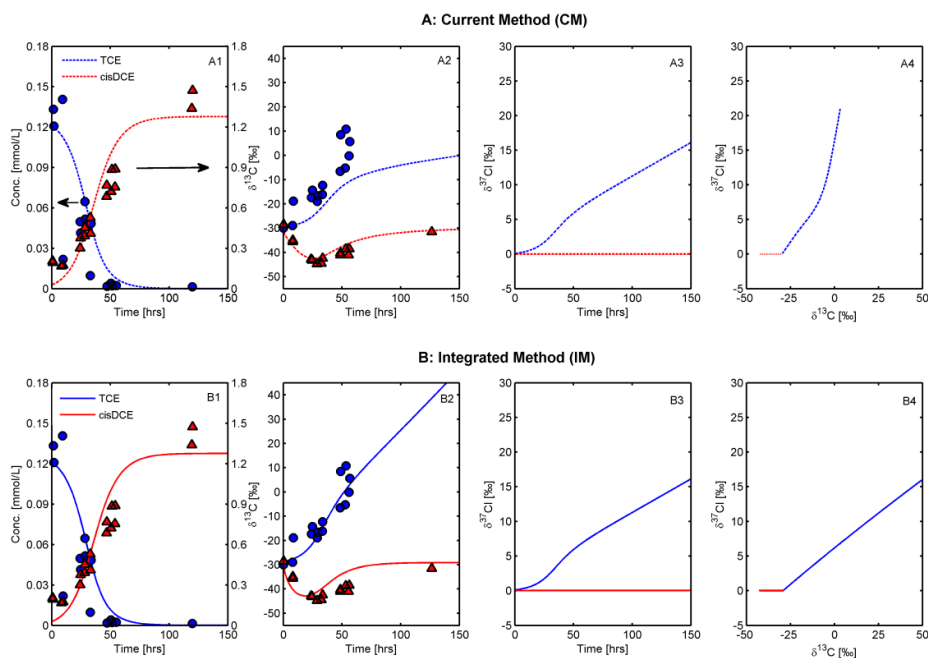


**Figure 3.3.** Changes of aqueous concentration and carbon and chlorine isotope signatures during dechlorination of TCE to cis-DCE in the aqueous phase of the three-phase system (i.e. gas-organic-aqueous). Dotted lines in Panel A are the results using CM, solid lines in Panel B are the results using IM, blue circles and red triangles are the experimental data for TCE and cis-DCE reported in Aeppli et al. [20]. The kinetic parameters and the simulation results for the organic phase and the total system are available in the Supporting Information (Table S2.4 and Figure S2.3).

To further illustrate the potential of the presented IM approach we consider a scenario where a mass-transfer limited step is followed either by aerobic or anaerobic degradation. We consider the setup of the previous application for mass-transfer limited biodegradation of TCE. Besides anaerobic reductive dechlorination we allow TCE undergoing an aerobic degradation pathway and we use dual isotope analysis to detect the actual degradation mechanism. For anaerobic degradation we consider the formulation described above, whereas under oxic conditions we allow TCE degradation through an aerobic cometabolic pathway and we select the enrichment factors  $\epsilon_{C,TCE} = -20\text{‰}$  from [35] and  $\epsilon_{Cl,TCE} = -1\text{‰}$ . We performed the simulations of aerobic and anaerobic TCE

degradation in both well-mixed and mass-transfer limited systems. The results using the CM and IM approaches are reported in Fig.3.4. It can be noticed that, in agreement to the applications described in the previous section, CM and IM give similar results in well-mixed systems with differences that become significant only at late reaction times. Under such conditions both methods allow identifying the reaction mechanism and to clearly discern between aerobic and anaerobic degradation. Completely different is the outcome in the mass-transfer limited setup. In fact, under such conditions the bias of CM is magnified and the outcomes show a variable slope in the dual isotope plot (Fig. 3.4, A2). For instance, the computed slope for aerobic degradation covers a range which overlaps the one characteristic of the anaerobic process. Therefore, under such conditions, by applying CM it is not possible to reliably evaluate the isotopic data and to identify the underlying degradation mechanism. Using the proposed, integrated and unbiased approach (IM) we can accurately “de-mask” the effect of mass-transfer limitations. The lines in panel B2 agree perfectly with the outcomes under well-mixed conditions. The integrated method allows a meaningful evaluation of the dual isotope data. Thus, such modeling approach allows one to fully take advantage of the potential of dual isotope analysis to identify, elucidate and quantify environmental transformation processes even in complex mass-transfer limited systems.

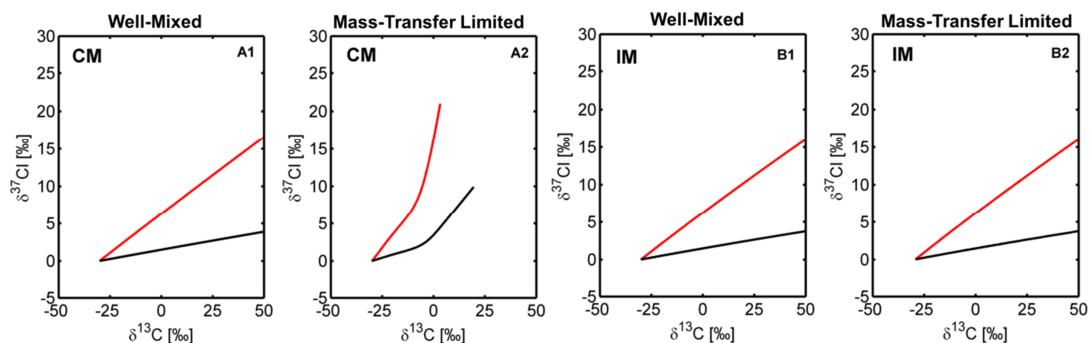


**Figure 3.4.** Simulated TCE carbon and chlorine isotope ratios using CM and IM in well-mixed (A1 and B1) and mass-transfer limited systems (A2 and B2). The red and black lines indicate reductive dechlorination and aerobic degradation, respectively.

## Implications for Environmental Applications

There has been increasing interest in the dual carbon and chlorine isotope approach, since it improves the understanding of the reaction mechanisms of chlorinated organic contaminants degradation. Recent advances have covered analytical techniques, in particular the on-line measurement of chlorine stable isotopes, as well as laboratory and field applications. In this contribution, we propose a modeling approach which represents a suitable framework for the quantitative interpretation of dual C and Cl isotope data. In fact, our approach naturally integrates carbon and chlorine isotope modeling schemes by considering the simultaneous evolution of all carbon-chlorine isotopologues. The three different applications shown in this study demonstrate the validity and the potential of the proposed modeling approach. Particularly promising are the outcomes of the simulations of the mass-transfer limited biodegradation example which demonstrate the capability of the method to correctly “de-mask” the effects of interphase mass-transfer. Mass-transfer limitations in environmental processes occur at a variety of scales and in different natural and engineered systems and should be taken into account when evaluating isotope data [34]. For instance, our method could be applied in reactive transport models of contaminant fate in groundwater systems, where mass-transfer limitations are extremely common and are often found to limit the overall contaminant degradation.

In this study we have focused exclusively on carbon and chlorine stable isotopes, but the proposed framework is versatile and can be applied to any dual-element isotope analysis (36-38) of reactive processes where the cleavage of a certain bond involves simultaneous isotope fractionation of both elements.

## Supporting Information Available

Additional material includes initial abundances of carbon-chlorine isotopologues, validation of the proposed approach with data from a well-mixed experimental setup, the governing equations and the kinetic parameters used in the mass-transfer limited TCE biodegradation example. For the latter application, also the simulation outcomes for the organic phase and the total system are provided.

## References

- (1) Wiedemeier, T. H.; Rifai H. S.; Newell, C. J.; Wilson, J. T.; Natural Attenuation of Fuels and Chlorinated Solvents in the Subsurface; John Wiley & Sons: NY, USA, **1999**.
- (2) Hunkeler, D., Meckenstock, R.U., Sherwood-Lollar, B., Schmidt, T., Wilson, J.T.; A Guide for Assessing Biodegradation and Source Identification of Organic Groundwater Contaminants using Compound Specific Isotope Analysis (CSIA). US Environmental Protection Agency (EPA) EPA 600/R-08/148, **2008**.
- (3) Meckenstock, R. U.; Morasch, B.; Griebler, C.; Richnow, H. H., Stable isotope fractionation analysis as a tool to monitor biodegradation in contaminated aquifers. *J. Contam. Hydrol.* **2004**, *75*, (3-4), 215-255.
- (4) Schmidt, T. C.; Zwank, L.; Elsner, M.; Berg, M.; Meckenstock, R. U.; Haderlein, S. B., Compound-specific stable isotope analysis of organic contaminants in natural environments: a critical review of the state of the art, prospects, and future challenges. *Analytical and Bioanalytical Chemistry* **2004**, *378*, (2), 283-300.
- (5) Elsner, M.; Zwank, L.; Hunkeler, D.; Schwarzenbach, R. P., A new concept linking observable stable isotope fractionation to transformation pathways of organic pollutants. *Environ. Sci. Technol.* **2005**, *39*, (18), 6896-6916.
- (6) Hofstetter, T. B.; Schwarzenbach, R. P.; Bernasconi, S. M., Assessing transformation processes of organic compounds using stable isotope fractionation. *Environ. Sci. Technol.* **2008**, *42*, (21), 7737-7743.
- (7) Cook, P. F.; *Enzyme Mechanism from Isotope Effects*; CRC Press, Boca Raton, FL, U.S., **1991**, pp 3-69.
- (8) Hunkeler, D.; Aravena, R.; Cox, E., Carbon isotopes as a tool to evaluate the origin and fate of vinyl chloride: Laboratory experiments and modeling of isotope evolution. *Environ. Sci. Technol.* **2002**, *36*, (15), 3378-3384.
- (9) Slater, G. F.; Lollar, B. S.; Lesage, S.; Brown, S., Carbon isotope fractionation of PCE and TCE during dechlorination by vitamin B12. *Ground Water Monit. Remediat.* **2003**, *23*, (4), 59-67.
- (10) Blessing, M.; Schmidt, T. C.; Dinkel, R.; Haderlein, S. B., Delineation of multiple chlorinated ethene sources in an industrialized area - A forensic field study using compound-specific isotope analysis. *Environ. Sci. Technol.* **2009**, *43*, (8), 2701-2707.
- (11) Aeppli, C.; Hofstetter, T. B.; Amaral, H. I. F.; Kipfer, R.; Schwarzenbach, R. P.; Berg, M., Quantifying In Situ Transformation Rates of Chlorinated Ethenes by Combining Compound-Specific Stable Isotope Analysis, Groundwater Dating, And Carbon Isotope Mass Balances. *Environ. Sci. Technol.* **2010**, *44*, (10), 3705-3711.
- (12) Sakaguchi-Soder, K.; Jager, J.; Grund, H.; Matthaus, F.; Schuth, C., Monitoring and evaluation of dechlorination processes using compound-specific chlorine isotope analysis. *Rapid Commun. Mass Spectrom.* **2007**, *21*, (18), 3077-3084.
- (13) Aeppli, C.; Holmstrand, H.; Adersson, P.; Gustafsson, Ö., Direct compound-specific stable chlorine isotope analysis of organic compounds with quadrupole GC/MS using standard isotope bracketing. *Anal. Chem.* **2010**, *82*, (1), 420-426 .
- (14) Jin, B. A.; Laskov, C.; Rolle, M.; Haderlein, S. B., Chlorine Isotope Analysis of Organic Contaminants Using GC-qMS: Method Optimization and Comparison of Different Evaluation Schemes. *Environ. Sci. Technol.* **2011**, *45*, (12), 5279-5286.
- (15) Bernstein, A.; Shouakar-Stash, O.; Ebert, K.; Laskov, C.; Hunkeler, D.; Jeannotat, S.; Sakaguchi-Soder, K.; Laaks, J.; Jochmann, M. A.; Cretnik, S.; Jager, J.; Haderlein, S. B.; Schmidt, T. C.; Aravena, R.; Elsner, M., Compound-Specific Chlorine Isotope Analysis: A Comparison of Gas Chromatography/Isotope Ratio Mass Spectrometry and Gas Chromatography/Quadrupole Mass Spectrometry Methods in an Interlaboratory Study. *Anal. Chem.* **2011**, *83*, (20), 7624-7634.
- (16) Heraty, L. J.; Fuller, M. E.; Huang, L.; Abrajano, T.; Sturchio, N. C., Isotopic fractionation of carbon and chlorine by microbial degradation of dichloromethane. *Org.*

- Geochem.* **1999**, *30*, (8A), 793-799.
- (17) Hofstetter, T. B.; Reddy, C. M.; Heraty, L. J.; Berg, M.; Sturchio, N. C., Carbon and chlorine isotope effects during abiotic reductive dechlorination of polychlorinated ethanes. *Environ. Sci. Technol.* **2007**, *41*, (13), 4662-4668.
- (18) Abe, Y.; Aravena, R.; Zopfi, J.; Shouakar-Stash, O.; Cox, E.; Roberts, J. D.; Hunkeler, D., Carbon and chlorine isotope fractionation during aerobic oxidation and reductive dechlorination of vinyl chloride and cis-1,2-dichloroethene. *Environ. Sci. Technol.* **2009**, *43*, (1), 101-107.
- (19) van Breukelen, B. M.; Hunkeler, D.; Volkering, F., Quantification of sequential chlorinated ethene degradation by use of a reactive transport model incorporating isotope fractionation. *Environ. Sci. Technol.* **2005**, *39*, (11), 4189-4197.
- (20) Aeppli, C.; Berg, M.; Cirpka, O. A.; Holliger, C.; Schwarzenbach, R. P.; Hofstetter, T. B., Influence of Mass-Transfer Limitations on Carbon Isotope Fractionation during Microbial Dechlorination of Trichloroethene. *Environ. Sci. Technol.* **2009**, *43*, (23), 8813-8820.
- (21) de Laeter, J. R.; Bohlke, J. K.; De Bièvre, P.; Hidaka, H.; Peiser, H. S.; Rosman, K. J. R.; Taylor, P. D. P., Atomic weights of the elements. *Pure Appl. Chem.* **2009**, *81*, (8), 1535-1536.
- (22) Elsner, M.; Hunkeler, D., Evaluating chlorine isotope effects from isotope ratios and mass spectra of polychlorinated molecules. *Anal. Chem.* **2008**, *80*, (12), 4731-4740.
- (23) Hunkeler, D.; Van Breukelen, B. M.; Elsner, M., Modeling Chlorine Isotope Trends during Sequential Transformation of Chlorinated Ethenes. *Environ. Sci. Technol.* **2009**, *43*, (17), 6750-6756.
- (24) Hunkeler, D.; Aravena, R.; Shouakar-Stash, O.; Weisbrod, N.; Nasser, A.; Netzer, L.; Ronen, D., Carbon and Chlorine Isotope Ratios of Chlorinated Ethenes Migrating through a Thick Unsaturated Zone of a Sandy Aquifer. *Environ. Sci. Technol.* **2011**, *45*, (19), 8247-8253.
- (25) Van Breukelen, B. M.; Rolle, M., Transverse hydrodynamic dispersion effects on isotope signals in groundwater chlorinated solvents' plumes. *Environ. Sci. Technol.* **2012**, *46*, (14), 7700-8.
- (26) Numata, M.; Nakamura, N.; Koshikawa, H.; Terashima, Y., Chlorine isotope fractionation during reductive dechlorination of chlorinated ethenes by anaerobic bacteria. *Environ. Sci. Technol.* **2002**, *36*, (20), 4389-4394.
- (27) Sabalowsky, A. R.; Semprini, L., Trichloroethene and cis-1,2-dichloroethene Concentration-Dependent Toxicity Model Simulates Anaerobic Dechlorination at High Concentrations: I. Batch-Fed Reactors. *Biotechnol. Bioeng.* **2010**, *107*, (3), 529-539.
- (28) Nijenhuis, I.; Andert, J.; Beck, K.; Kastner, M.; Diekert, G.; Richnow, H. H., Stable isotope fractionation of tetrachloroethene during reductive dechlorination by *Sulfurospirillum multivorans* and *Desulfotobacterium* sp strain PCE-S and abiotic reactions with cyanocobalamin. *Appl. Environ. Microbiol.* **2005**, *71*, (7), 3413-3419.
- (29) Tobler, N. B.; Hofstetter, T. B.; Schwarzenbach, R. P., Carbon and Hydrogen Isotope Fractionation during Anaerobic Toluene Oxidation by *Geobacter metallireducens* with Different Fe(III) Phases as Terminal Electron Acceptors. *Environ. Sci. Technol.* **2008**, *42*, (21), 7786-7792.
- (30) Thullner, M.; Kampara, M.; Richnow, H. H.; Harms, H.; Wick, L. Y., Impact of bioavailability restrictions on microbially induced stable isotope fractionation. 1. Theoretical calculation. *Environ. Sci. Technol.* **2008**, *42*, (17), 6544-6551.
- (31) Rolle, M.; Chiogna, G.; Bauer, R.; Griebler, C.; Grathwohl, P., Isotopic Fractionation by Transverse Dispersion: Flow-through Microcosms and Reactive Transport Modeling Study. *Environ. Sci. Technol.* **2010**, *44*, (16), 6167-6173.
- (32) Thullner, M.; Centler, F.; Richnow, H. H.; Fischer, A., Quantification of organic pollutant degradation in contaminated aquifers using compound specific stable isotope analysis - Review of recent developments. *Org. Geochem.* **2012**, *42*, (12), 1440-1460.

- (33) Eckert, D.; Rolle, M.; Cirpka, O.A., Numerical simulation of isotope fractionation in bioreactive transport controlled by transverse mixing. *J. Contam. Hydrol.* **2012**, *140-141*, 95-106.
- (34) Thullner, M.; Fisher, A.; Richnow, H.H.; L.Y. Wick, Influence of mass transfer on stable isotope fractionation. *Appl. Microbiol. Biotechnol.*, **2012**, DOI: 10.1007/s00253-012-4537-7.
- (35) Barth, J. A. C.; Slater, G.; Schuth, C.; Bill, M.; Downey, A.; Larkin, M.; Kalin, R. M., Carbon isotope fractionation during aerobic biodegradation of trichloroethene by Burkholderia cepacia G4: a tool to map degradation mechanisms. *Appl. Environ. Microbiol.* **2002**, *68*, (4), 1728-1734.
- (36) Mancini, S. A.; Ulrich, A. C.; Lacrampe-Couloume, G.; Sleep, B.; Edwards, E. A.; Lollar, B. S., Carbon and hydrogen isotopic fractionation during anaerobic biodegradation of benzene. *Appl. Environ. Microbiol.* **2003**, *69*, (1), 191-198.
- (37) Hofstetter, T. B.; Spain, J. C.; Nishino, S. F.; Bolotin, J.; Schwarzenbach, R. P., Identifying competing aerobic nitrobenzene biodegradation pathways by compound-specific isotope analysis. *Environ. Sci. Technol.* **2008**, *42*, (13), 4764-4770.
- (38) Elsner, M., Stable isotope fractionation to investigate natural transformation mechanisms of organic contaminants: principles, prospects and limitations. *J. Environ. Monit.* **2010**, *12*, (11), 2005-2031.

## Chapter 4

---

### Mechanistic Approach to Multi-Element Isotope Modeling of Organic Contaminant Degradation<sup>3</sup>

#### Abstract

We propose a multi-element isotope modeling approach to simultaneously predict the evolution of different isotopes during the transformation of organic contaminants. The isotopic trends of different elements are explicitly simulated by tracking position-specific isotopologues that contain the isotopes located at fractionating positions. Our approach is self-consistent and provides a mechanistic description of different degradation pathways that accounts for the influence of both primary and secondary isotope effects during contaminant degradation. The method is particularly suited to quantitatively describe the isotopic evolution of relatively large organic contaminant molecules. For such compounds, an integrated approach, simultaneously considering all possible isotopologues, would be impractical due to the large number of isotopologues. We apply the proposed modeling approach to the degradation of toluene, methyl tert-butyl ether (MTBE) and nitrobenzene observed in previous experimental studies. Our model successfully predicts the multi-element isotope data (both 2D and 3D), and accurately captures the distinct trends observed for different reaction pathways. The proposed approach provides an improved and mechanistic methodology to interpret multi-element isotope data and to predict the extent of multi-element isotope fractionation that goes beyond commonly applied modeling descriptions and simplified methods based on the ratio between bulk enrichment factors or on linear regression in dual-isotope plots.

---

<sup>3</sup> Modified from Jin, B.; Rolle, M., 2014. Mechanistic Approach to Multi-Element Isotope Modeling of Organic Contaminant Degradation. *Chemosphere*, 95, 131-139. Copyright 2014 Elsevier.

## 4.1 Introduction

Compound specific isotope analysis (CSIA) is a valuable tool for assessing the transformation and fate of organic contaminants in environmental systems (Schmidt et al., 2004). To date, carbon has been the most commonly analyzed element for practical applications of CSIA to investigate the degradation of various organic contaminants in both laboratory and field studies (Bill et al., 2001; Sherwood Lollar et al., 2001; Hunkeler et al., 2002; Slater et al., 2002; Blessing et al., 2009; Liang et al., 2009; Amaral et al., 2011). In recent years, stable isotope techniques have been extended to other elements such as hydrogen, oxygen, nitrogen and chlorine. For instance, recent advances in analytical techniques promoted the development and implementation of chlorine CSIA (Sakaguchi-Soder et al., 2007; Aeppli et al., 2010; Bernstein et al., 2011; Hitzfeld et al., 2011; Jin et al., 2011). The possibility to analyze the isotopic evolution of different elements has led to an increasing number of applications of dual-element (2D) isotope approaches that have shown considerable advantages compared to single-element CSIA and a great potential to identify, elucidate and quantify environmental transformation processes (Morasch et al., 2001; Mancini et al., 2003; Zwank et al., 2005; Vogt et al., 2008; Abe et al., 2009; Fischer et al., 2010; Kumar et al., 2013). By combining CSIA of different isotope pairs, reaction pathways can be identified and effectively visualized in dual-isotope plots. Numerous experimental studies have applied 2D isotope approaches to investigate the transformation of common groundwater organic contaminants including toluene (Morasch et al., 2001; Fischer et al., 2008; Vogt et al., 2008), MTBE (Kuder et al., 2005; Elsner et al., 2007) and nitrobenzene (Hofstetter et al., 2008b).

The assessment of 2D isotope experimental data commonly relies on the interpretation of dual-isotope plots based on the ratio between bulk enrichment factors or on linear regression of measured dual-isotope data. As we discussed in a previous study focused on chlorinated ethenes degradation (Jin et al., 2013), the interpretation of dual-isotope data becomes more challenging when the bulk enrichment factors of the different fractionating elements differ significantly and in the presence of mass-transfer limitations which can occur in both batch (Thullner et al., 2008; Tobler et al., 2008; Aeppli et al., 2009; Thullner et al., 2012) and flow-through systems (Rolle et al., 2010; Eckert et al., 2012).

Despite the fact that modeling approaches are required to improve the interpretation of multi-element isotope data for environmentally-relevant transformation processes of



organic contaminants, their development and application are still rather limited and have been mainly focused on carbon and chlorine isotopes to predict C and Cl isotope fractionation of chlorinated solvents during degradation reactions (Hunkeler et al., 2009; Van Breukelen and Rolle, 2012; Jin et al., 2013).

This study aims at contributing to fill the gap between the mechanistic understanding of contaminants transformation based on multi-element isotope analysis, which has considerably improved, facilitated by the advances in analytical techniques, and the current state of the art of modeling approaches to quantitatively describe and interpret multi-element isotope evolution. We study the degradation of important organic contaminants such as toluene, MTBE and nitrobenzene and we focus on the evolution of carbon-hydrogen (C, H) and carbon-nitrogen (C, N) isotope pairs as well as on 3D (C, H, N) isotope fractionation as in the case of nitrobenzene oxidative transformation. The organic contaminants selected for this study are relatively large molecules for which an integrated method, simultaneously tracking all isotopologues, such as the one we recently proposed for chlorinated solvents (Jin et al., 2013), would not be practical due to the large number of isotopologues. Therefore, we propose a new multi-element modeling approach based on position-specific isotopologues which only considers isotopically-sensitive atoms (i.e., atoms directly located at reactive positions or at positions adjacent to a reactive bond). To illustrate and validate the proposed methodology, we apply the model to predict the multi-element isotopic evolution for different degradation pathways observed in previous experimental studies.

## 4.2 Modeling Approach

During the transformation of organic contaminants the cleavage of chemical bonds results in primary or secondary isotope effects for the atoms located at the reacting bond positions or in adjacent positions, respectively. As mentioned above, for relatively large organic contaminant molecules an integrated approach, based on the simultaneous tracking of all multi-element isotopologues, is impractical due to the large number of isotopologues (i.e., 72, 78 and 84 molecular isotopologues for the organic compounds considered in this study: toluene, MTBE and nitrobenzene, respectively). Therefore, we define a limited number of position-specific isotopologues which are exclusively based

on the isotopically-sensitive atoms. We start to illustrate the proposed methodology for dual-element (2D) isotope modeling.

The relative abundances of position-specific isotopologues containing two elements, X and Y, can be computed with a binomial distribution combining the occurrence of both X and Y isotopes:

$$A_j = \binom{u}{v} \cdot X_H^v \cdot X_L^{u-v} \cdot \binom{h}{i} \cdot Y_H^i \cdot Y_L^{h-i} \quad (4.1)$$

where  $A_j$  is the relative abundance of the  $j^{\text{th}}$  position-specific isotopologue containing  $v$  heavy X- isotopes out of total  $u$  X-atoms and  $i$  heavy Y-isotopes out of total  $h$  Y-atoms and  $X$  and  $Y$  are the abundances of X and Y isotopes.

When a reaction occurs, each isotope of a position-specific isotopologue is fractionating and the corresponding apparent kinetic isotope effects (AKIEs) are given as (Elsner et al., 2005):

$$AKIE \approx \frac{1}{1 + n/x \cdot \varepsilon_{bulk}} \quad (4.2)$$

$$\alpha = \frac{1}{AKIE} \quad (4.3)$$

where  $n$  is the number of atoms of the element considered,  $x$  is the number of the atoms of the element located at fractionating position,  $\varepsilon_{bulk}$  is the bulk enrichment factor,  $\alpha$  is the fractionation factor at fractionating position.

Assuming first-order kinetics, the reaction rate of the  $j^{\text{th}}$  position-specific isotopologue,  $X_u Y_h$ , reads as:

$${}^j r_{X_u Y_h} = -k \cdot (\alpha_X)^v \cdot (\alpha_Y)^i \cdot C_j \quad (4.4)$$

where  ${}^j r_{X_u Y_h}$  is the reaction rate for the  $j^{\text{th}}$  position-specific isotopologue,  $X_u Y_h$ , which contains  $v$  heavy X-isotopes out of total  $u$  X-atoms and  $i$  heavy Y-isotopes out of  $h$  Y-atoms,  $C_j$  is the concentration of the  $j^{\text{th}}$  position-specific isotopologue, and  $\alpha_X$  and  $\alpha_Y$  are the fractionation factors on the isotopically-sensitive positions for X and Y, respectively (see Eq. 4.3). The product of the fractionation factors takes into account that both X and Y can fractionate during the considered reaction. The exponents  $v$  and  $i$  of  $\alpha_X$  and  $\alpha_Y$  indicate that several atoms of the same element can simultaneously fractionate. This

occurs, for instance, when several atoms of the same element are located adjacent to a reactive position and undergo secondary isotope effects.

The concentration change of a certain organic compound can be described by tracking each position-specific isotopologue. Therefore, the governing mass balance equation for a given organic compound consists of a system of ordinary differential equations based on the degradation rates of the position-specific isotopologues:

$$\frac{dC}{dt} = -\sum_{j=1}^m {}^j r_{X_u Y_h} \quad (4.5)$$

where  $C$  is the total concentration of the organic compound,  $t$  is the time,  $m$  is the number of all possible position-specific isotopologues, and  ${}^j r_{X_u Y_h}$  is the reaction rate of a position-specific isotopologue that, in case of first order reaction kinetics, reads as Eq. 4.4.

We solve the differential equations using Matlab and we run the models for a simulation time corresponding to 90% reduction of the initial contaminant concentrations. The computed concentrations of each position-specific isotopologue are used to determine the isotope ratios. The position-specific isotope ratios of element X and Y for the isotopologues  $X_u Y_h$  are calculated by considering the total number of heavy and light isotopes, and are described by the equations proposed in Jin et al. (2011):

$$R'_X = \frac{\text{Tot}(X_H)}{\text{Tot}(X_L)} = \frac{\sum_{j=1}^m v \cdot {}^j C_{X_u Y_h}}{\sum_{j=1}^m (u-v) \cdot {}^j C_{X_u Y_h}} \quad (4.6)$$

$$R'_Y = \frac{\text{Tot}(Y_H)}{\text{Tot}(Y_L)} = \frac{\sum_{j=1}^m i \cdot {}^j C_{X_u Y_h}}{\sum_{j=1}^m (h-i) \cdot {}^j C_{X_u Y_h}} \quad (4.7)$$

in which  $R'_X$  and  $R'_Y$  are the isotope ratios of all the X and Y atoms on isotopically-sensitive positions,  $C$  is the concentration of the  $j^{\text{th}}$  position-specific isotopologue, and  $u$ ,  $v$ ,  $h$  and  $i$  are the same as defined in Eq. 4.4.

With the exception of a few studies that have provided position-specific isotope ratios (Corso and Brenna, 1997; McKelvie et al., 2010; Breider and Hunkeler, 2011; Wuerfel et al., 2013) in most practical applications the bulk isotope ratios are reported. Therefore, to derive the bulk isotope ratios from the position specific ratios ( $R'_X$  and  $R'_Y$  computed in

Eq. 4.6 and Eq. 4.7) it is necessary to account for the dilution of non-reactive molecular positions:

$$R_X = R'_X \cdot \frac{x}{n_x} + R_{0,X} \cdot \frac{n_x - x}{n_x} \quad (4.8)$$

$$R_Y = R'_Y \cdot \frac{y}{n_y} + R_{0,Y} \cdot \frac{n_y - y}{n_y} \quad (4.9)$$

where  $R_X$  and  $R_Y$  are the bulk isotope ratios for the elements, X and Y, respectively,  $R'_X$  and  $R'_Y$  are the position-specific isotope ratios (Eqs. 4.6-7),  $R_{0,X}$  and  $R_{0,Y}$  are the initial isotope ratios for X and Y.  $n_x$  and  $n_y$  are the total number of X and Y atoms in the organic molecule, and  $x$  and  $y$  are the number of X or Y atoms at fractionating positions.

### *2.1. Reaction mechanisms and evolution of position-specific isotopologues: illustrative examples*

The compounds selected to illustrate the proposed modeling approach are toluene, MTBE and nitrobenzene. Due to their widespread use in many industrial activities these organic contaminants are frequently found in different environmental compartments such as soil and aquifer systems where they can undergo degradation through a number of reaction pathways. Recent experimental studies showed that multi-element isotope analysis is a powerful tool to identify and elucidate the different reaction mechanisms. To quantitatively describe the degradation of these contaminants and the associated multi-element fractionation we apply the procedure outlined above for each compound and reaction pathway.

Toluene degradation can occur, under both aerobic and anaerobic conditions, through the breaking of one C-H bond in the methyl group (Elsner et al., 2005; Vogt et al., 2008). We consider the C-H bond cleaved in the enzymatic attack to the methyl group and we define position-specific isotopologues which include all possible combinations of C and H atoms affected, through primary or secondary isotope effects, by the cleavage of this bond. Therefore, four position-specific isotopologues have been considered for the selected reaction pathways: aerobic degradation, nitrate reduction and sulfate reduction for which the bulk enrichment factors of both C and H are reported in Vogt et al. (2008). The relative abundances of the position-specific isotopologues are determined based on Eq. 1 and their degradation rates are computed according to Eq. 4.4.

A number of studies have investigated the mechanisms of MTBE degradation under different environmental conditions (Gray et al., 2002; Kuder et al., 2005; Elsner et al., 2007). Three main mechanisms: methyl group oxidation,  $S_N1$ -type hydrolysis and  $S_N2$ -type hydrolysis have been identified by dual-isotope analysis. The methyl group oxidation was observed during aerobic biodegradation of MTBE (Gray et al., 2002) and involves the cleavage of a C-H bond in the methyl group. To model MTBE degradation according to this mechanistic pathway we consider, as done for toluene, the four position-specific isotopologues associated with the C-H bond. Under anaerobic conditions biodegradation of MTBE was observed to occur through an enzymatic nucleophilic attack,  $S_N2$ -type hydrolysis (Kuder et al., 2005; Elsner et al., 2007). The C-O bond is cleaved resulting in primary carbon isotope effects and in secondary isotope effects on the adjacent hydrogen atoms in the methyl group. We model this reaction mechanism considering eight carbon-hydrogen position-specific isotopologues ( $C-H_3$ ), representing all possible combinations of C and H atoms for the methyl group, with abundances and degradation rates computed as Eq. 1 and Eq. 4, respectively. A similar mechanism occurs during the acidic hydrolysis ( $S_N1$  reaction), which also involves the cleavage of a C-O bond and primary C isotope effects. However, this mechanism involves secondary hydrogen isotope effects for nine hydrogen atoms located at the three adjacent methyl groups. The modeling of MTBE degradation through this reaction pathway requires the consideration of twenty position-specific carbon-hydrogen ( $C-H_9$ ) isotopologues.

Biodegradation of nitrobenzene has been shown to occur under aerobic conditions through both a reductive and an oxidative transformation pathways (Hofstetter et al., 2008a; Hofstetter et al., 2008b). Concerning the reductive mechanism, primary nitrogen isotope and secondary carbon isotope effects occur (Hofstetter et al., 2008b). Therefore, we apply dual-isotope modeling considering the four position-specific isotopologues associated with the C-N bond. The oxidative transformation mechanism of nitrobenzene proceeds with an initial dioxygenation at the aromatic ring (Hofstetter et al., 2008b, Scheme 2). Such enzymatic attack causes primary carbon isotope fractionation and secondary isotope effects on the hydrogen and nitrogen atoms located at adjacent positions. In this case, we need to consider the position-specific isotopologues of the three elements, C, N and H at the reactive positions or at adjacent positions to the attacked bond in the aromatic ring,  $N-C=C-H$ . Therefore, a 3D isotope modeling approach is

required to describe this reactive system which involves twelve position-specific isotopologues whose relative abundances are computed as:

$$A_{NB,j} = \binom{u}{v} \cdot X_{13C}^v \cdot X_{12C}^{u-v} \cdot \binom{h}{i} \cdot Y_{15N}^i \cdot Y_{14N}^{h-i} \cdot \binom{e}{f} \cdot Z_{2H}^f \cdot Z_{1H}^{e-f} \quad (4.10)$$

where  $A_{NB,j}$  is the relative abundance of  $j^{\text{th}}$  position-specific isotopologue of nitrobenzene,  $X$ ,  $Y$  and  $Z$  represent the relative abundances of carbon, hydrogen and nitrogen isotopes,  $v$ ,  $i$  and  $f$  are the number of heavy isotopes of carbon, nitrogen and hydrogen, respectively,  $u$ ,  $h$  and  $e$  are the total number of certain atoms in the  $j^{\text{th}}$  isotopologue. Accordingly, the reaction rate of the  $j^{\text{th}}$  position-specific C-H-N isotopologue needs to be modified to include the dependency on the fractionation factors of the three elements.

A summary of the illustrative examples considered in this study including the reaction pathways, the stable isotope pairs, the bulk enrichment factors and the number of position-specific isotopologues is reported in Table 4.1.

Table 4.1. Degradation pathways of the selected organic contaminants, enrichment factors and number of position-specific isotopologues

| Compound   | Reaction<br>(and Mechanism)  | Isotope  | n <sup>§</sup>                   | x <sup>†</sup> | ε <sub>bulk</sub><br>[‰] | ε <sup>‡</sup><br>[‰] | Position-Specific<br>Isotopologues |   |
|--|--|--|----------------------------------|----------------|--------------------------|-----------------------|------------------------------------|---|
| Toluene  | aerobic degradation <sup>a</sup><br>(methyl monooxygenase)             | <sup>13</sup> C/ <sup>12</sup> C                             | 7                                | 1              | -3                       | -21                   | 4                                  |   |
|  |  | <sup>2</sup> H/ <sup>1</sup> H                               | 8                                | 3              | -135                     | -360                  |                                    |   |
|  | anaerobic nitrate reduction <sup>a</sup><br>(benzilsuccinate synthase) | <sup>13</sup> C/ <sup>12</sup> C                             | 7                                | 1              | -3                       | -21                   | 4                                  |   |
|  |  | <sup>2</sup> H/ <sup>1</sup> H                               | 8                                | 3              | -40                      | 106.<br>7             |                                    |   |
|  | anaerobic sulfate reduction <sup>a</sup><br>(benzilsuccinate synthase) | <sup>13</sup> C/ <sup>12</sup> C                             | 7                                | 1              | -2.5                     | -17.5                 | 4                                  |   |
|  |  | <sup>2</sup> H/ <sup>1</sup> H                               | 8                                | 3              | -64                      | 170.<br>7             |                                    |   |
|  | MTBE   | aerobic degradation <sup>b</sup><br>(methyl group oxidation) | <sup>13</sup> C/ <sup>12</sup> C | 5              | 1                        | -2                    | -10                                | 4 |
|  |  |  | <sup>2</sup> H/ <sup>1</sup> H   | 12             | 3                        | -37                   | -148                               |   |
| acidic hydrolysis <sup>c</sup><br>(S <sub>N</sub> 1-type)                |  | <sup>13</sup> C/ <sup>12</sup> C                             | 5                                | 1              | -4.9                     | -24.5                 | 20                                 |   |
|  |  | <sup>2</sup> H/ <sup>1</sup> H                               | 12                               | 9              | -55                      | -73.3                 |                                    |   |
| anaerobic degradation <sup>d</sup><br>(S <sub>N</sub> 2-type hydrolysis) |  | <sup>13</sup> C/ <sup>12</sup> C                             | 5                                | 1              | -13                      | -65                   | 8                                  |   |
|  | <sup>2</sup> H/ <sup>1</sup> H   | 12   | 3                                | -16            | -64                      |                       |                                    |   |
| Nitrobenzene   | aerobic degradation <sup>e</sup><br>(partial reduction)                | <sup>13</sup> C/ <sup>12</sup> C                             | 6                                | 1              | -0.5                     | -3                    | 4                                  |   |
|  |  | <sup>15</sup> N/ <sup>14</sup> N                             | 1                                | 1              | -27                      | -27                   |                                    |   |
|  | aerobic degradation <sup>f</sup><br>(dioxygenation)                    | <sup>13</sup> C/ <sup>12</sup> C                             | 6                                | 2              | -3.9                     | -11.7                 | 12                                 |   |
|  |  | <sup>2</sup> H/ <sup>1</sup> H                               | 6                                | 1              | -7                       | -42                   |                                    |   |
| <sup>15</sup> N/ <sup>13</sup> N   | 1  | 1  | -0.8                             | -0.8           |                          |                       |                                    |   |

<sup>§</sup> number of atoms of the element considered;

<sup>†</sup> number of atoms of the element located at the fractionating position

<sup>‡</sup> position-specific enrichment factor

<sup>a</sup>Vogt et al., 2008; <sup>b</sup>Gray et al., 2002; <sup>c</sup>Elsner et al., 2007; <sup>d</sup>Kuder et al., 2005; <sup>e</sup>Hofstetter et al., 2008b; <sup>f</sup>Hofstetter et al., 2008a

## 4.3 Results and Discussion

### 4.3.1. Toluene degradation

Toluene was selected as first model compound and its biodegradation under aerobic, nitrate-reducing and sulfate-reducing conditions was considered. Dual carbon and hydrogen compound specific isotope analysis was performed in previous experimental studies and the observations are reported in Figure 1A. The three distinct reaction pathways show a similar extent ( $\sim 7\text{‰}$ ) of C isotope fractionation, whereas the H fractionation is significantly larger during aerobic degradation ( $67.6\text{‰} - 429.9\text{‰}$ ), followed by sulfate reduction ( $-0.1\text{‰} - 209.7\text{‰}$ ) and by nitrate reduction ( $13.6\text{‰} - 97.0\text{‰}$ ). In the same figure the lines represent the outcome of the modeling approach outlined in the previous section. For each of the considered reaction pathways (aerobic degradation: pathway 1; nitrate reduction: pathway 2 and sulfate reduction: pathway 3) the modeling results allowed us to accurately predict the evolution of both C and H isotopes observed in the experimental studies. The comparison between the data and the simulation results is reported in terms of bulk isotope ratios (Eq. 4.8 and Eq. 4.9) since such compound average values were observed in the experimental studies. However, as shown in the previous section, the proposed modeling approach is based on the evolution of position-specific isotopologues; thus, it allows tracking position-specific isotope ratios (Eq. 4.6 and Eq. 4.7). The simulated results for the “undiluted”, position-specific isotope fractionation are reported in Figure 4.1B. Notice that the obtained patterns are similar to the ones shown in Figure 4.1A but the extent of both carbon and hydrogen fractionation associated with the oxidation of the methyl group of the toluene molecule through the three distinct reaction pathways is considerably more significant. Values of up to  $50\text{‰}$  are obtained for  $\delta^{13}\text{C}$ , whereas hydrogen fractionation ( $\delta^2\text{H}$ ) are in the range  $60\text{‰}$ - $1177.3\text{‰}$  for aerobic degradation,  $15.6\text{‰}$ - $248.4\text{‰}$  for nitrate reduction and  $-7.5\text{‰}$ - $610.0\text{‰}$  for sulfate reduction.



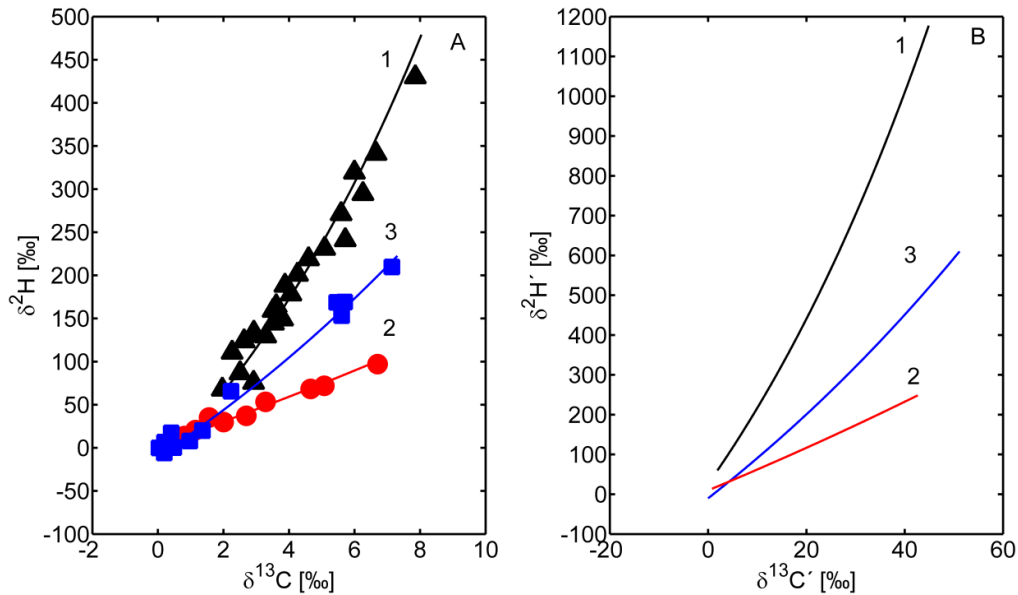


Fig. 4.1. Evolution of carbon and hydrogen isotope ratios during different toluene degradation pathways (A). The symbols represent the experimental data reported by Vogt et al. (2008), and the solid lines represent the simulation results. The numbers indicate the three distinct reaction pathways (1: aerobic degradation, 2: anaerobic nitrate reduction, 3: anaerobic sulfate reduction). Panel B shows the corresponding position-specific isotope fractionation at the methyl group for the three different reaction mechanisms.

The dual isotope trends show a significant bending which is caused by the different change between isotope ratios of the two elements which becomes increasingly important at late reaction times (Jin et al., 2013). The ratio between the incremental changes in hydrogen ( $\Delta\delta^2H$ ) and carbon ( $\Delta\delta^{13}C$ ) isotope values can be expressed as:

$$\frac{\Delta\delta^2H}{\Delta\delta^{13}C} = \frac{\varepsilon_H \times (\delta^2H + 1)}{\varepsilon_C \times (\delta^{13}C + 1)} \quad (4.11)$$

where  $\varepsilon_H$  and  $\varepsilon_C$  are the bulk hydrogen and carbon enrichment factors. By combining Eq. 4.2 and Eq. 4.11, a similar expression can be obtained for the position-specific isotope fractionation of C and H via the three distinct reaction pathways:

$$\frac{\Delta\delta^2H'}{\Delta\delta^{13}C'} = \frac{\varepsilon_H}{\varepsilon_C} \cdot \frac{n_H}{x_H} \cdot \frac{x_C}{n_C} \cdot \frac{(\delta^2H' + 1)}{(\delta^{13}C' + 1)} \quad (4.12)$$

Figure 4.2 shows the experimental data (symbols) and the modeling results using our mechanistic modeling approach (solid line) and a separate dual-isotope approach (dashed line), respectively. The latter is a typical approach used to simulate isotope evolution which considers the average behavior of light and heavy isotope species. In the case of

multi-element modeling such light and heavy species are computed separately for the different elements. In Figure 4.2 we also show the linear trends (dotted line) given by the ratio of the bulk enrichment factors ( $\epsilon_H/\epsilon_C$ ), which represent a simplified and commonly adopted approach to interpret dual-isotope data. Both modeling approaches predict dual-isotope trends which are initially close to the linear approximation ( $\epsilon_H/\epsilon_C$ ) but tend to deviate from the linear relation as the reaction proceeds. Such deviations from the linear approximation are more pronounced in the cases of aerobic degradation and sulfate reduction for which the differences between the C and H bulk enrichment factors are larger. Notice that significant differences exist between the two simulation approaches. The proposed mechanistic position-specific isotopologue approach shows a more remarkable non-linear behavior with slopes in a range: 46.0-137.5 for aerobic degradation, 13.5-18.6 for nitrate reduction, and 25.4-56.6 for sulfate reduction. The dual-isotope trends computed with the separate isotope method have less pronounced slopes and show a less satisfactory agreement with the experimental results at later times (Fig. 4.2A and 4.2B). The differences between the two simulation approaches stem from the inconsistencies introduced by the simplified isotope approach in computing separately C and H isotope evolution. Such shortcomings are avoided with the proposed mechanistic method, since it consistently takes into account, with a more fundamental and integrated approach, the evolution of each position-specific isotopologue.

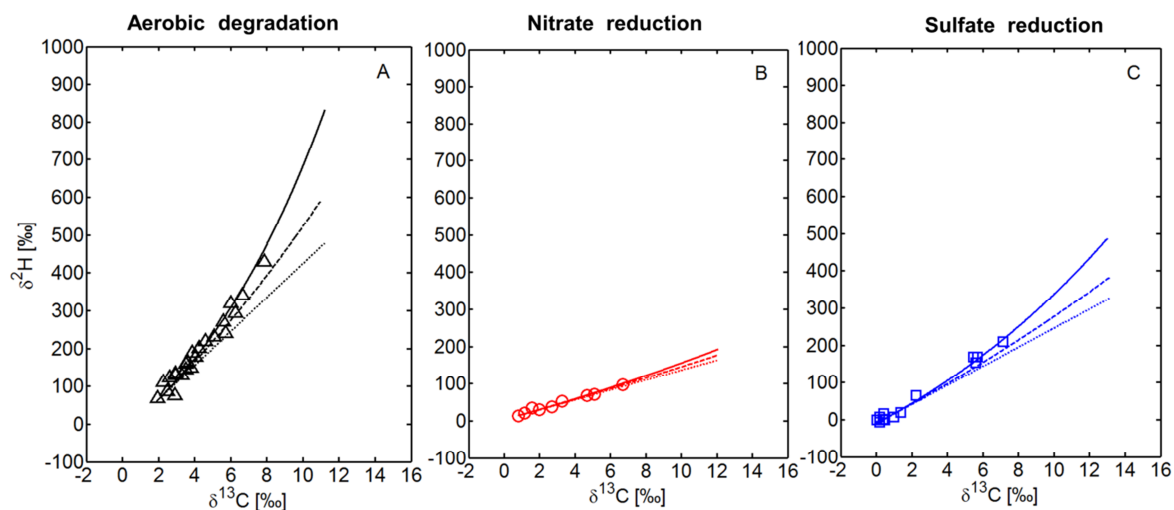


Fig.4.2. Observed (symbols) and simulated (solid lines) dual-isotope ratios using the mechanistic position-specific isotopologue method of this study (solid line) and a separate isotope approach (dashed line). The dotted line is the approximated linear interpretation with constant slope given

by  $\epsilon_H/\epsilon_C$ . The comparison is reported for the three distinct reaction pathways of toluene degradation (panels A, B and C).

### 4.3.2 MTBE degradation.

Previous experimental studies (Gray et al., 2002; Kuder et al., 2005; Elsner et al., 2007) have shown that different reaction mechanisms of MTBE degradation result in different extents of carbon and hydrogen isotope fraction.

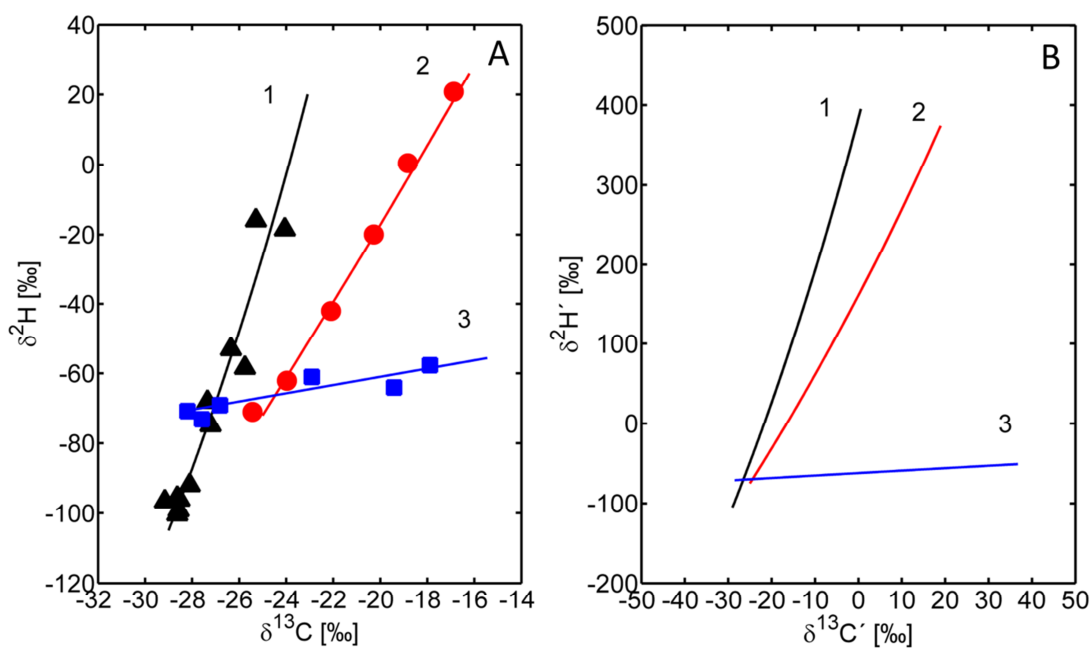


Fig. 4.3. Evolution of carbon and hydrogen isotope ratios during different MTBE degradation pathways (1: methyl group oxidation; 2: acidic hydrolysis,  $S_N1$ -type; 3: hydrolysis by nucleophilic attack,  $S_N2$ -type). In panel A the symbols represent published experimental data (Gray et al., 2002; Kuder et al., 2005; Elsner et al., 2007) and the lines are the simulated bulk isotope ratios. Panel B shows the corresponding position-specific isotope fractionation at the methyl group for the three different reaction mechanisms.

We simulate MTBE degradation and the evolution of carbon and hydrogen isotope ratios via the identified reaction pathways: methyl group oxidation (reaction 1 in Fig. 4.3), acidic hydrolysis (reaction 2 in Fig. 4.3), and hydrolysis by nucleophilic attack (reaction 3 in Fig. 4.3). We obtain a good agreement between the experimental data and the simulation results for all three reaction pathways (Fig. 4.3). The methyl group oxidation (reaction 1) shows a remarkable variation of  $\delta^2H'$  values, ranging from -96.6‰ to -18.5‰. This is due to large hydrogen isotope fractionation caused by primary isotope effects

associated with the mechanism of methyl group oxidation. The observed hydrogen fractionation is also substantial for the  $S_N1$ -type hydrolysis (reaction pathway 2) although only secondary hydrogen isotope effects are associated with this pathway. Conversely, the extent of H fractionation is considerably smaller for reaction pathway 3 ( $S_N2$ -type hydrolysis) where the secondary isotope effects only result in a small change of  $\delta^2H$  (13‰). The most significant variation on  $\delta^{13}C$  values, from -28.2‰ to -17.9‰, was observed for the hydrolysis of MTBE by nucleophilic attack (reaction pathway 3). Notice that for MTBE the bending of the dual isotope plots is less important than in the case of toluene degradation. The model results indicate that the slopes of the dual isotope plots of MTBE show a remarkable deviation from a linear trend (18.0 - 25.8) only for reaction pathway 1, for which the difference between bulk carbon and hydrogen enrichment factors are more relevant (Table 1). Figure 4.3B reports the corresponding position-specific dual-isotope evolution that can be described by the proposed mechanistic modeling approach. The position-specific fractionation of both C and H is considerably larger than the bulk values:  $\delta^{13}C'$  values vary from -29‰ to 0.6‰ (reaction pathway 1), from -25‰ to 19‰ (reaction pathway 2), and from -28.5‰ to 36.7‰ (reaction pathway 3);  $\delta^2H'$  values vary from -105‰ to 395‰ (reaction pathway 1), from -75‰ to -374‰ (reaction pathway 2), and from -71‰ to -51‰ (reaction pathway 3).

### 4.3.3. Nitrobenzene degradation

In this section, we consider nitrobenzene degradation occurring through two distinct reaction mechanisms and the associated multi-element isotopic changes observed in previous experimental studies and predicted using our modeling approach.

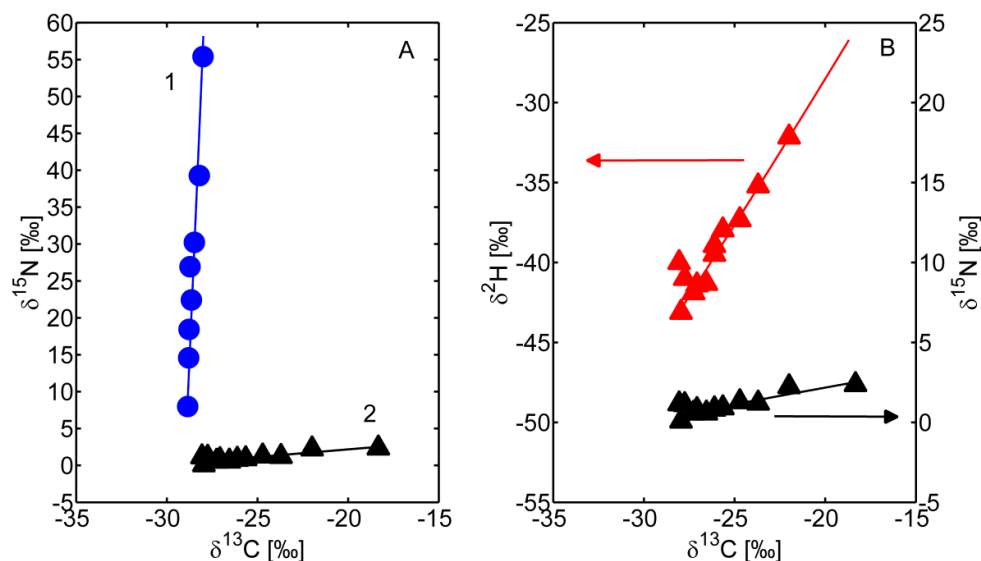


Fig. 4.4 Nitrogen and carbon isotope fractionation during partial reduction and oxidation of nitrobenzene (A). The symbols represent the published experimental data (Hofstetter et al., 2008b), and the lines are the model results. The numbers indicate the different reaction pathways (1: partial reduction, 2: oxidation). Panel B shows the 3D (C, N and H) isotope plot for nitrobenzene oxidative transformation with observed data (Hofstetter et al., 2008a) and simulated results for C and H (red symbols and line) and for C and N (black symbols and line). The red and black arrows indicate the corresponding y-axis for the two datasets.

For the considered cases of nitrobenzene degradation the selected experimental references (Hofstetter et al., 2008a; Hofstetter et al., 2008b) also include data on the temporal evolution of nitrobenzene concentrations during both microbially-mediated partial reduction by *Pseudomonas pseudoalcaligenes* strain JS45 (reaction 1) and oxidation (dioxygenation) by *Comamonas sp.* strain JS765 (reaction 2), thus allowing a direct comparison between the progress of the reaction and the extent of multi-element fractionation. To reproduce the observed concentration trends, we modeled the biodegradation reaction with a Michaelis-Menten kinetic formulation. As supplementary material we provide the governing equations, the parameter values and the comparison between observed and simulated nitrobenzene concentrations (Fig. S3.1 and Fig. S3.2). Here we focus on the multi-element isotopic evolution during nitrobenzene degradation. In the partial reduction reaction, a significant nitrogen isotope fractionation (8.0‰ to 55.4‰), but only a small carbon isotope fractionation (-28.9‰ to -28.0‰) were observed (reaction 1 in Fig. 4A). This is due to the fact that the cleavage of the N-O bond in the rate-determining step of the transformation (Hofstetter et al., 2008b, Scheme 2) results in primary nitrogen isotope fractionation, while the carbon atom in the adjacent position is

only affected by a small secondary isotope effect. Conversely, significant carbon isotope fractionation (-28.0‰ to -18.3‰) and a much smaller nitrogen isotope fractionation (0.5‰ to 2.36‰) were observed during oxidation of nitrobenzene (reaction 2). As shown by Hofstetter et al. (2008b), a primary carbon isotope effect occurs during the attack of the aromatic ring, while only secondary isotope effects affect the nitrogen and hydrogen atoms in the adjacent positions (Hofstetter et al., 2008a). For this reaction pathway, the simulation of the multi-element isotopic evolution requires a 3D approach to simultaneously consider the changes in C, N and H. The modeling results are reported in Figure 4B and show a good agreement with the experimental data presented by (Hofstetter et al., 2008a).

#### **4.3.4. Comparison of mechanistic isotopologue approach and separate bulk isotope method in presence of position-specific isotopic signatures**

Since bulk isotope ratios are typically measured and reported in most experimental investigations, isotope modeling studies are commonly conducted with the aim of capturing the bulk isotopic evolution during transformation of organic compounds. However, recent advances on position-specific isotope analysis allow tracking position-specific isotope signatures at reactive positions. Such applications are not yet widespread, and experimental data are reported only for a few organic compounds (McKelvie et al., 2010; Breider and Hunkeler, 2011; Wuerfel et al., 2013). It is very likely that position-specific isotope techniques will be applied in an increasing number of studies in the near future and they will provide essential data for an improved mechanistic understanding of contaminant transformation. In this section we illustrate the capability of our mechanistic modeling approach to capture the position-specific evolution of isotopic signatures and we highlight the differences with conventional bulk isotope modeling. We selected, as an illustrative example, the aerobic degradation of toluene. We performed scenario modeling of dual C and H fractionation considering toluene molecules with 0‰ bulk carbon and hydrogen isotope values but different carbon isotope compositions at the reactive methyl group: -30‰, 0‰ and 30‰, respectively. The results for the bulk and position-specific dual-isotope evolution are reported in Fig. 4.5. The outcomes of the bulk isotope evolution are shown in panels A1, B1 and C1 for both modeling approaches. The scenario shown in panel B1, with no distinction between the bulk and the position specific isotopic signatures, represents the same results shown in the comparison with the experimental

data (Fig. 4.2A). As shown in Fig. 4.5 (A1-C1), the variation of the  $\delta^{13}\text{C}'$  signatures at the methyl group, leads to changes in the slopes of the dual-isotope trends in the three cases: 46.5–141.7 (A1), 46.1–137.5 (B1) and 43.8–133.5 (C1), respectively. These differences on the slopes are observed since more enriched  $\delta^{13}\text{C}'$  values result in higher abundances of  $^{13}\text{C}$  at the reactive methyl group, thus causing a decrease of the overall position-specific reaction rates. Such effects are captured by the proposed mechanistic approach but cannot be reproduced by the separate dual-isotope method. In fact, the latter produces exactly the same dual isotope plots (red solid lines in Fig. 4.5, A1-C1) for the three cases since it only considers the bulk  $\delta^{13}\text{C}$  values (i.e., 0 ‰) under the assumption of even distribution of isotopes in all molecular positions. Thus, such method is not sensitive to the variation of the isotopic composition at the reactive position and cannot capture its influence on the overall bulk isotope evolution. The differences between the two modeling approaches become more evident considering the isotopic evolution at the reactive position. The results in panel A2-C2 show that the mechanistic approach can capture the significant effect of the different isotopic signatures in the reactive methyl group position. On the contrary, the conventional dual-isotope approach cannot reproduce such mechanistic effects since it assumes the same isotopic composition at each molecular position, thus resulting in the same outcomes as for the bulk ratios' evolution (i.e., same red lines in panels A1-C1 and A2-C2).

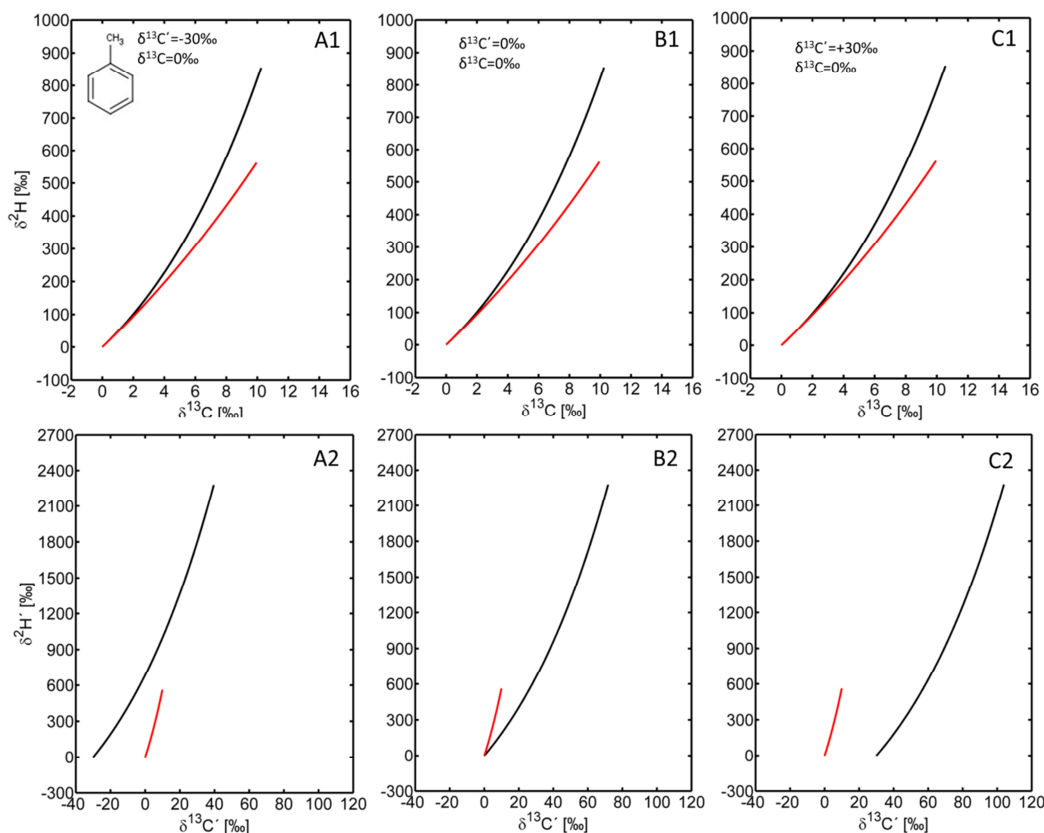


Fig. 4.5. Results of bulk (panels A1, B1, C1) and position-specific (panels A2, B2, C2) isotope fractionation using the mechanistic isotopologue-specific modeling approach (black lines) and the separate isotope modeling method (red lines). The simulations were performed for toluene aerobic degradation in three distinct scenarios with different  $\delta^{13}\text{C}^1$  values at the methyl group:  $-30\text{‰}$ ,  $0\text{‰}$  and  $+30\text{‰}$ .

## Conclusions

The development of analytical techniques allows measuring an increasing number of stable isotope ratios of different elements. For assessing the fate of organic contaminants in the environment it is important to determine ratios such as:  $^{13}\text{C}/^{12}\text{C}$ ,  $^2\text{H}/^1\text{H}$ ,  $^{15}\text{N}/^{14}\text{N}$ ,  $^{18}\text{O}/^{16}\text{O}$ ,  $^{34}\text{S}/^{32}\text{S}$  and  $^{37}\text{Cl}/^{35}\text{Cl}$ . Multi-element isotope analysis offers the possibility to obtain mechanistic information valuable for identifying and elucidating transformation processes (Elsner, 2010; Elsner et al., 2012; Schmidt and Jochmann, 2012). For an improved interpretation of multi-element isotope data, the development of analytical techniques and mechanistic understanding of isotope evolution should be accompanied by advances in modeling approaches. In fact, mathematical modeling is a critical tool to



transfer detailed and mechanistic laboratory observations to practical applications in complex environmental systems. In this study we proposed a new modeling approach to simulate multi-element isotope evolution during the degradation of organic contaminants. Specifically, the advantages of the proposed methodology can be summarized in the following key aspects:

- The proposed modeling approach allows the mechanistic description of contaminant degradation through different reaction pathways and the associated multi-element isotope evolution, including both primary and secondary isotope effects. This goes beyond current interpretation practices and modeling techniques. For instance, as shown for the case of toluene degradation, the model allowed us to better capture the non-linearity of dual isotope plots which arises when the bulk enrichment factors are significantly different.
- The modeling methodology described in this study is based on position-specific isotopologues. This allows tracking directly the isotopic evolution that occurs at fractionating positions specific for distinct compounds and reaction mechanisms. Such possibility is of great advantage also for a quantitative interpretation of position-specific isotope analysis which is developing at a fast pace due to the advances of analytical techniques (McKelvie et al., 2010; Breider and Hunkeler, 2011; Wuerfel et al., 2013).

Further investigation is required to assess the capabilities of the proposed mechanistic approach to describe multi-element isotope evolution in complex environmental systems, where coupled physical and transformation processes determine the fate of organic contaminants.

### **Supporting Information Available**

Supplementary material (S3) associated with this work includes the computed relative abundances of the different isotopologues for the considered compounds as well as the concentration evolution and modeling description for nitrobenzene degradation.

## References

- Abe, Y., Aravena, R., Zopfi, J., Shouakar-Stash, O., Cox, E., Roberts, J.D., Hunkeler, D., 2009. Carbon and Chlorine Isotope Fractionation during Aerobic Oxidation and Reductive Dechlorination of Vinyl Chloride and cis-1,2-Dichloroethene. *Environ. Sci. Technol.* 43, 101-107.
- Aeppli, C., Berg, M., Cirpka, O.A., Holliger, C., Schwarzenbach, R.P., Hofstetter, T.B., 2009. Influence of Mass-Transfer Limitations on Carbon Isotope Fractionation during Microbial Dechlorination of Trichloroethene. *Environ. Sci. Technol.* 43, 8813-8820.
- Aeppli, C., Holmstrand, H., Andersson, P., Gustafsson, O., 2010. Direct Compound-Specific Stable Chlorine Isotope Analysis of Organic Compounds with Quadrupole GC/MS Using Standard Isotope Bracketing. *Anal. Chem.* 82, 420-426.
- Amaral, H.I.F., Aeppli, C., Kipfer, R., Berg, M., 2011. Assessing the transformation of chlorinated ethenes in aquifers with limited potential for natural attenuation: Added values of compound-specific carbon isotope analysis and groundwater dating. *Chemosphere* 85, 774-781.
- Bernstein, A., Shouakar-Stash, O., Ebert, K., Laskov, C., Hunkeler, D., Jeannotat, S., Sakaguchi-Soder, K., Laaks, J., Jochmann, M.A., Cretnik, S., Jager, J., Haderlein, S.B., Schmidt, T.C., Aravena, R., Elsner, M., 2011. Compound-Specific Chlorine Isotope Analysis: A Comparison of Gas Chromatography/Isotope Ratio Mass Spectrometry and Gas Chromatography/Quadrupole Mass Spectrometry Methods in an Interlaboratory Study. *Anal. Chem.* 83, 7624-7634.
- Bill, M., Schuth, C., Barth, J.A.C., Kalin, R.M., 2001. Carbon isotope fractionation during abiotic reductive dehalogenation of trichloroethene (TCE). *Chemosphere* 44, 1281-1286.
- Blessing, M., Schmidt, T.C., Dinkel, R., Haderlein, S.B., 2009. Delineation of Multiple Chlorinated Ethene Sources in an Industrialized Area-A Forensic Field Study Using. *Environ. Sci. Technol.* 43, 2701-2707.
- Breider, F., Hunkeler, D., 2011. Position-specific carbon isotope analysis of trichloroacetic acid by gas chromatography/isotope ratio mass spectrometry. *Rapid Commun. Mass Spectrom.* 25, 3659-3665.
- Corso, T.N., Brenna, J.T., 1997. High-precision position-specific isotope analysis. *Proc. Natl. Acad. Sci. U. S. A.* 94, 1049-1053.
- Eckert, D., Rolle, M., Cirpka, O.A., 2012. Numerical simulation of isotope fractionation in steady-state bioreactive transport controlled by transverse mixing. *J. Contam. Hydrol.* 140, 95-106.
- Elsner, M., 2010. Stable isotope fractionation to investigate natural transformation mechanisms of organic contaminants: principles, prospects and limitations. *J. Environ. Monit.* 12, 2005-2031.
- Elsner, M., Jochmann, M.A., Hofstetter, T.B., Hunkeler, D., Bernstein, A., Schmidt, T.C., Schimmelmann, A., 2012. Current challenges in compound-specific stable isotope analysis of environmental organic contaminants. *Anal. Bioanal. Chem.* 403, 2471-2491.
- Elsner, M., McKelvie, J., Couloume, G.L., Lollar, B.S., 2007. Insight into methyl tert-butyl ether (MTBE) stable isotope Fractionation from abiotic reference experiments. *Environ. Sci. Technol.* 41, 5693-5700.

Elsner, M., Zwank, L., Hunkeler, D., Schwarzenbach, R.P., 2005. A new concept linking observable stable isotope fractionation to transformation pathways of organic pollutants. *Environ. Sci. Technol.* 39, 6896-6916.

Fischer, A., Herklotz, I., Herrmann, S., Thullner, M., Weelink, S.A.B., Stams, A.J.M., Schlomann, M., Richnow, H.H., Vogt, C., 2008. Combined carbon and hydrogen isotope fractionation investigations for elucidating benzene biodegradation pathways. *Environ. Sci. Technol.* 42, 4356-4363.

Fischer, A., Weber, S., Reineke, A.K., Hollender, J., Richnow, H.H., 2010. Carbon and hydrogen isotope fractionation during anaerobic quinoline degradation. *Chemosphere* 81, 400-407.

Gray, J.R., Lacrampe-Couloume, G., Gandhi, D., Scow, K.M., Wilson, R.D., Mackay, D.M., Lollar, B.S., 2002. Carbon and hydrogen isotopic fractionation during biodegradation of methyl tert-butyl ether. *Environ. Sci. Technol.* 36, 1931-1938.

Hitzfeld, K.L., Gehre, M., Richnow, H.H., 2011. A novel online approach to the determination of isotopic ratios for organically bound chlorine, bromine and sulphur. *Rapid Commun. Mass Spectrom.* 25, 3114-3122.

Hofstetter, T.B., Schwarzenbach, R.P., Bernasconi, S.M., 2008a. Assessing Transformation Processes of Organic Compounds Using Stable Isotope Fractionation. *Environ. Sci. Technol.* 42, 7737-7743.

Hofstetter, T.B., Spain, J.C., Nishino, S.F., Bolotin, J., Schwarzenbach, R.P., 2008b. Identifying competing aerobic nitrobenzene biodegradation pathways by compound-specific isotope analysis. *Environ. Sci. Technol.* 42, 4764-4770.

Hunkeler, D., Aravena, R., Cox, E., 2002. Carbon isotopes as a tool to evaluate the origin and fate of vinyl chloride: Laboratory experiments and modeling of isotope evolution. *Environ. Sci. Technol.* 36, 3378-3384.

Hunkeler, D., Van Breukelen, B.M., Elsner, M., 2009. Modeling Chlorine Isotope Trends during Sequential Transformation of Chlorinated Ethenes. *Environ. Sci. Technol.* 43, 6750-6756.

Jin, B., Haderlein, S.B., Rolle, M., 2013. Integrated carbon and chlorine isotope modeling: applications to chlorinated aliphatic hydrocarbons dechlorination. *Environ. Sci. Technol.* 47, 1443-1451.

Jin, B.A., Laskov, C., Rolle, M., Haderlein, S.B., 2011. Chlorine Isotope Analysis of Organic Contaminants Using GC-qMS: Method Optimization and Comparison of Different Evaluation Schemes. *Environ. Sci. Technol.* 45, 5279-5286.

Kuder, T., Wilson, J.T., Kaiser, P., Kolhatkar, R., Philp, P., Allen, J., 2005. Enrichment of stable carbon and hydrogen isotopes during anaerobic biodegradation of MTBE: Microcosm and field evidence. *Environ. Sci. Technol.* 39, 213-220.

Kumar, N., Millot, R., Battaglia-Brunet, F., Negrel, P., Diels, L., Rose, J., Bastiaens, L., 2013. Sulfur and oxygen isotope tracing in zero valent iron based In situ remediation system for metal contaminants. *Chemosphere* 90, 1366-1371.

Liang, X.M., Philp, R.P., Butler, E.C., 2009. Kinetic and isotope analyses of tetrachloroethylene and trichloroethylene degradation by model Fe(II)-bearing minerals. *Chemosphere* 75, 63-69.

Mancini, S.A., Ulrich, A.C., Lacrampe-Couloume, G., Sleep, B., Edwards, E.A., Lollar, B.S., 2003. Carbon and hydrogen isotopic fractionation during anaerobic biodegradation of benzene. *Appl. Environ. Microbiol.* 69, 191-198.

McKelvie, J.R., Elsner, M., Simpson, A.J., Lollar, B.S., Simpson, M.J., 2010. Quantitative Site-Specific H-2 NMR Investigation of MTBE: Potential for Assessing Contaminant Sources and Fate. *Environ. Sci. Technol.* 44, 1062-1068.

Morasch, B., Richnow, H.H., Schink, B., Meckenstock, R.U., 2001. Stable hydrogen and carbon isotope fractionation during microbial toluene degradation: Mechanistic and environmental aspects. *Appl. Environ. Microbiol.* 67, 4842-4849.

Rolle, M., Chiogna, G., Bauer, R., Griebler, C., Grathwohl, P., 2010. Isotopic Fractionation by Transverse Dispersion: Flow-through Microcosms and Reactive Transport Modeling Study. *Environ. Sci. Technol.* 44, 6167-6173.

Sakaguchi-Soder, K., Jager, J., Grund, H., Matthaus, F., Schuth, C., 2007. Monitoring and evaluation of dechlorination processes using compound-specific chlorine isotope analysis. *Rapid Commun. Mass Spectrom.* 21, 3077-3084.

Schmidt, T.C., Jochmann, M.A., 2012. Origin and Fate of Organic Compounds in Water: Characterization by Compound-Specific Stable Isotope Analysis. in: Cooks, R.G., Yeung, E.S. (Eds.). *Annual Review of Analytical Chemistry*, Vol 5. Annual Reviews, Palo Alto, pp. 133-155.

Schmidt, T.C., Zwank, L., Elsner, M., Berg, M., Meckenstock, R.U., Haderlein, S.B., 2004. Compound-specific stable isotope analysis of organic contaminants in natural environments: a critical review of the state of the art, prospects, and future challenges. *Anal. Bioanal. Chem.* 378, 283-300.

Sherwood Lollar, B., Slater, G.F., Sleep, B., Witt, M., Klecka, G.M., Harkness, M., Spivack, J., 2001. Stable carbon isotope evidence for intrinsic bioremediation of tetrachloroethene and trichloroethene at area 6, Dover Air Force Base. *Environmental Science and Technology* 35, 261-269.

Slater, G.F., Lollar, B.S., King, R.A., O'Hannesin, S., 2002. Isotopic fractionation during reductive dechlorination of trichloroethene by zero-valent iron: influence of surface treatment. *Chemosphere* 49, 587-596.

Thullner, M., Centler, F., Richnow, H.H., Fischer, A., 2012. Quantification of organic pollutant degradation in contaminated aquifers using compound specific stable isotope analysis - Review of recent developments. *Org. Geochem.* 42, 1440-1460.

Thullner, M., Kampara, M., Richnow, H.H., Harms, H., Wick, L.Y., 2008. Impact of bioavailability restrictions on microbially induced stable isotope fractionation. 1. Theoretical calculation. *Environ. Sci. Technol.* 42, 6544-6551.

Tobler, N.B., Hofstetter, T.B., Schwarzenbach, R.P., 2008. Carbon and Hydrogen Isotope Fractionation during Anaerobic Toluene Oxidation by *Geobacter metallireducens* with Different Fe(III) Phases as Terminal Electron Acceptors. *Environ. Sci. Technol.* 42, 7786-7792.

Van Breukelen, B.M., Rolle, M., 2012. Transverse Hydrodynamic Dispersion Effects on Isotope Signals in Groundwater Chlorinated Solvents' Plumes. *Environ. Sci. Technol.* 46, 7700-7708.

Vogt, C., Cyrus, E., Herklotz, I., Schlosser, D., Bahr, A., Herrmann, S., Richnow, H.H., Fischer, A., 2008. Evaluation of Toluene Degradation Pathways by Two-Dimensional Stable Isotope Fractionation. *Environ. Sci. Technol.* 42, 7793-7800.

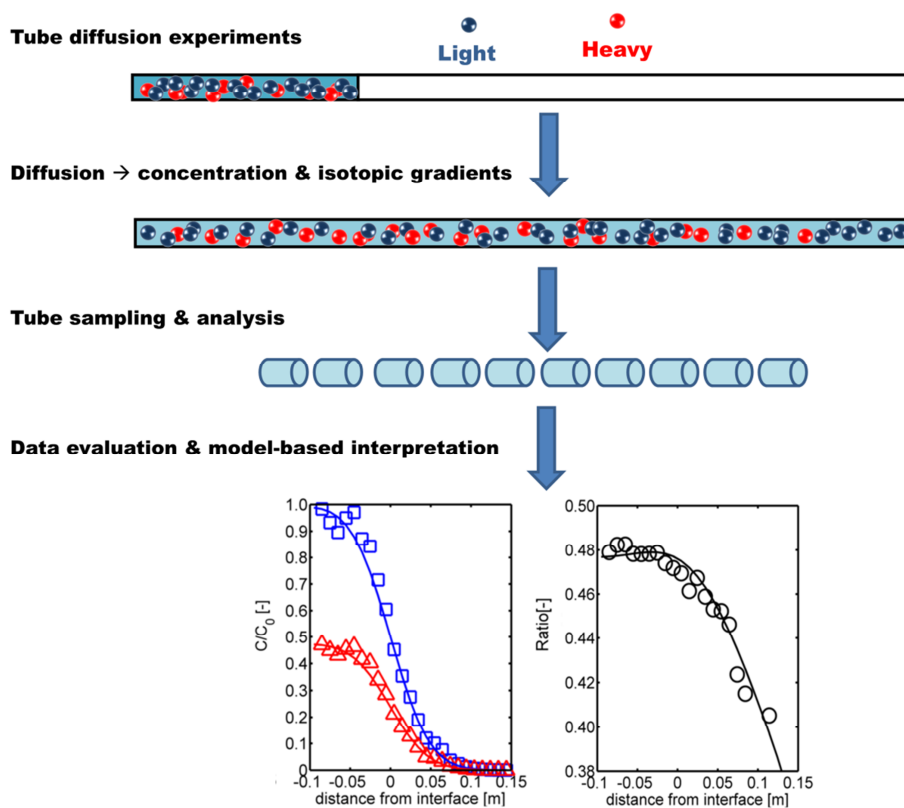
Wuerfel, O., Greule, M., Keppler, F., Jochmann, M.A., Schmidt, T.C., 2013. Position-specific isotope analysis of the methyl group carbon in methylcobalamin for the investigation of biomethylation processes. *Anal. Bioanal. Chem.* 405, 2833-2841.

Zwank, L., Berg, M., Elsner, M., Schmidt, T.C., Schwarzenbach, R.P., Haderlein, S.B., 2005. New evaluation scheme for two-dimensional isotope analysis to decipher biodegradation processes: Application to groundwater contamination by MTBE (vol 39, pg 1018, 2005). *Environ. Sci. Technol.* 39, 7344-7344.



# Chapter 5

## Diffusive Fractionation of Organic Contaminants in Aqueous Solution: Quantification of Spatial Isotope Gradients<sup>4</sup>



<sup>4</sup> Modified from Jin, B.; Haderlein, S.B.; Li T.; Rolle, M., Diffusive Fractionation of Organic Contaminants in Aqueous Solution: Quantification of Spatial Isotope Gradients. Environ. Sci. Technol. (submitted). Copyright 2014 American Chemical Society.

## Abstract

Laboratory experiments were performed to investigate and quantify the extent of diffusive isotope fractionation of organic contaminants in aqueous solution. We selected petroleum hydrocarbons (toluene and ethylbenzene, in 1:2 mixtures of labeled (perdeuterated) and non-labeled isotopologues) and chlorinated solvents (trichloroethene (TCE) and cis-dichloroethene (cisDCE), at their natural isotopic abundance) as model compounds. The experimental approach using gel diffusion tubes allowed us to resolve concentration and isotopic gradients induced by isotopologue-specific diffusion, and to determine aqueous diffusion coefficients in agreement with the values calculated using published empirical correlations. The experimental results were quantitatively evaluated with numerical simulations to determine the aqueous diffusion coefficients,  $D$ , and the exponent of the inverse power-law relation between  $D$  and the molecular mass of the isotopologues. The results show remarkable diffusive isotope fractionation for all the investigated organic compounds. The outcomes of this study are relevant for the interpretation of the isotopic signatures of organic contaminants in environmental systems and for the quantitative application of compound specific isotope analysis (CSIA) that needs to take into account the fractionation effects of both physical and transformation processes.



## 5.1 Introduction

Compound specific isotope analysis (CSIA) is a powerful tool to assess transformations of various organic pollutants in environmental systems [1-3]. This technique is finding an increasing number of applications as summarized in recent reviews [2, 4, 5]. The basic principle of the CSIA approach for organic contaminants is that light isotopes located at a certain reactive position react faster than the heavy ones. The isotopic composition in the remaining organic compound fraction is monitored by CSIA, which allows obtaining direct information on (bio)degradation and other transformation processes. An increasing number of investigations have demonstrated the important role of physical processes on isotope fractionation of organic contaminants. Such processes include mass transfer limitations [6-8], sorption [9, 10], volatilization [11, 12], aqueous diffusion [13] and transverse dispersion [14-16]. In particular, a sound understanding of the impact of aqueous diffusion on isotope fractionation is of primary importance for a quantitative interpretation of isotopic data in many fields of applied and environmental geosciences. The research in this direction has been mainly focused on the investigation of diffusion-induced isotope fractionation of dissolved trace gases (e.g., noble gases, methane and CO<sub>2</sub>) [17-20], and ionic species (e.g., Br<sup>-</sup>, Cl<sup>-</sup>, SO<sub>4</sub><sup>2-</sup>, Mg<sup>2+</sup> and Ca<sup>2+</sup>) [21-27] in various diffusion-dominated laboratory and environmental systems. Important experimental evidence was provided in the studies of Richter et al. [24] and Eggenkamp and Coleman [23], who showed the effects of kinetic isotope fractionation during diffusion of selected cations and anions in aqueous systems. Furthermore, the work of Bourg and Sposito [19, 21] and Bourg et al. [25], based on molecular dynamics simulations, helped to interpret the experimental observations and to deepen the understanding on the mass dependence of the aqueous diffusion coefficient for monoatomic solutes in liquid water. Such advances are yet not well documented for diffusion of uncharged polyatomic species, such as organic contaminants, in aqueous systems, although an improved understanding of diffusive isotopic fractionation of such compounds is of critical importance for a correct interpretation of isotopic data in groundwater systems, allowing a quantitative assessment of contaminant transport and transformation by CSIA techniques. In fact, the importance of diffusion as major transport mechanism in saturated porous media is increasingly acknowledged in studies on plume migration in groundwater. For instance,

several investigations have pointed out the role of back diffusion from silt and clay aquitards for the persistence of organic plumes [13, 28, 29]. Also, recent high-resolution investigations in contaminated aquifers point to an effect of diffusion on the observed isotopic signatures at the plume fringes [30, 31]. Moreover, experimental and modeling investigation of transverse hydrodynamic dispersion in advection-dominated flow-through systems has shown an explicit dependence of mechanical dispersion on the aqueous diffusion coefficients of the transported species. These findings have significant implications for conservative and mixing-controlled reactive transport in porous media [32, 33], for coupled displacement of charged species leading to multicomponent ionic dispersion [34], for transport of different organic contaminant isotopologues and for the interpretation of isotopic signatures in groundwater [14, 16]. The latter task requires high-resolution data and a quantitative understanding of the effects of aqueous diffusion on isotope fractionation of organic pollutants in aqueous systems.

In this work we performed controlled laboratory experiments to quantify the effect of diffusive isotope fractionation on the displacement of neutral organic contaminant isotopologues. We selected, model compounds, representative of organic contaminants frequently found in groundwater, including petroleum hydrocarbons (toluene; ethylbenzene) and chlorinated solvents (cis-dichloroethene; trichloroethene). The experiments with toluene and ethylbenzene were performed using mixtures of labeled (perdeuterated) and non-labeled isotopologues, whereas the experiments with cisDCE and TCE were carried out using these compounds at their natural isotopic abundance and determining the spatial and temporal evolution of the chlorine isotope ratio. The results allowed us to clearly capture the effects of diffusion-induced spatial isotope gradients and their temporal evolution. A one-dimensional modeling approach was used to quantitatively interpret the experimental observations and to extrapolate the findings to a larger scale scenario relevant for practical application of CSIA in subsurface systems.

## **5.2 Materials and Methods**

### **5.2.1 Diffusion Experiments**

The experiments were performed in cylindrical glass tubes filled with agarose gel. We prepared the gel using deionized water and a minimal concentration of phyto agar (1% w/w) to obtain a medium in which the extent of diffusion is very similar to the one that would be observed in purely aqueous systems [35]. The experimental setup is similar to the one used to investigate fractionation of chlorine and bromine stable isotopes during diffusive transport of chloride and bromide ions [23]. The glass tubes (25 cm long; 1.1 cm inner diameter) are glass sealed on one end, and can be closed using crimp caps on the open opposite side. We prepared solutions with agar containing the organic contaminants as well as blank solutions (i.e., without contaminant). The glass tubes were partially filled up to 15 cm with a volume of 14.2 ml of solution containing the blank liquid agar representing the pristine fraction of the test tube into which diffusion occurs. After solidification of this blank medium, agar solutions (9.5 mL) containing the individual dissolved organic contaminants were added to fill up the tubes. These solutions contained known concentrations of different isotopologues (1:2 mixture perdeuterated: non-deuterated for toluene and ethylbenzene; natural abundance of isotopologues of cisDCE and TCE). Once solidified, these solutions acted as contamination sources, progressively releasing the organic contaminant to the adjacent blank medium. During the setup preparation, the hot agar medium was injected using a 25-ml gas-tight syringe (Hamilton, Bonaduz, Switzerland) with a 20 cm stainless steel needle (UNIMED; Lausanne, Switzerland). After filling the agar medium containing the contaminant, the glass tubes were first covered with aluminum foil and crimp-sealed using caps with Teflon-coated silicone septa. To prevent gas exchange and contaminant mass losses we applied an additional sealing using wax. For a given experiment, several tubes were prepared starting from the same contaminant solution. The tubes were placed horizontally in a thermally-insulated box and kept at a constant temperature of 20°C. As shown in the schematic description of the experimental protocol provided in the Supporting Information, after several days necessary for diffusive isotopic gradients to establish, the tubes were sacrificed and sampled. The sampling procedure started with breaking the glass tube and removing the gel that was successively cut into 1 cm slices with a scalpel. Each slice was immediately put in a 10 ml glass vial for subsequent headspace GC-analysis and closed with screw caps with Teflon coated silicone septa. To correct for small errors due to uneven cutting, we weighted each vial on a precision scale and used these data as a gravimetric correction of the concentration measurements. The 25 vials were heated to

melt the gel and measurements were performed using GC-MS at an incubation temperature of 50°C. An overview of the experiments is provided in Table 1 and Table 2 for the petroleum hydrocarbons and the chlorinated solvents, respectively.

### 5.2.2 Chemicals

The organic compounds (acronym; manufacturer) used in the experiments include: ethylbenzene (ETB, ACROS, New Jersey, USA), perdeuterated ethylbenzene (D-ETB, Sigma-Aldrich, Steinheim, Germany), toluene (TOL, Merck, Darmstadt, Germany), perdeuterated toluene (D-TOL, Sigma-Aldrich, Seelze, Germany), cis-1,2-dichloroethene (cisDCE, Sigma-Aldrich, Steinheim, Germany), trichloroethene (TCE, Merck, Darmstadt, Germany), and phyto agar in powder (Duchefa, Haarlem, Netherland).

### 5.2.3 Analytical Methods

Gas chromatography (GC) was used to determine the concentrations of all analytes as well as the chlorine isotope ratios for the chlorinated compounds. Compound specific chlorine isotope analysis using quadrupole MS has recently been enabled by advances in analytical techniques [36-40] and evaluation methods [41, 42] and fostered new experimental and modeling applications [43-46]. In this study we used a 7890A gas chromatograph connected to a 5975C quadrupole mass selective detector (MSD) (Agilent, Santa Clara, CA, USA) for both concentration and chlorine isotope analysis. Automated headspace sample injection was performed with a COMBIPAL multipurpose auto-sampler (Gerstel, Australia). The GC was equipped with a split/splitless injector and a capillary column (60 m × 250 μm, 1.4 μm film thickness; Restek, USA). Helium at 1 ml/min was used as carrier gas. The GC oven program was set as follows: 40 °C (2 min) → 110 °C at a rate of 25 °C /min → 200 °C at a rate of 15 °C /min (5min). 250 μL of headspace for each sample were injected for analysis. The quadrupole mass spectrometer was operated in the selected ion mode (SIM) with a dwell time of 50 ms applied to each target ion. The analysis was conducted considering the ions of different analytes: TOL (91.1 m/z) and D-TOL (98.1 m/z) for toluene, and the most abundant ions ETB (91.1 m/z) and D-ETB (98.1 m/z) for ethylbenzene. The target ions for the chlorinated ethenes were: TCE (130, 132, 134, 136 m/z) and cis-DCE (96, 98, 100 m/z). The sample concentration was determined by calibration with external standards.

The isotopic ratios of perdeuterated and light toluene and ethylbenzene were determined by calculating the ratio of the corresponding molar concentrations, and the chlorine isotope ratios of chlorinated organic compounds were determined using the method proposed by Jin et al. [38]:

$$R_{Cl} = \frac{Tot(^{37}Cl)}{Tot(^{35}Cl)} = \frac{\sum_{j=1}^t i \cdot C_j}{\sum_{j=1}^t (h-i) \cdot C_j} \quad (5.1)$$

where  $R_{Cl}$  is the chlorine isotope ratio,  $Tot(^{37}Cl)$  and  $Tot(^{35}Cl)$  are the total number of heavy and light chlorine isotopes,  $h$  and  $i$  are the total number of chlorine atoms and the number of heavy chlorine atoms in a certain molecular chlorine isotopologue, respectively.

**Modeling Diffusive Isotope Fractionation.** Diffusion of dissolved organic contaminants in the glass tubes filled with agarose gel is described by Fick's second law in one dimension:

$$\frac{\partial c}{\partial t} = D_{av} \frac{\partial^2 c}{\partial x^2} \quad (5.2)$$

where  $c = c(x,t)$  is the contaminant concentration, which is function of space ( $x$ ) and time ( $t$ ).  $D_{av}$  is the diffusion coefficient of the organic compound. Tracking independently the concentration of each isotopologue, eq 5.2 can be expressed as:

$$\frac{\partial c_j}{\partial t} = D_j \frac{\partial^2 c_j}{\partial x^2} \quad (5.3)$$

where  $c_j$  is the concentration of a given isotopologue and  $D_j$  is the isotopologue-specific diffusion coefficient.

The diffusion coefficients of the different isotopologues are related to their molecular masses ( $m_j$ ). Based on the outcomes of previous experimental investigations of isotopic fractionation during diffusion of ionic species in water, we used an inverse power law model:  $D_j \propto m_j^{-\beta}$  to describe the dependency of isotopologue-specific diffusion coefficients on the molar masses of the considered isotopologues. Given any two distinct

isotopologues of an organic compound, the inverse power law relation can be written as [24]:

$$\frac{D_1}{D_2} = \left( \frac{m_2}{m_1} \right)^\beta \quad (5.4)$$

where  $D_1$  and  $D_2$  are the diffusion coefficients of the two isotopologues with molecular masses  $m_1$  and  $m_2$ .  $\beta$  is the inverse power law exponent, which equals 0.5 in the ideal case of kinetic gas theory. The magnitude of  $\beta$  and the value of this coefficient used to model diffusive fractionation in aqueous systems caused some discussion in the geochemistry literature [22, 47, 48]. In this study we determined the value of the diffusion coefficient as well as the parameter  $\beta$  from the experimental data.

In the experiments with petroleum hydrocarbons each light and heavy (perdeuterated) isotopologue could be measured individually. Therefore, to evaluate the experimental results, we solved eq 5.3 for each toluene and ethylbenzene isotopologue in a one-dimensional system with same geometry, initial and boundary conditions as the experimental setup. We used a numerical approach with an implicit finite-difference scheme to solve the forward problem and an automated procedure to fit the model to the experimental data, using  $D_j$  as fitting parameter. The fitting procedure was implemented using the capability of the Matlab function `lsqnonlin` to solve nonlinear least square problems. Details on the optimization procedure and on error propagation are provided in the Supporting Information.

In the experiments with chlorinated compounds at natural isotopic abundances, we could not directly measure the concentrations of each isotopologue. Therefore, eq 5.2 was used to describe the spatial and temporal evolution of cisDCE and TCE and to fit the values of  $D_{av}$  from the measured concentration data. The average diffusion coefficient of a given compound can be expressed by the geometric mean of the individual diffusion coefficients of an isotopologue  $j$ , weighted by its relative abundance ( $F_j$ ) [49]:

$$D_{av} = \frac{1}{\frac{F_1}{D_1} + \frac{F_2}{D_2} + \frac{F_3}{D_3} + \dots + \frac{F_j}{D_j}} \quad (5.5)$$

By combining eq 5.4 and eq 5.5, the isotopologue-specific diffusion coefficients ( $D_j$ ) can be written as:

$$D_j = D_{av} \cdot \left( F_1 \cdot \left( \frac{m_1}{m_j} \right)^\beta + F_2 \cdot \left( \frac{m_2}{m_j} \right)^\beta + \dots + F_{j-1} \cdot \left( \frac{m_{j-1}}{m_j} \right)^\beta + F_j \right) \quad (5.6)$$

Using the  $D_{av}$  obtained from the measured concentrations and knowing the relative abundances of the chlorine isotopologues of cisDCE and TCE as well as the measured isotope ratios, the value of the exponent  $\beta$  is fitted for each experimental run.

## 5.3 Results and Discussion

### 5.3.1 Diffusive isotope fractionation of isotopically-labeled petroleum hydrocarbons

Diffusive isotope fractionation of isotopically-labeled petroleum hydrocarbons. Diffusion experiments using 1:2 mixtures of labeled (perdeuterated) and non-labeled toluene and ethylbenzene were conducted and the measured concentration and isotopic gradients are shown in Figure 5.1.

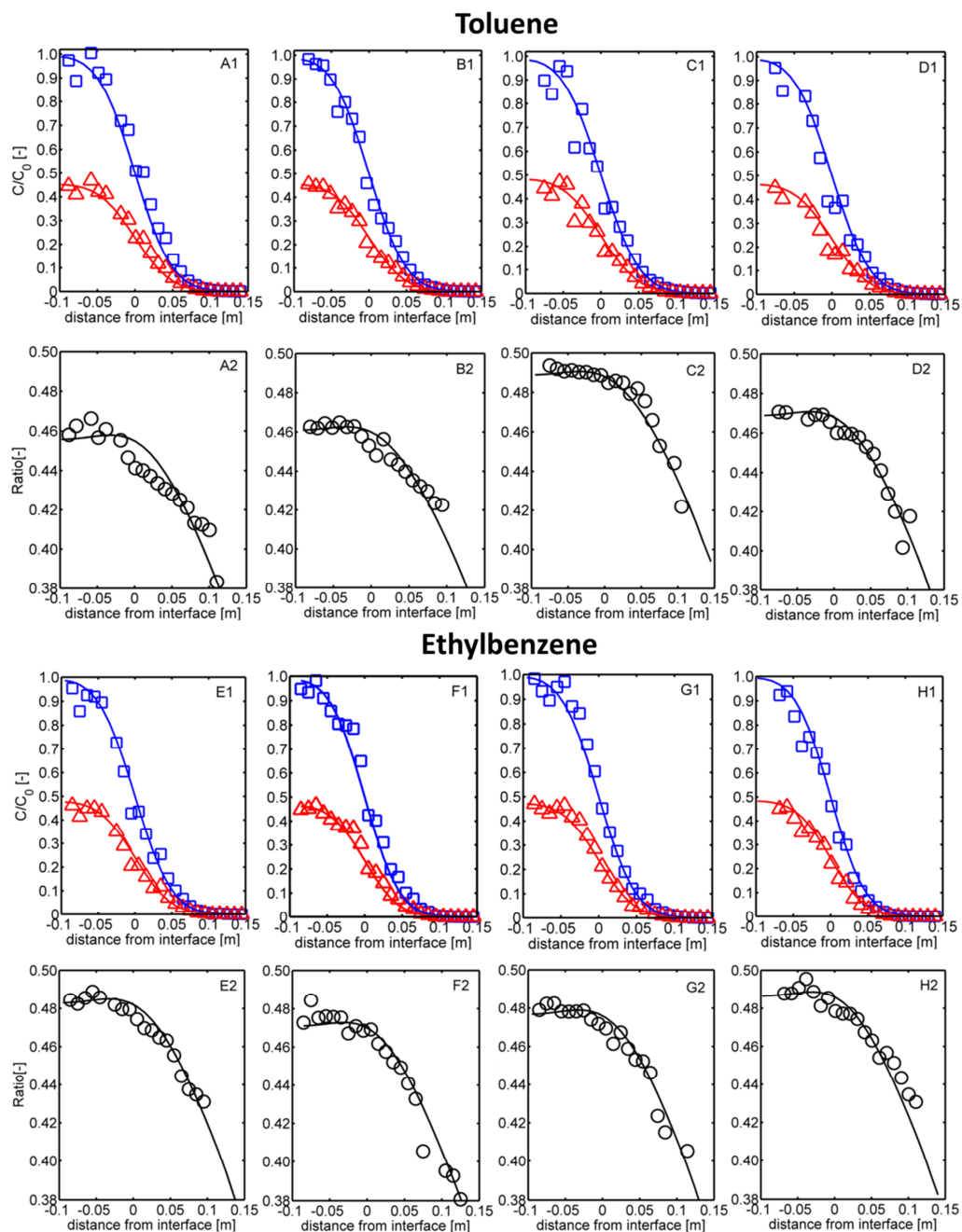


**Figure 5.1.** Spatial gradients of isotopologue concentrations and ratios for toluene and ethylbenzene diffusion experiments. The symbols (squares: light (nondeuterated) isotopologue; triangles: heavy (perdeuterated) isotopologue) represent the measured concentrations (normalized with respect to the initial source concentration of the light isotopologue) and isotope ratios (circles); the solid lines are the best-fit model results (see Table 5.1 for further details).

All experiments showed consistent results and were highly reproducible. The concentration of both light (blue square) and heavy (red triangle) toluene and



ethylbenzene isotopologues show clear spatial gradients along the direction of the diffusive flux, from the source zone towards the initially pristine gel medium. Since the light isotopologues tend to diffuse slightly faster than the heavy ones, the isotopic ratio between the heavy and the light isotopologues changed with the distance from the interphase along the tube. Diffusive isotope fractionation results in a significant decrease of the isotope ratio (up to 0.08) for both toluene (Figure 5.1, A2-D2) and ethylbenzene (Figure 5.1, E2-H2). We fitted the one-dimensional diffusion model (eq 5.2) to the experimental data to estimate the diffusion coefficients of the light and heavy isotopologues ( $D_L$  and  $D_H$ ), and we obtained the inverse power law exponent ( $\beta$ ) expressing the dependence of  $D$  on the molecular mass. The outcomes of the evaluation are summarized in Table 5.1.

**DIFFUSIVE FRACTIONATION OF ORGANIC CONTAMINANTS IN AQUEOUS SOLUTION:  
QUANTIFICATION OF SPATIAL ISOTOPE GRADIENTS**

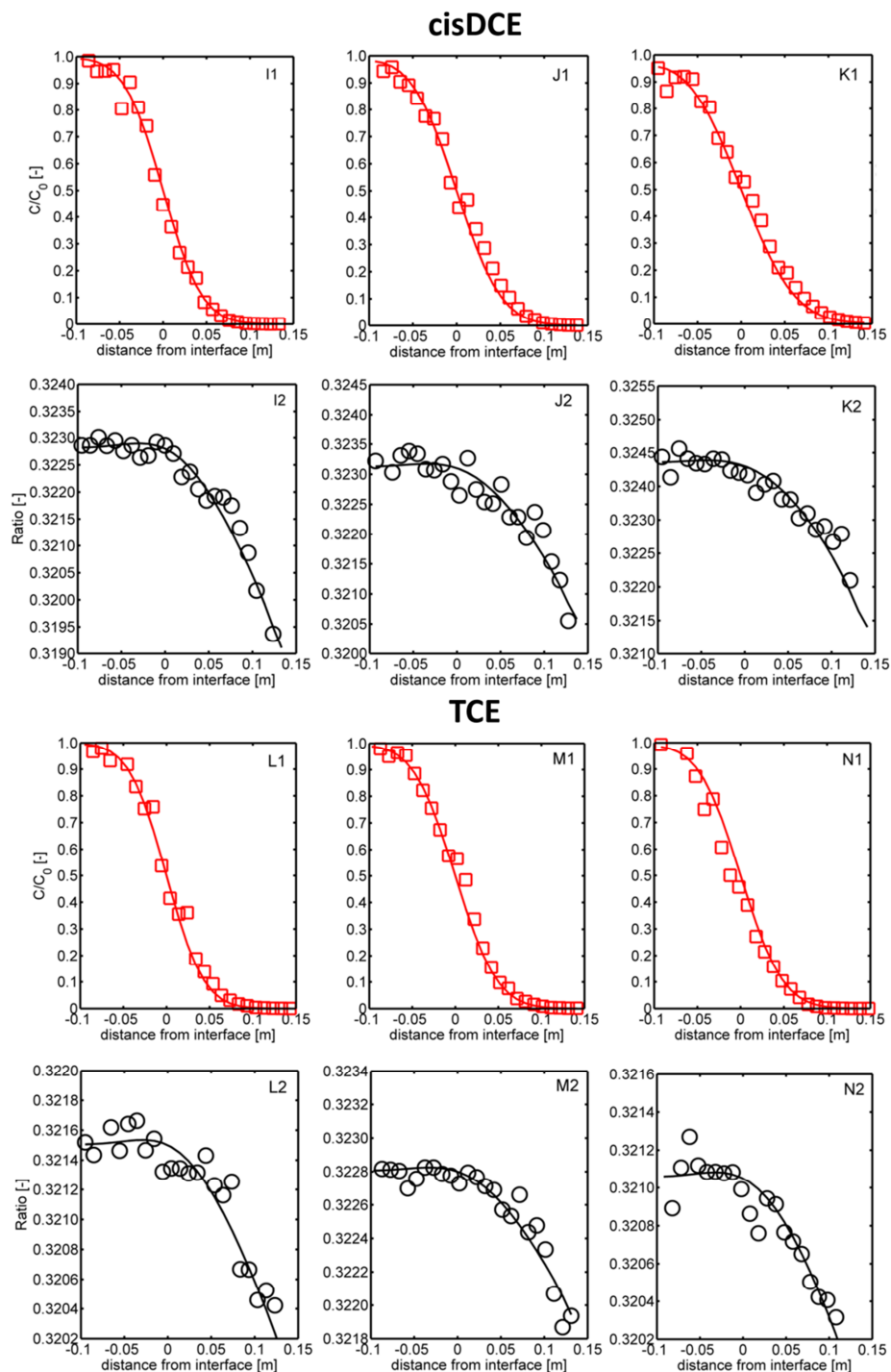
**Table 5. 1.** Overview of the experiments and best-fit parameters for toluene and ethylbenzene diffusion.

| Compound     | Experiment | Time<br>[Days] | $D_L$<br>[ $\times 10^{-9} \text{ m}^2 \text{ s}^{-1}$ ] | $D_H$<br>[ $\times 10^{-9} \text{ m}^2 \text{ s}^{-1}$ ] | $\beta$<br>[-] | Average   |   |             |
|--------------|------------|----------------|--|--|----------------|---|---|-------------|
|              |            |                |  |  |                | $D_L$ [ $\times 10^{-9} \text{ m}^2 \text{ s}^{-1}$ ] | $D_H$ [ $\times 10^{-9} \text{ m}^2 \text{ s}^{-1}$ ] | $\beta$ [-] |
| toluene      | A          | 10.0           | 0.859±0.061  | 0.829±0.060  | 0.430±0.074    | 0.805±0.037   | 0.775±0.037   | 0.455±0.023 |
|              | B          | 10.8           | 0.800±0.032  | 0.769±0.031  | 0.485±0.031    |   |   |             |
|              | C          | 12.5           | 0.779±0.053  | 0.750±0.051  | 0.455±0.054    |   |   |             |
|              | D          | 12.8           | 0.780±0.048  | 0.752±0.046  | 0.450±0.027    |   |   |             |
| ethylbenzene | E          | 10.0           | 0.764±0.025  | 0.734±0.025  | 0.450±0.076    | 0.757±0.017   | 0.727±0.017   | 0.455±0.027 |
|              | F          | 10.5           | 0.761±0.024  | 0.733±0.024  | 0.421±0.080    |   |   |             |
|              | G          | 12.0           | 0.733±0.027  | 0.702±0.026  | 0.483±0.088    |   |   |             |
|              | H          | 12.3           | 0.770±0.028  | 0.738±0.027  | 0.466±0.086    |   |   |             |

The determined diffusion coefficients for the light and heavy isotopologues were  $0.805 \times 10^{-9}$  m<sup>2</sup>/s and  $0.775 \times 10^{-9}$  m<sup>2</sup>/s for toluene, and  $0.757 \times 10^{-9}$  m<sup>2</sup>/s and  $0.727 \times 10^{-9}$  m<sup>2</sup>/s for ethylbenzene. The higher diffusivities of the non-labeled compared to the labeled isotopologues substantiate, for both toluene ( $D_L/D_H=1.039$ ) and ethylbenzene ( $D_L/D_H=1.041$ ), the isotopic diffusive fractionation in the investigated experimental setup. Furthermore, the magnitude of the diffusion coefficient values is consistent with the values computed using the empirical correlations proposed by Wilke and Chang [50] and Worch [51]. The experimental results corrected by the effective volume fraction of the gel and the coefficient of obstruction according to Lauffer [35] as well as the values computed using the above-mentioned empirical correlations are reported in Table S4.1 of the Supporting Information. An average  $\beta$  value of 0.455 was obtained for both toluene and ethylbenzene, close to the upper square root limit. It is considerably larger than the ones reported for ionic species but lower than the ones for helium and for deuterated benzene in water, from the experiments of Jaehne et al. [20] and Mills [52], respectively.

### 5.3.2 Diffusive isotope fractionation of chlorinated compounds at natural abundance

The experiments with chlorinated compounds were conducted in the same experimental setup using cisDCE and TCE at their natural isotopic abundance and measuring the evolution of the chlorine isotope ratio. The measured concentrations and isotope ratios are reported in Figure 5.2.

DIFFUSIVE FRACTIONATION OF ORGANIC CONTAMINANTS IN AQUEOUS SOLUTION:  
QUANTIFICATION OF SPATIAL ISOTOPE GRADIENTS

**Figure 5.2.** Spatial gradients of concentrations and isotope ratios for cisDCE and TCE diffusion experiments. The symbols represent the measured concentrations (squares) and chlorine isotope ratios (circles) sampled at different days; the solid lines are the best-fit model results (see Table 5.2 for further details).

The results are qualitatively similar to the outcomes for the petroleum hydrocarbons. The concentrations of both cisDCE and TCE show a diffusive profile from the source zone towards the initially pristine gel medium. Clear spatial isotopic gradients are obtained due to the different displacement of cisDCE and TCE isotopologues. The extent of change in the chlorine isotope ratio is larger for cisDCE (0.0025-0.0035) than for TCE (0.009-0.011). The values of  $D$  and  $\beta$  were determined with the fitting procedure outlined above, based on eqs. 5.2, 5.5 and 5.6. The values of diffusion coefficients and beta obtained in the different experiments are reported in Table 5.2, whereas the detailed isotopologue-specific properties including computed relative abundances of the cisDCE and TCE chlorine isotopologues and their aqueous diffusivity are summarized in Table S4.2 (Supporting Information (S4)).

**Table 5.2.** Overview of the experiments and best-fit parameters for cisDCE and TCE.

| Compound | Experiment | Time<br>[Days] | D<br>[ $\times 10^{-9} \text{ m}^2 \text{ s}^{-1}$ ] | $\beta$<br>[-]    | Average   |                   |
|----------|------------|----------------|--|-------------------|---|-------------------|
|          |            |                |  |                   | D [ $\times 10^{-9} \text{ m}^2 \text{ s}^{-1}$ ] | $\beta$ [-]       |
| cisDCE   | I          | 7.0            | 1.098 $\pm$ 0.109                                    | 0.104 $\pm$ 0.006 | 1.108 $\pm$ 0.011                                 | 0.088 $\pm$ 0.015 |
|          | J          | 9.0            | 1.105 $\pm$ 0.128                                    | 0.075 $\pm$ 0.006 |   |                   |
|          | K          | 12.8           | 1.120 $\pm$ 0.141                                    | 0.086 $\pm$ 0.007 |   |                   |
| TCE      | L          | 8.0            | 0.898 $\pm$ 0.252                                    | 0.049 $\pm$ 0.007 | 0.898 $\pm$ 0.002                                 | 0.043 $\pm$ 0.008 |
|          | M          | 9.0            | 0.899 $\pm$ 0.523                                    | 0.034 $\pm$ 0.001 |   |                   |
|          | N          | 10.3           | 0.896 $\pm$ 0.218                                    | 0.046 $\pm$ 0.006 |   |                   |

The values obtained for the average diffusion coefficients are  $1.108 \times 10^{-9} \text{ m}^2/\text{s}$  and  $0.898 \times 10^{-9} \text{ m}^2/\text{s}$  for cisDCE and TCE, respectively. As in the case of toluene and ethylbenzene, also the determined diffusion coefficients for the considered chlorinated compounds are in fairly good agreement with the values calculated using published empirical correlations (Table S4.1, Supporting Information (S4)). The values of  $\beta$  for the chlorinated ethenes are 0.088 for cisDCE and 0.043 for TCE. These values are larger but comparable to the ones reported for charged ions [25] and calculated from data reported for dissolved methane and ethane [17]. In comparison to the results for toluene and ethylbenzene, the values of  $\beta$  found for cisDCE and TCE are considerably smaller. A possible reason of such remarkable dissimilarity is that the deuterium substitutions in the case of labeled hydrocarbon molecules do not only imply a

significant difference in the mass but also in the size of the toluene and ethylbenzene molecules. Recently, it was shown by high-resolution neutron powder diffractometry and by theoretical arguments [53] that, starting from a temperature of 170 K, the molecular volume of fully-deuterated benzene ( $C_6D_6$ ) was greater than the one of the light molecule ( $C_6H_6$ ). This could explain the large difference in aqueous diffusion coefficient between  $C_6H_6$  and  $C_6D_6$  reported in the early work of Mills [52] as well as the extensive diffusive fractionation between labeled and non-labeled petroleum hydrocarbons (toluene:  $C_7H_8/C_7D_8$ ; ethylbenzene:  $C_8H_{10}/C_8D_{10}$ ) observed in our diffusion experiments and quantified by an average beta of 0.455 (Table 5.1). Moreover, additional factors that contribute to the different beta values observed in our experiments for the petroleum hydrocarbons and for the chlorinated compounds can be the polarity and the solute-solvent interactions. In fact, similarly to what observed for ionic species, the more polar chlorinated molecules interact more strongly with the water molecules thus leading to more attenuated diffusive fractionation effects. Such arguments, although still rather qualitative and requiring further evidence, might also explain the relative difference between the beta values of cisDCE and TCE, with the latter being smaller due to stronger solute-solvent interaction.

Using the average values for the diffusion coefficients ( $D$ ) and for the exponent ( $\beta$ ) of the inverse power law relation between  $D$  and the molecular mass determined from the experiments, we performed forward modeling to assess the temporal evolution of the chlorine isotopic gradients for both cisDCE and TCE. We consider a time period that covers and goes beyond the one of the experiments and we show the results of chlorine isotope ratios as  $\delta^{37}Cl$ , referenced to the chlorine isotope ratio of standard mean ocean chloride (SMOC) (Figure 5.3). The outcomes of the simulations clearly show remarkable isotopic gradients for both cisDCE and TCE. Accordingly to the experimental findings, cisDCE shows the largest isotopic differences (up to -5‰) compared to TCE (up to -3‰). The profiles have steeper isotope gradients at early times when the sharp concentration fronts of the different isotopologues propagate in the tube from the source zone towards the pristine gel medium. As time progresses, the diffusion fronts reach the boundary and the spatial concentration and isotope gradients tend to be smoothed and they finally tend to disappear at late times (200 days). This effect depends on the geometry and boundary conditions of our

experimental setup. The conditions are likely to be different in environmental systems, which are typically open systems characterized by larger scales compared to the ones of our experimental setup.

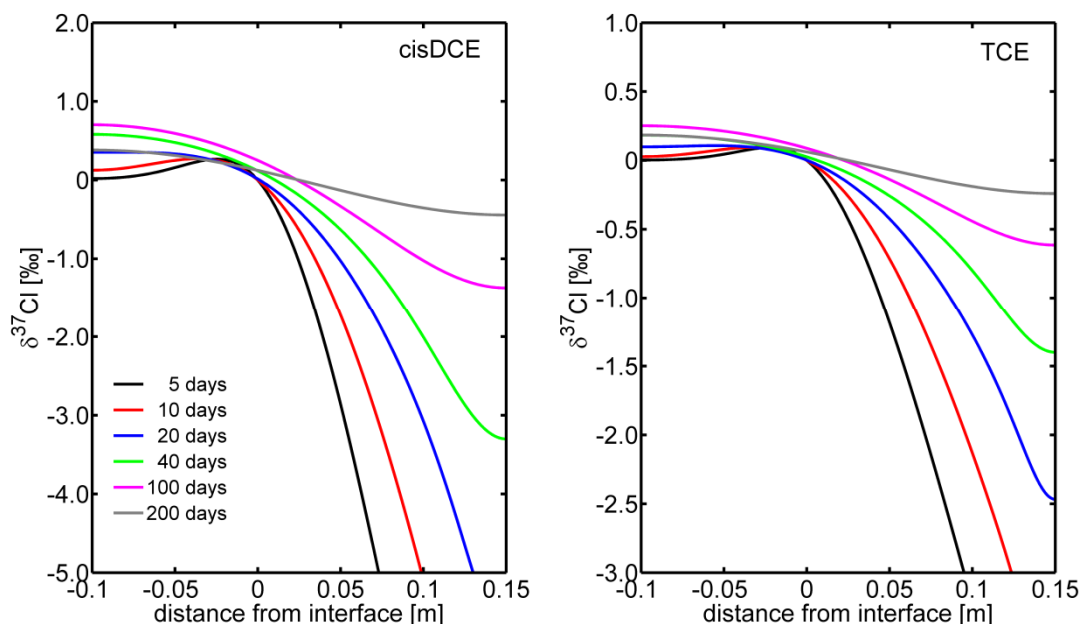


**Figure 5. 3.** Spatial and temporal change of  $\delta^{37}\text{Cl}$  values for cisDCE and TCE diffusion.

## Environmental Significance

The development of diffusive isotope gradients during transport of organic contaminants has important environmental implications. For instance, many subsurface environments (e.g., clay and silt aquitards, unweathered and unfractured rocks, lake and marine sediments etc.) are diffusion-dominated systems. The migration of organic compounds in such environments is likely to be strongly affected by isotopologue-specific diffusion. As an example, Figure 5.4 reports the expected extent of diffusive isotope fractionation in an unbounded aquitard. Simulations of diffusion were performed in a one-dimensional domain representing a vertical profile in a low-permeability porous medium. The contaminant source containing cisDCE and TCE was initially located at the bottom 0.5 m of the profiles. The parameter  $D$  and  $\beta$

were selected identical to the ones experimentally-determined in this study with the only exception that, in the simulations, the effective aqueous diffusion coefficients were corrected by a tortuosity of 2.5, taking into account that in this scenario diffusion occurs only through the void space of the porous medium. The resulting spatial isotopic gradients computed after a 10-year diffusion period are shown in Fig. 5.4. Significant  $\delta^{37}\text{Cl}$  gradients were obtained for both cisDCE and TCE with more depleted values in the initially pristine region at the top, towards which the contaminants diffuse, and slightly enriched values at the bottom due to the faster migration of light isotopologues, which tend to leave the source zone at a slightly faster diffusive rate.

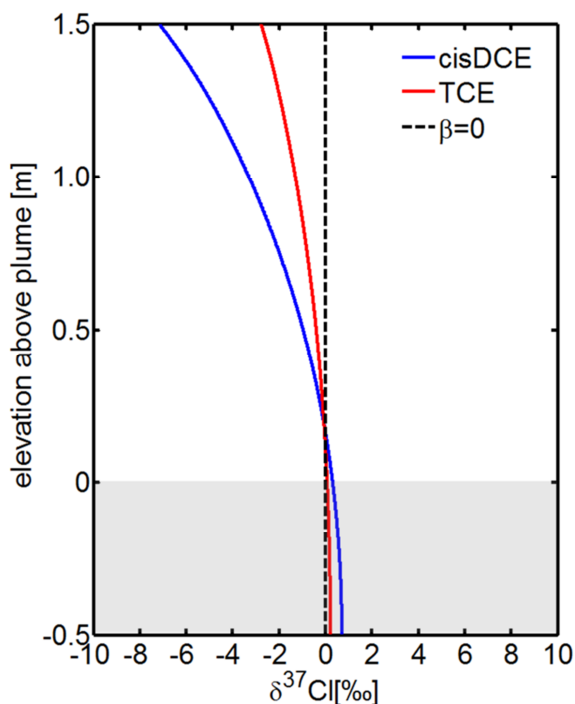


**Figure 5. 4.** Diffusion-induced chlorine isotope fractionation in a low-permeability subsurface layer. The continuous lines represent the values for cisDCE and TCE, after a simulation time of 10 years, with the parameters  $D$  and  $\beta$  determined in this study; the dashed line is the case with no diffusive isotope fractionation. The gray area delineates the location of the initial source zone.

Besides the cases of purely diffusion-dominated transport, the findings of this study are important also for other conditions frequently found in natural porous media. In fact, aquifer



systems are complex heterogeneous formations where diffusion-limited mass transfer occurs between high and low flow velocity zones. For instance, solute back-diffusion from silt and clay aquitards into more permeable layers has been recognized as an important process controlling the persistence of organic contaminant plumes in groundwater [28, 29]. Furthermore, also in cases in which mass-transfer is advection-dominated, recent experimental and multi-scale modeling studies have shown a critical and quantitatively important role of diffusion [34, 54]. The outcomes of the present work help understanding and quantifying the significance of isotopologue-specific diffusion of selected widespread organic contaminants. Due to the scarcity of currently available data on diffusive isotope fractionation of organic compounds in water and to the crucial importance of diffusion for contaminant mass transport in many environmental systems such as geologic formations, further research is required to extend the investigation to other common groundwater contaminants. This will produce high-resolution experimental data that are instrumental for an integrated interpretation of isotopic signatures in environmental systems and for the quantitative application of CSIA taking into account the fractionation effects of both physical and transformation processes. Moreover, we think that further experimental investigation and studies based on molecular dynamics simulations will help to shed light on the role of factors such as the molecular structure of the solute, temperature, polarity and the interaction between solute and solvents molecule, on diffusive isotopic fractionation of organic compounds in aqueous systems.

### **Supporting Information Available**

Schematic descriptions of the experimental protocol, the parameter-fitting approach, the comparison of the experimental results with the values of aqueous diffusion coefficients based on empirical correlations and a summary of the isotopologue-specific properties of the compounds at natural isotopic abundance are available in the Supporting Information.

## References

1. Elsner, M.; Zwank, L.; Hunkeler, D.; Schwarzenbach, R. P., A new concept linking observable stable isotope fractionation to transformation pathways of organic pollutants. *Environ. Sci. Technol.* **2005**, *39*, (18), 6896-6916.
2. Elsner, M., Stable isotope fractionation to investigate natural transformation mechanisms of organic contaminants: principles, prospects and limitations. *J. Environ. Monit.* **2010**, *12*, (11), 2005-2031.
3. Schmidt, T. C.; Zwank, L.; Elsner, M.; Berg, M.; Meckenstock, R. U.; Haderlein, S. B., Compound-specific stable isotope analysis of organic contaminants in natural environments: a critical review of the state of the art, prospects, and future challenges. *Anal. Bioanal. Chem.* **2004**, *378*, (2), 283-300.
4. Thullner, M.; Centler, F.; Richnow, H. H.; Fischer, A., Quantification of organic pollutant degradation in contaminated aquifers using compound specific stable isotope analysis - Review of recent developments. *Org. Geochem.* **2012**, *42*, (12), 1440-1460.
5. Hatzinger, P. B.; Bohlke, J.; Sturchio, N. C., Application of stable isotope ratio analysis for biodegradation monitoring in groundwater. *Current opinion in biotechnology* **2013**, *24*, (3), 542-9.
6. Thullner, M.; Kampara, M.; Richnow, H. H.; Harms, H.; Wick, L. Y., Impact of bioavailability restrictions on microbially induced stable isotope fractionation. 1. Theoretical calculation. *Environ. Sci. Technol.* **2008**, *42*, (17), 6544-6551.
7. Tobler, N. B.; Hofstetter, T. B.; Schwarzenbach, R. P., Carbon and Hydrogen Isotope Fractionation during Anaerobic Toluene Oxidation by *Geobacter metallireducens* with Different Fe(III) Phases as Terminal Electron Acceptors. *Environ. Sci. Technol.* **2008**, *42*, (21), 7786-7792.
8. Aeppli, C.; Berg, M.; Cirpka, O. A.; Holliger, C.; Schwarzenbach, R. P.; Hofstetter, T. B., Influence of Mass-Transfer Limitations on Carbon Isotope Fractionation during Microbial Dechlorination of Trichloroethene. *Environ. Sci. Technol.* **2009**, *43*, (23), 8813-8820.
9. Kopinke, F. D.; Georgi, A.; Voskamp, M.; Richnow, H. H., Carbon isotope fractionation of organic contaminants due to retardation on humic substances: Implications for natural attenuation studies in aquifers. *Environ. Sci. Technol.* **2005**, *39*, (16), 6052-6062.
10. Hohener, P.; Yu, X. J., Stable carbon and hydrogen isotope fractionation of dissolved organic groundwater pollutants by equilibrium sorption. *J. Contam. Hydrol.* **2012**, *129*, 54-61.
11. Bouchard, D.; Hohener, P.; Hunkeler, D., Carbon Isotope Fractionation During Volatilization of Petroleum Hydrocarbons and Diffusion Across a Porous Medium: A Column Experiment. *Environ. Sci. Technol.* **2008**, *42*, (21), 7801-7806.
12. Jeannotat, S.; Hunkeler, D., Chlorine and Carbon Isotopes Fractionation during Volatilization and Diffusive Transport of Trichloroethene in the Unsaturated Zone. *Environ. Sci. Technol.* **2012**, *46*, (6), 3169-3176.
13. LaBolle, E. M.; Fogg, G. E.; Eweis, J. B.; Gravner, J.; Leaist, D. G., Isotopic fractionation by diffusion in groundwater. *Water Resour. Res.* **2008**, *44*, (7).
14. Rolle, M.; Chiogna, G.; Bauer, R.; Griebler, C.; Grathwohl, P., Isotopic Fractionation by Transverse Dispersion: Flow-through Microcosms and Reactive Transport Modeling Study. *Environ. Sci. Technol.* **2010**, *44*, (16), 6167-6173.
15. Eckert, D.; Rolle, M.; Cirpka, O. A., Numerical simulation of isotope fractionation in steady-state bioreactive transport controlled by transverse mixing. *J. Contam. Hydrol.* **2012**, *140*, 95-106.
16. Van Breukelen, B. M.; Rolle, M., Transverse Hydrodynamic Dispersion Effects on Isotope Signals in Groundwater Chlorinated Solvents' Plumes. *Environ. Sci. Technol.* **2012**, *46*, (14), 7700-7708.

17. Schloemer, S.; Krooss, B. M., Molecular transport of methane, ethane and nitrogen and the influence of diffusion on the chemical and isotopic composition of natural gas accumulations. *Geofluids* **2004**, *4*, (1), 81-108.
18. Risk, D.; Kellman, L., Isotopic fractionation in non-equilibrium diffusive environments. *Geophys. Res. Lett.* **2008**, *35*, (2).
19. Bourg, I. C.; Sposito, G., Isotopic fractionation of noble gases by diffusion in liquid water: Molecular dynamics simulations and hydrologic applications. *Geochim. Cosmochim. Acta* **2008**, *72*, (9), 2237-2247.
20. Jaehne B., H. G., Dietrich W., Measurement of the diffusion coefficients of sparingly soluble gases in water. *Journal of Geophysical Research: Oceans* **1987**, *92*, (C10).
21. Bourg, I. C.; Sposito, G., Molecular dynamics simulations of kinetic isotope fractionation during the diffusion of ionic species in liquid water. *Geochim. Cosmochim. Acta* **2007**, *71*, (23), 5583-5589.
22. Donahue, M. A.; Werne, J. P.; Meile, C.; Lyons, T. W., Modeling sulfur isotope fractionation and differential diffusion during sulfate reduction in sediments of the Cariaco Basin. *Geochim. Cosmochim. Acta* **2008**, *72*, (9), 2287-2297.
23. Eggenkamp, H. G. M.; Coleman, M. L., The effect of aqueous diffusion on the fractionation of chlorine and bromine stable isotopes. *Geochim. Cosmochim. Acta* **2009**, *73*, (12), 3539-3548.
24. Richter, F. M.; Mendybaev, R. A.; Christensen, J. N.; Hutcheon, I. D.; Williams, R. W.; Sturchio, N. C.; Beloso, A. D., Kinetic isotopic fractionation during diffusion of ionic species in water. *Geochim. Cosmochim. Acta* **2006**, *70*, (2), 277-289.
25. Bourg, I. C.; Richter, F. M.; Christensen, J. N.; Sposito, G., Isotopic mass dependence of metal cation diffusion coefficients in liquid water. *Geochim. Cosmochim. Acta* **2010**, *74*, (8), 2249-2256.
26. Wortmann, U. G.; Chernyavsky, B. M., The significance of isotope specific diffusion coefficients for reaction-transport models of sulfate reduction in marine sediments. *Geochim. Cosmochim. Acta* **2011**, *75*, (11), 3046-3056.
27. Beekman, H. E.; Eggenkamp, H. G. M.; Appelo, C. A. J., An integrated modelling approach to reconstruct complex solute transport mechanisms - Cl and delta Cl-37 in pore water of sediments from a former brackish lagoon in The Netherlands. *Appl. Geochem.* **2011**, *26*, (3), 257-268.
28. Rasa, E.; Chapman, S. W.; Bekins, B. A.; Fogg, G. E.; Scow, K. M.; Mackay, D. M., Role of back diffusion and biodegradation reactions in sustaining an MTBE/TBA plume in alluvial media. *J. Contam. Hydrol.* **2011**, *126*, (3-4), 235-247.
29. Mackay, D. M.; Cherry, J. A., GROUNDWATER CONTAMINATION - PUMP-AND-TREAT REMEDIATION .2. *Environ. Sci. Technol.* **1989**, *23*, (6), 630-636.
30. Hunkeler, D.; Chollet, N.; Pittet, X.; Aravena, R.; Cherry, J. A.; Parker, B. L., Effect of source variability and transport processes on carbon isotope ratios of TCE and PCE in two sandy aquifers. *J. Contam. Hydrol.* **2004**, *74*, (1-4), 265-282.
31. Hunkeler, D.; Aravena, R.; Shouakar-Stash, O.; Weisbrod, N.; Nasser, A.; Netzer, L.; Ronen, D., Carbon and Chlorine Isotope Ratios of Chlorinated Ethenes Migrating through a Thick Unsaturated Zone of a Sandy Aquifer. *Environ. Sci. Technol.* **2011**, *45*, (19), 8247-8253.
32. Rolle, M.; Hochstetler, D.; Chiogna, G.; Kitanidis, P. K.; Grathwohl, P., Experimental Investigation and Pore-Scale Modeling Interpretation of Compound-Specific Transverse Dispersion in Porous Media. *Transp. Porous Media* **2012**, *93*, (3), 347-362.
33. Hochstetler, D. L.; Rolle, M.; Chiogna, G.; Haberer, C. M.; Grathwohl, P.; Kitanidis, P. K., Effects of compound-specific transverse mixing on steady-state reactive plumes: Insights from pore-scale simulations and Darcy-scale experiments. *Adv. Water Resour.* **2013**, *54*, 1-10.
34. Rolle, M., Muniruzzaman, M., Haberer, C.M., Grathwohl, P., , Coulombic effects in advection-dominated transport of electrolytes in porous media: Multicomponent ionic dispersion. *Geochim. Cosmochim. Acta* **2013**.

35. Lauffer, M. A., Theory of diffusion in gels. *Biophys Jour* **1961**, *1*, ((3)), 205-213.
36. Sakaguchi-Soder, K.; Jager, J.; Grund, H.; Matthaus, F.; Schuth, C., Monitoring and evaluation of dechlorination processes using compound-specific chlorine isotope analysis. *Rapid Commun. Mass Spectrom.* **2007**, *21*, (18), 3077-3084.
37. Aeppli, C.; Holmstrand, H.; Andersson, P.; Gustafsson, O., Direct Compound-Specific Stable Chlorine Isotope Analysis of Organic Compounds with Quadrupole GC/MS Using Standard Isotope Bracketing. *Anal. Chem.* **2010**, *82*, (1), 420-426.
38. Jin, B. A.; Laskov, C.; Rolle, M.; Haderlein, S. B., Chlorine Isotope Analysis of Organic Contaminants Using GC-qMS: Method Optimization and Comparison of Different Evaluation Schemes. *Environ. Sci. Technol.* **2011**, *45*, (12), 5279-5286.
39. Bernstein, A.; Shouakar-Stash, O.; Ebert, K.; Laskov, C.; Hunkeler, D.; Jeannotat, S.; Sakaguchi-Soder, K.; Laaks, J.; Jochmann, M. A.; Cretnik, S.; Jager, J.; Haderlein, S. B.; Schmidt, T. C.; Aravena, R.; Elsner, M., Compound-Specific Chlorine Isotope Analysis: A Comparison of Gas Chromatography/Isotope Ratio Mass Spectrometry and Gas Chromatography/Quadrupole Mass Spectrometry Methods in an Interlaboratory Study. *Anal. Chem.* **2011**, *83*, (20), 7624-7634.
40. Cincinelli, A.; Pieri, F.; Zhang, Y.; Seed, M.; Jones, K. C., Compound Specific Isotope Analysis (CSIA) for chlorine and bromine: A review of techniques and applications to elucidate environmental sources and processes. *Environ. Pollut.* **2012**, *169*, 112-127.
41. Hofstetter, T. B.; Reddy, C. M.; Heraty, L. J.; Berg, M.; Sturchio, N. C., Carbon and chlorine isotope effects during abiotic reductive dechlorination of polychlorinated ethanes. *Environ. Sci. Technol.* **2007**, *41*, (13), 4662-4668.
42. Elsner, M.; Hunkeler, D., Evaluating chlorine isotope effects from isotope ratios and mass spectra of polychlorinated molecules. *Anal. Chem.* **2008**, *80*, (12), 4731-4740.
43. Heraty, L. J.; Fuller, M. E.; Huang, L.; Abrajano, T.; Sturchio, N. C., Isotopic fractionation of carbon and chlorine by microbial degradation of dichloromethane. *Org. Geochem.* **1999**, *30*, (8A), 793-799.
44. Numata, M.; Nakamura, N.; Koshikawa, H.; Terashima, Y., Chlorine isotope fractionation during reductive dechlorination of chlorinated ethenes by anaerobic bacteria. *Environ. Sci. Technol.* **2002**, *36*, (20), 4389-4394.
45. Hunkeler, D.; Van Breukelen, B. M.; Elsner, M., Modeling Chlorine Isotope Trends during Sequential Transformation of Chlorinated Ethenes. *Environ. Sci. Technol.* **2009**, *43*, (17), 6750-6756.
46. Jin, B.; Haderlein, S. B.; Rolle, M., Integrated carbon and chlorine isotope modeling: applications to chlorinated aliphatic hydrocarbons dechlorination. *Environ. Sci. Technol.* **2013**, *47*, (3), 1443-51.
47. Donahue, M. A.; Werne, J. P.; Meile, C.; Lyons, T. W., Response to comment by IC Bourg on "Modeling sulfur isotope fractionation and differential diffusion during sulfate reduction in sediments of the Cariaco Basin" by MA Donahue, JP Werne, C. Meile, and TW Lyons. *Geochim. Cosmochim. Acta* **2008**, *72*, (23), 5855-5856.
48. Bourg, I. C., Comment on "Modeling sulfur isotope fractionation and differential diffusion during sulfate reduction in sediments of the Cariaco Basin" by MA Donahue, JP Werne, C. Meile and TW Lyons. *Geochim. Cosmochim. Acta* **2008**, *72*, (23), 5852-5854.
49. Wilke, C. R., a viscosity equation for gas mixtures. In *The journal of chemical physics*, 1950; p 3.
50. Wilke, C. R. C., P.C., *American Institute of Chemical Engineers Journal* **1955**, *1*, 264.
51. Worch, E., A new equation for the calculation of diffusion coefficients for dissolved substances. In 1993; Vol. 81, pp 289-297.
52. Mills, R., Diffusion relationships in the binary system benzene-perdeuteriobenzene at 25 C. *the journal of physical chemistry* **1976**, *80*.
53. Dunitz, J. D.; Ibberson, R. M., Is deuterium always smaller than protium? *Angewandte Chemie-International Edition.* **2008**, *47*, (22), 4208-4210.

54. Rolle, M., Chiogna, G., Hochstetler, D.L., Kitanidis, P.K., On the importance of diffusion and compound-specific mixing for groundwater transport: an investigation from pore to field scale. *J. Contam. Hydrol.* **2013**.



# Chapter 6

---

## Conclusions and Outlook

### 6.1 Conclusions

This thesis focuses on the implementation of isotope techniques to understand transformation and physical processes that influence the fate of groundwater organic contaminants. The different works conducted within the thesis, include the analytical method for chlorine CSIA using GC-qMS, the integrated carbon–chlorine dual-isotope modeling approach, the mechanistic multi-element isotope modeling method, and the laboratory experiments to quantify diffusion-induced isotope fractionation of organic contaminants. In the following, we summarize the main conclusions of each study.

- *Chlorine CSIA using GC-qMS.* Our results demonstrate that the GC-qMS method needs proper validation as its performance depends on the applied evaluation scheme, the selected instrumental parameters and the compound analyzed. All these factors need to be considered and optimized in order to obtain high quality GC-qMS measurements. Also, it is important to note that the chlorine isotope ratios tend to be overestimated in the presence of an increasing number of  $^{13}\text{C}$  atoms in the analyte. This error is neglectable for chlorinated ethenes, but becomes significant for chlorinated compounds containing a higher number of carbon atoms such as chlorinated benzenes. Therefore, a correction on the chlorine isotope ratio is necessary in these cases.
- *Integrated C–Cl isotope modeling approach.* Our approach naturally integrates carbon and chlorine isotope modeling schemes by considering the simultaneous evolution of all carbon-chlorine isotopologues. The three different applications shown in chapter 2 demonstrate the validity and the potential of the proposed modeling approach. Particularly promising are the outcomes of the simulations of the mass-transfer limited biodegradation example which demonstrates the capability of the method to correctly “de-mask” the effects of interphase mass-transfer.

- *Mechanistic multi-element isotope modeling method.* The modeling approach proposed in chapter 3 allows the mechanistic description of contaminant degradation through different reaction pathways and the associated multi-element isotope evolution, including both primary and secondary isotope effects. The modeling methodology described in this study is based on position-specific isotopologues. This allows tracking directly the isotopic evolution that occurs at fractionating positions specific for distinct compounds and reaction mechanisms. Such possibility is of great advantage also for a quantitative interpretation of position-specific isotope analysis which is developing the advances of analytical techniques (McKelvie et al., 2010; Breider and Hunkeler, 2011; Wuerfel et al., 2013).
- *Diffusion-induced isotope fractionation of organic contaminants.* The outcomes of the experimental work allow to understand and quantify the significance of isotopologue-specific diffusion of selected widespread organic contaminants. The  $\beta$  values observed for the organic compounds directly relate the isotopologue-specific diffusion coefficients with the ratio of molecular masses. The  $\beta$  values obtained for the experiments using mixture of perdeuterated and nondeuterated ETB and TOL are much bigger than those obtained for cisDCE and TCE at natural abundances. The differences on  $\beta$  values can be influenced by several possible factors, such as the relative mass difference between isotopologues, the molecular structure of the solute, temperature, polarity and the interaction between solute and solvents molecules.

## 6.2 Outlook

Stable isotope techniques significantly improve the understanding of the fate of organic contaminants in aquatic environmental systems, and thus, have been increasingly applied in contaminant hydrology during the last decade. Recent advances on analytical techniques allows precise measurements of isotope ratios of different elements, and therefore extended this approach from single element to multi-dimension (i.e. 2D and 3D), offering new possibility to obtain mechanistic information valuable for identifying and elucidating transformation processes (Elsner, 2010; Elsner et al., 2012).



Based on the results of this work, possible directions for further developments of the multi-element isotope approaches can be summarized in the following points:

- *GC-qMS approach for Cl CSIA.* So far, this approach has been mainly applied to volatile compounds using headspace injection. However, headspace analysis is not feasible for some chlorinated organic compounds that have relatively low air–water partitioning coefficients, such as chlorinated benzenes, as well as for samples at low concentrations. In these cases, no sufficient peak intensity can be achieved for chlorine isotope ratio determinations. Therefore, different injection (e.g., liquid injection) or extraction techniques (e.g., solid phase micro extraction; purge and trap) are necessary to increase the masses that are injected on-column. Moreover, brominated organic contaminants are also of great environmental concern, and bromine CSIA has great potential to study the fate of brominated compounds. In principle, the GC-qMS approach is also able to be adapted for on-line bromine CSIA. Thus, the applied evaluation scheme and the selected instrumental parameters also need to be carefully evaluated for brominated organic compounds.
- *Modeling multi-dimensional isotope evolutions.* The assessment of 2D isotope experimental data commonly relies on the interpretation of dual-isotope plots based on the ratio between bulk enrichment factors or on linear regression of measured dual-isotope data. Despite the fact that modeling approaches are required to improve the interpretation of multi-element isotope data for environmentally-relevant transformation processes of organic contaminants, their development and application are still rather limited. For an improved interpretation of multi-element isotope data, the development of analytical techniques and mechanistic understanding of isotope evolution should be accompanied by advances in modeling approaches. During a reaction, isotope fractionation often simultaneously involves two or even more elements and one compound might also degrade simultaneously through different reaction pathways. To address these complex cases, advanced multi-dimensional isotope modeling should be self-consistent and mechanism-specific.
- *Diffusion-induced isotope fractionation.* Due to the scarcity of currently available data on diffusive isotope fractionation of organic compounds in water and to the

crucial importance of diffusion for contaminant mass transport in many environmental systems such as geologic formations, further research is required to extend the investigation to other common groundwater contaminants. This will produce high-resolution experimental data that are instrumental for an integrated interpretation of isotopic signatures in environmental systems and for the quantitative application of CSIA taking into account the fractionation effects of both physical and transformation processes. Moreover, we think that further experimental investigation and studies based on molecular dynamics simulations will help to shed light on the role of factors such as the molecular structure of the solute, temperature, polarity, and the interaction between solute and solvent molecules, on diffusive isotopic fractionation of organic compounds in aqueous systems.

## References

- Breider, F., Hunkeler, D., 2011. Position-specific carbon isotope analysis of trichloroacetic acid by gas chromatography/isotope ratio mass spectrometry. *Rapid Communications in Mass Spectrometry* 25, 3659-3665.
- Elsner, M., 2010. Stable isotope fractionation to investigate natural transformation mechanisms of organic contaminants: principles, prospects and limitations. *J. Environ. Monit.* 12, 2005-2031.
- Elsner, M., Jochmann, M.A., Hofstetter, T.B., Hunkeler, D., Bernstein, A., Schmidt, T.C., Schimmelmann, A., 2012. Current challenges in compound-specific stable isotope analysis of environmental organic contaminants. *Anal. Bioanal. Chem.* 403, 2471-2491.
- McKelvie, J.R., Elsner, M., Simpson, A.J., Lollar, B.S., Simpson, M.J., 2010. Quantitative Site-Specific H-2 NMR Investigation of MTBE: Potential for Assessing Contaminant Sources and Fate. *Environmental Science & Technology* 44, 1062-1068.
- Wuerfel, O., Greule, M., Keppler, F., Jochmann, M.A., Schmidt, T.C., 2013. Position-specific isotope analysis of the methyl group carbon in methylcobalamin for the investigation of biomethylation processes. *Anal. Bioanal. Chem.* 405, 2833-2841.



## Acknowledgement

There are group of people that I would like to thank

**Professor Stefan Haderlein** for continuously helping and inspiring me during my Ph.D work. His excellent supports and useful discussions are always appreciated.

**Dr.-Ing Massimo Rolle** for intensively guiding my work during my entire Ph.D. Without his great support, no work can be organized and accomplished in such an efficient way. Specially, I would like to thank him for backing me up when I was down in the valley of my Ph.D life (i.e. 2010 summer).

**Professor Peter Grathwohl, Professor Christian Zwiener, Prof. Olaf Cirpka, Dr. Martin Elsner, Dr. Christine Laskov, Dr. Satoshi Endo, Dr. Raul Martinez and Dr. Gabriele Chiogna** for useful discussions during my master and Ph.D studies.

**Ting Li** for contributing to the study in chapter 5 during her master thesis.

**Karin Ebert and Daniel Buchner** for sharing their information and experience during my lab work.

**The mensa team (Dominik Eckert, Alexander Lübben, Chuanhe Lu, Doro Kennedy, Stephane Ngueleu, Muhammad Muniruzzaman)**, without you guys, lunch would be boring.

**All my friends in Europe and China.**

**My parents** for their unconditional support, understanding and love.

Last but not least, **IPSWaT (BMBF)** for funding my master and Ph.D studies in Germany.



## Supporting Information

### S1. Chlorine Isotope Analysis of Organic Contaminants Using GC-qMS: Method Optimization and Comparison of Different Evaluation Schemes

#### S1.3 Details on Chlorine Isotope Ratio Computations

*Deriving Relative Isotopologue Abundances.* Expressing the relative isotopologue abundances of molecular chlorinated compounds and corresponding fragments is the first step to compute the chlorine isotope ratio. Taking PCE as an example and light  $^{35}\text{Cl}$  (L %) and heavy  $^{37}\text{Cl}$  (H %) chlorine atoms; the probability of encountering a PCE molecule containing two  $^{35}\text{Cl}$  and two  $^{37}\text{Cl}$  is 6·H·H·L·L. The number, “6”, indicates six possible patterns of heavy and light isotope compositions (i.e. HHLL, HLHL, HLLH, LHHL, LHLH and LLHH). The computed probability stands for the relative abundance of  $\text{C}_2^{35}\text{Cl}_2^{37}\text{Cl}_2$ . The probability that an event will occur “ $k$ ” times out of “ $n$ ” trials can be computed by the binomial formula (1):

$$P = \binom{n}{k} p^k (1-p)^{n-k} \quad (\text{S1.1})$$

$$\binom{n}{k} = \frac{(n-k+1) \cdot (n-k+2) \cdots (n-1) \cdot (n)}{k!} \quad (\text{S1.2})$$

where  $n$  is the number of trials,  $k$  is the specific number that an event will occur, and  $p$  is the probability that the event is to occur on each particular trial. Eqn. S1.2 expresses the binomial coefficient, which represents the number of possible patterns (1).

For the general case of chlorinated compounds, this equation can be used to compute the relative abundance of the chlorinated isotopologue containing “ $k$ ”  $^{37}\text{Cl}$  atoms out of a total of “ $n$ ” chlorine atoms. This corresponds to:

$$A = \binom{n}{k} H^k L^{n-k} \quad (\text{S1.3})$$

where  $A$  is the relative abundance of a certain isotopologue of a chlorinated compound,  $H$  (%) is the abundance of  $^{37}\text{Cl}$ ,  $L$  (%) is the abundance of  $^{35}\text{Cl}$ ,  $n$  is the total number of

chlorine atoms in a certain chlorinated compound,  $k$  is the number of  $^{37}\text{Cl}$  atoms in a specified isotopologue. Here, the binomial coefficient is defined as the number of possible positions of chlorine atoms on a certain molecule.

Due to the excessive electron impact (EI) energy in the ion source of mass spectrometry, not only charged molecular ions but also fragment ions exist in the mass spectrum. Isotopologues with different chlorine isotope compositions are identified by the corresponding mass over charge ratios ( $m/z$ ). Based on the statistical method explained above, all the relative ion abundances of molecular chlorinated ethenes and their corresponding fragments are mathematically expressed and summarized in Figure S1.1.



| PCE | Molecular group   | Mass | Relative abundance             |      | Chlorine isotope ratio        |               |
|-----|---|------|--------------------------------|------|-------------------------------|---------------|
|     | $^{12}\text{C}_2^{35}\text{Cl}_4$                       | 164* | L <sup>4</sup>                 | (1)  | $\xrightarrow{\text{R}_M}$    |               |
|     | $^{12}\text{C}_2^{35}\text{Cl}_3^{37}\text{Cl}$         | 166* | 4L <sup>3</sup> H              | (2)  |                               | 1/4·(2)/(1)   |
|     | $^{12}\text{C}_2^{35}\text{Cl}_2^{37}\text{Cl}_2$       | 168  | 6L <sup>2</sup> H <sup>2</sup> | (3)  |                               | 2/3·(3)/(2)   |
|     | $^{12}\text{C}_2^{35}\text{Cl}^{37}\text{Cl}_3$         | 170  | 4LH <sup>3</sup>               | (4)  |                               | 3/2·(4)/(3)   |
|     | $^{12}\text{C}_2^{37}\text{Cl}_4$                       | 172  | H <sup>4</sup>                 | (5)  |                               | 4·(5)/(4)     |
|     | <b>Fragment group 1</b>                                 |      |                                |      |                               |               |
|     | $^{12}\text{C}_2^{35}\text{Cl}_3$                       | 129* | L <sup>3</sup>                 | (6)  | $\xrightarrow{\text{R}_{F1}}$ |               |
|     | $^{12}\text{C}_2^{35}\text{Cl}_2^{37}\text{Cl}$         | 131* | 3L <sup>2</sup> H              | (7)  |                               | 1/3·(7)/(6)   |
|     | $^{12}\text{C}_2^{35}\text{Cl}^{37}\text{Cl}_2$         | 133  | 3LH <sup>2</sup>               | (8)  |                               | (8)/(7)       |
|     | $^{12}\text{C}_2^{37}\text{Cl}_3$                       | 135  | H <sup>3</sup>                 | (9)  |                               | 3·(9)/(8)     |
|     | <b>Fragment group 2</b>                                 |      |                                |      |                               |               |
|     | $^{12}\text{C}_2^{35}\text{Cl}_2$                       | 94*  | L <sup>2</sup>                 | (10) | $\xrightarrow{\text{R}_{F2}}$ |               |
|     | $^{12}\text{C}_2^{35}\text{Cl}^{37}\text{Cl}$           | 96*  | 2LH                            | (11) |                               | 1/2·(11)/(10) |
|     | $^{12}\text{C}_2^{37}\text{Cl}_2$                       | 98   | H <sup>2</sup>                 | (12) |                               | 2·(12)/(11)   |
|     | <b>Fragment group 3</b>                                 |      |                                |      |                               |               |
|     | $^{12}\text{C}_2^{35}\text{Cl}$                         | 59*  | L                              | (13) | $\xrightarrow{\text{R}_{F3}}$ |               |
|     | $^{12}\text{C}_2^{37}\text{Cl}$                         | 61*  | H                              | (14) |                               | (14)/(13)     |
|     | <b>TCE</b>  |      |                                |      |                               |               |
|     | <b>Molecular group</b>                                  |      |                                |      |                               |               |
|     | $^{12}\text{C}_2\text{H}^{35}\text{Cl}_3$               | 130* | L <sup>3</sup>                 | (15) | $\xrightarrow{\text{R}_M}$    |               |
|     | $^{12}\text{C}_2\text{H}^{35}\text{Cl}_2^{37}\text{Cl}$ | 132* | 3L <sup>2</sup> H              | (16) |                               | 1/3·(16)/(15) |
|     | $^{12}\text{C}_2\text{H}^{35}\text{Cl}^{37}\text{Cl}_2$ | 134  | 3LH <sup>2</sup>               | (17) |                               | (17)/(16)     |
|     | $^{12}\text{C}_2\text{H}^{37}\text{Cl}_3$               | 136  | H <sup>3</sup>                 | (18) |                               | 3·(18)/(17)   |
|     | <b>Fragment group 1</b>                                 |      |                                |      |                               |               |
|     | $^{12}\text{C}_2^{35}\text{Cl}_2\text{H}$               | 95*  | L <sup>2</sup>                 | (19) | $\xrightarrow{\text{R}_{F1}}$ |               |
|     | $^{12}\text{C}_2^{35}\text{Cl}^{37}\text{ClH}$          | 97*  | 2LH                            | (20) |                               | 1/2·(20)/(19) |
|     | $^{12}\text{C}_2^{37}\text{Cl}_2\text{H}$               | 99   | H <sup>2</sup>                 | (21) |                               | 2·(21)/(20)   |
|     | <b>Fragment group 2</b>                                 |      |                                |      |                               |               |
|     | $^{12}\text{C}_2\text{H}^{35}\text{Cl}$                 | 60*  | L                              | (22) | $\xrightarrow{\text{R}_{F2}}$ |               |
|     | $^{12}\text{C}_2\text{H}^{37}\text{Cl}$                 | 62*  | H                              | (23) |                               | (23)/(22)     |
|     | <b>DCE</b>  |      |                                |      |                               |               |
|     | <b>Molecular group</b>                                  |      |                                |      |                               |               |
|     | $^{12}\text{C}_2\text{H}_2^{35}\text{Cl}_2$             | 96*  | L <sup>2</sup>                 | (24) | $\xrightarrow{\text{R}_M}$    |               |
|     | $^{12}\text{C}_2\text{H}_2^{35}\text{Cl}^{37}\text{Cl}$ | 98*  | 2LH                            | (25) |                               | 1/2·(25)/(24) |
|     | $^{12}\text{C}_2\text{H}_2^{37}\text{Cl}_2$             | 100  | H <sup>2</sup>                 | (26) |                               | 2·(26)/(25)   |
|     | <b>Fragment group 1</b>                                 |      |                                |      |                               |               |
|     | $^{12}\text{C}_2\text{H}_2^{35}\text{Cl}$               | 61*  | L                              | (27) | $\xrightarrow{\text{R}_{F1}}$ |               |
|     | $^{12}\text{C}_2\text{H}_2^{37}\text{Cl}$               | 63*  | H                              | (28) |                               | (28)/(27)     |
|     | <b>VC</b>   |      |                                |      |                               |               |
|     | <b>Molecular group</b>                                  |      |                                |      |                               |               |
|     | $^{12}\text{C}_2\text{H}_3^{35}\text{Cl}$               | 62*  | L                              | (29) | $\xrightarrow{\text{R}_M}$    |               |
|     | $^{12}\text{C}_2\text{H}_3^{37}\text{Cl}$               | 64*  | H                              | (30) |                               | (30)/(29)     |

**Figure S1.1.** Evaluation scheme for chlorine isotope ratio determination of chlorinated ethenes based on relative abundances of different isotopologues. The masses selected in the multiple ion method are labelled (\*). Arrows indicate the expression for chlorine isotope ratio determination.  $R_M$  and  $R_F$  are the partial chlorine isotope ratios from the molecular and fragment ion groups, respectively.

**Conversion of Mass Spectra into Partial Chlorine Isotope Ratios.** The partial chlorine isotope ratio can be determined indirectly using the relative abundances of neighboring isotopologues with a difference of two-mass units. For instance, the partial chlorine isotope ratios of PCE can be determined as follows:

$$R_{M(PCE)} = \frac{1}{4} \cdot \frac{I_{166}}{I_{164}} \quad (S1.4)$$

$$R_{F1(PCE)} = \frac{1}{3} \cdot \frac{I_{131}}{I_{129}} \quad (S1.5)$$

$$R_{F2(PCE)} = \frac{1}{2} \cdot \frac{I_{96}}{I_{94}} \quad (S1.6)$$

$$R_{F3(PCE)} = \frac{I_{61}}{I_{59}} \quad (S1.7)$$

For TCE similar equations can be derived as follow:

$$R_{M(TCE)} = \frac{1}{3} \cdot \frac{I_{132}}{I_{130}} \quad (S1.8)$$

$$R_{F1(TCE)} = \frac{1}{2} \cdot \frac{I_{97}}{I_{95}} \quad (S1.9)$$

$$R_{F2(TCE)} = \frac{I_{62}}{I_{60}} \quad (S1.10)$$

**Calculation of Overall Chlorine Isotope Ratios.** In order to calculate the overall chlorine isotope ratio that represents the isotopic composition of a specific compound, the weighted average of partial  $^{37}\text{Cl}/^{35}\text{Cl}$  ratios from different ion groups needs to be taken into account. In comparison to the previous work of Sakaguchi-Soeder et al. (2), here, the weight factors are defined as the relative abundance of the two most abundant ions in each ion group, instead of only the major ion. Hence, both ions contributing to the partial chlorine isotope ratio computation are taken into account. The overall isotope ratio can then be determined as follows:

$$R_{PCE} = a \times R_M + b \times R_{F1} + c \times R_{F2} + d \times R_{F3} \quad (\text{S1.11})$$

$$a = \frac{I_{166} + I_{164}}{(I_{166} + I_{164}) + (I_{131} + I_{129}) + (I_{96} + I_{94}) + (I_{61} + I_{59})}$$

$$b = \frac{I_{131} + I_{129}}{(I_{166} + I_{164}) + (I_{131} + I_{129}) + (I_{96} + I_{94}) + (I_{61} + I_{59})}$$

$$c = \frac{I_{96} + I_{94}}{(I_{166} + I_{164}) + (I_{131} + I_{129}) + (I_{96} + I_{94}) + (I_{61} + I_{59})}$$

$$d = \frac{I_{61} + I_{59}}{(I_{166} + I_{164}) + (I_{131} + I_{129}) + (I_{96} + I_{94}) + (I_{61} + I_{59})} \quad (\text{S1.12})$$

where  $I$  is the corresponding molecular/fragment ion abundance at different  $m/z$  values. The weight factors  $a$ ,  $b$ ,  $c$  and  $d$  are defined as the relative ion intensities among two major ions from each group.  $R_M$ ,  $R_{F1}$ ,  $R_{F2}$  and  $R_{F3}$  are the partial chlorine isotope ratios determined from two major ions of each group. Similarly, for TCE, DCE and VC (vinyl chloride) the equations are:

$$R_{TCE} = a \times R_M + b \times R_{F1} + c \times R_{F2} \quad (\text{S1.13})$$

$$a = \frac{I_{130} + I_{132}}{(I_{132} + I_{130}) + (I_{97} + I_{95}) + (I_{62} + I_{60})} \quad b = \frac{I_{97} + I_{95}}{(I_{132} + I_{130}) + (I_{97} + I_{95}) + (I_{62} + I_{60})}$$

$$c = \frac{I_{62} + I_{60}}{(I_{132} + I_{130}) + (I_{97} + I_{95}) + (I_{62} + I_{60})} \quad (\text{S1.14})$$

$$R_{DCE} = a \times R_M + b \times R_{F1} \quad (\text{S1.15})$$

$$a = \frac{I_{96} + I_{98}}{(I_{96} + I_{98}) + (I_{61} + I_{63})} \quad b = \frac{I_{61} + I_{63}}{(I_{96} + I_{98}) + (I_{61} + I_{63})} \quad (\text{S1.16})$$

$$R_{VC} = R_M \quad (\text{S1.17})$$

Differently from the multiple ion method, the complete ion method uses complete mass spectral data to compute the total abundances of  $^{35}\text{Cl}$  and  $^{37}\text{Cl}$  atoms in each ion group. The partial  $^{35}\text{Cl}/^{37}\text{Cl}$  ratios of PCE molecule/fragment then can be determined by taking ratios of heavy over light chlorine atom abundance. For PCE the equations correspond to:

$$R_M = \frac{I_{166} + 2I_{168} + 3I_{170} + 4I_{172}}{4I_{164} + 3I_{166} + 2I_{168} + I_{170}} \quad (\text{S1.18})$$

$$R_{F1} = \frac{I_{131} + 2I_{133} + 3I_{135}}{3I_{129} + 2I_{131} + I_{133}} \quad (\text{S1.19})$$

$$R_{F2} = \frac{I_{96} + 2I_{98}}{2I_{94} + I_{96}} \quad (\text{S1.20})$$

$$R_{F3} = \frac{I_{61}}{I_{59}} \quad (\text{S1.21})$$

Then, the overall  $^{35}\text{Cl}/^{37}\text{Cl}$  ratio for PCE can be determined by taking weighted mean

$$R_{PCE} = a \cdot R_M + b \cdot R_{F1} + c \cdot R_{F2} + d \cdot R_{F3} \quad (\text{S1.22})$$

$$a = \frac{\sum_{j=1}^{n_M} I_j}{\sum_{k=1}^{n_T} I_k} \quad b = \frac{\sum_{j=1}^{n_{F1}} I_j}{\sum_{k=1}^{n_T} I_k}$$

$$c = \frac{\sum_{j=1}^{n_{F2}} I_j}{\sum_{k=1}^{n_T} I_k} \quad d = \frac{\sum_{j=1}^{n_{F3}} I_j}{\sum_{k=1}^{n_T} I_k} \quad (\text{S1.23})$$

where the  $n_M, n_{F1}, n_{F2}$ , and  $n_{F3}$  are the number of ions in each ion group, respectively,  $n_T$  is the total number of ion in the mass spectra,  $a, b, c$  and  $d$  are weight factors.

Similarly, the corresponding equations for TCE are:

$$R_M = \frac{I_{132} + 2I_{134} + 3I_{136}}{3I_{130} + 2I_{132} + I_{134}} \quad (\text{S1.24})$$

$$R_{F1} = \frac{I_{97} + 2I_{99}}{2I_{95} + I_{97}} \quad (\text{S1.25})$$

$$R_{F2} = \frac{I_{62}}{I_{60}} \quad (\text{S1.26})$$

$$R_{TCE} = a \cdot R_M + b \cdot R_{F1} + c \cdot R_{F2} \quad (\text{S1.27})$$

$a$ ,  $b$  and  $c$  are the weight factors which can be computed by eq. S1.23.

## S1.2. List of Instrumental Parameters

The principle GC-qMS settings used in this study are the following:

### Injection parameters

Injection mode: split

Split ratio: 10:1

Injected volume: 500  $\mu\text{L}$

### Column and oven parameters

GC column: 60 m  $\times$  250  $\mu\text{m}$ , 1.4  $\mu\text{m}$  film thickness; Restek, USA

Carrier gas: Helium at 1ml/min

Oven program: 40  $^{\circ}\text{C}$  (2 min)  $\rightarrow$  110  $^{\circ}\text{C}$  @ 25  $^{\circ}\text{C}/\text{min}$   $\rightarrow$  200  $^{\circ}\text{C}$  @ 15  $^{\circ}\text{C}/\text{min}$  (5min)

### Mass spectrometer parameters

Type of mode: selected ion monitoring (SIM)

Ion Source Temperature: 230  $^{\circ}\text{C}$

SIM list: See selected mass/ion (see Fig. 2) or complete mass/ion for cis-DCE

EI voltage: 70 eV

### S1.3. Experimental dataset

In the following we report in a tabular format the experimental data shown in Figure 2.3, and the comparison of the selected evaluation methods for TCE and PCE.

**Table S1.1.** Evaluation of chlorine isotope ratios of PCE and TCE using the conventional and modified multiple ion methods.

| Compound | n <sup>b</sup> | Aqueous Conc. [µg/L] | Conventional multiple ion method (2) |  |           | Modified multiple ion method |  |           |         |
|----------|----------------|----------------------|--------------------------------------|--|-----------|------------------------------|--|-----------|---------|
|          |                |                      | Mass on Column [pmol]                | <sup>37</sup> Cl/ <sup>35</sup> Cl Ratio | STDV (1σ) | RSD [%]                      | <sup>37</sup> Cl/ <sup>35</sup> Cl Ratio | STDV (1σ) | RSD [%] |
| TCE      | 5              | 20                   | 3.2                                  | 0.3237                                   | 0.00076   | 2.4                          | 0.32344                                  | 0.00066   | 2.0     |
|          | 5              | 50                   | 8                                    | 0.3230                                   | 0.00062   | 1.9                          | 0.32266                                  | 0.00061   | 1.9     |
|          | 5              | 100                  | 16                                   | 0.3224                                   | 0.00038   | 1.2                          | 0.32208                                  | 0.00039   | 1.2     |
|          | 5              | 200                  | 32                                   | 0.3227                                   | 0.00032   | 1.0                          | 0.32240                                  | 0.00032   | 1.0     |
|          | 5              | 300                  | 48                                   | 0.3231                                   | 0.00026   | 0.8                          | 0.32277                                  | 0.00022   | 0.7     |
|          | 5              | 400                  | 64                                   | 0.3229                                   | 0.00024   | 0.7                          | 0.32263                                  | 0.00025   | 0.8     |
|          | 5              | 500                  | 80                                   | 0.3230                                   | 0.00023   | 0.7                          | 0.32273                                  | 0.00023   | 0.7     |
| PCE      | 5              | 20                   | 4.6                                  | 0.32159                                  | 0.00053   | 1.7                          | 0.32144                                  | 0.00048   | 1.5     |
|          | 5              | 50                   | 11.5                                 | 0.32228                                  | 0.00030   | 0.9                          | 0.32216                                  | 0.00036   | 1.1     |
|          | 5              | 100                  | 23                                   | 0.32210                                  | 0.00026   | 0.8                          | 0.32195                                  | 0.00024   | 0.8     |
|          | 5              | 200                  | 46                                   | 0.32214                                  | 0.00038   | 1.2                          | 0.32199                                  | 0.00038   | 1.2     |
|          | 5              | 300                  | 69                                   | 0.32233                                  | 0.00028   | 0.9                          | 0.32217                                  | 0.00028   | 0.9     |
|          | 5              | 400                  | 92                                   | 0.32233                                  | 0.00018   | 0.6                          | 0.32217                                  | 0.00018   | 0.6     |
|          | 5              | 500                  | 115                                  | 0.32232                                  | 0.00012   | 0.4                          | 0.32216                                  | 0.00013   | 0.4     |

**Table S1.2.** Evaluation of chlorine isotope ratios of PCE and TCE mixtures (at 200 µg/L) using the conventional and modified multiple ion methods, the molecular ion method and the complete ion method.

| Evaluation schemes               | TCE |  |          |         | PCE |  |          |         |
|----------------------------------|-----|--|----------|---------|-----|--|----------|---------|
|                                  | n   | <sup>37</sup> Cl/ <sup>35</sup> Cl Ratio | STDV(1σ) | RSD [%] | n   | <sup>37</sup> Cl/ <sup>35</sup> Cl Ratio | STDV(1σ) | RSD [%] |
| Molecular ion method             | 5   | 0.32122                                  | 0.00039  | 1.2     | 5   | 0.32002                                  | 0.00062  | 1.9     |
| Conventional multiple ion method | 5   | 0.32270                                  | 0.00032  | 1.0     | 5   | 0.32214                                  | 0.00038  | 1.2     |
| Modified multiple ion method     | 5   | 0.32240                                  | 0.00032  | 1.0     | 5   | 0.32199                                  | 0.00038  | 1.2     |
| Complete ion method              | 5   | 0.32488                                  | 0.00055  | 1.7     | 5   | 0.33570                                  | 0.00083  | 2.5     |

As shown in table S1.2, the complete ion method resulted in the highest chlorine isotope ratios with the lowest precision (1.7‰ for TCE, 2.5‰ for PCE). The conventional and modified ion method showed the highest precision (1‰ for TCE, 1.2‰ for PCE). Note that here the results using the complete ion method are based on a full mass spectral data

of PCE and TCE (see Figure S1.1). A larger number of ions (i.e. 14 ions for PCE, 9 for TCE) were added into the SIM mode of MS, therefore significantly lowering the scan rates.

#### S1.4. Long-Time Monitoring of the Chlorine Isotope Ratios

Chlorine isotope ratios for PCE and TCE measured over a period of approximately 6 months are reported in Table S1.3.

**Table S1.3:** Chlorine isotope ratios of PCE and TCE over time

| Date                     | PCE                                   |                    | TCE                                   |                   |
|--------------------------|---------------------------------------|--------------------|---------------------------------------|-------------------|
|                          | $^{37}\text{Cl}/^{35}\text{Cl}$ Ratio | STDV (1 $\sigma$ ) | $^{37}\text{Cl}/^{35}\text{Cl}$ Ratio | STDV(1 $\sigma$ ) |
| 07-Jul-09                | 0.32107                               | 0.00034            | 0.32219                               | 0.00078           |
| 16-Jul-09                | 0.32163                               | 0.00064            | 0.32215                               | 0.00061           |
| 22-Jul-09                | 0.32159                               | 0.00032            | 0.32270                               | 0.00090           |
| 30-Jul-09                | 0.32222                               | 0.00039            | 0.32299                               | 0.00019           |
| 05-Jan-2010 <sup>a</sup> | 0.32195                               | 0.00026            | 0.32266                               | 0.00061           |
| 06-Jan-10                | 0.32217                               | 0.00028            | 0.32276                               | 0.00020           |
| 13-Jan-10                | 0.32199                               | 0.00038            | 0.32240                               | 0.00032           |

| PCE                             |       | TCE                |         |
|---------------------------------|-------|--------------------|---------|
| Average <sup>b</sup>            | 0.322 | Average            | 0.32255 |
| STDV (1 $\sigma$ ) <sup>c</sup> | 4E-04 | STDV (1 $\sigma$ ) | 0.00031 |

a: changing of GC column: before: DB-5 capillary column (30 m  $\times$  250  $\mu\text{m}$  I.D., 0.25  $\mu\text{m}$  film); after: Restek capillary column (60 m  $\times$  250  $\mu\text{m}$ , 1.4  $\mu\text{m}$  film thickness)

b: average of  $^{37}\text{Cl}/^{35}\text{Cl}$  ratio over time;

c: standard deviation of  $^{37}\text{Cl}/^{35}\text{Cl}$  ratio over time

#### S1.5. Evaluation of $^{13}\text{C}$ Error

Differences of two mass units in the MS spectra are not only caused by  $^{35}\text{Cl}$  and  $^{37}\text{Cl}$  atoms, but can also be caused by two  $^{13}\text{C}$  atoms. Neglecting the influence of  $^{13}\text{C}$  atoms results in an error on  $^{37}\text{Cl}/^{35}\text{Cl}$  ratios. This can be quantified using the equation reported by Aeppli et al. (3), which reads as:

$$\text{Error} = R_{\text{chlorine}} - R'_{\text{chlorine}} = \frac{1}{n_{\text{Cl}}} \times \frac{n_{\text{C}}(n_{\text{C}} - 1)}{2} \times R_{\text{C}}^2 \quad (\text{S1.28})$$

where  $R_{\text{chlorine}}$  is the apparent  $^{37}\text{Cl}/^{35}\text{Cl}$  ratios (experimental values),  $R'_{\text{chlorine}}$  is the theoretical  $^{37}\text{Cl}/^{35}\text{Cl}$  ratios (corrected values),  $n_{\text{Cl}}$  is the number of chlorine atoms per molecule,  $n_{\text{C}}$  is the number of carbon atoms per molecule.

**Table S1.4:** Quantification of error caused by  $^{13}\text{C}$ 

| $N_{\text{C}}^{\text{a}}$ | $N_{\text{Cl}}^{\text{b}}$ | $R_{\text{chlorine}} - R'_{\text{chlorine}}$ | Overestimated Error [%] <sup>c</sup> |
|---------------------------|----------------------------|--|--------------------------------------|
| 2                         | 1                          | $R_{\text{carbon}}^2$                        | 0.100                                |
| 2                         | 2                          | $\frac{1}{2} \cdot R_{\text{carbon}}^2$      | 0.050                                |
| 2                         | 3                          | $\frac{1}{3} \cdot R_{\text{carbon}}^2$      | 0.033                                |
| 2                         | 4                          | $\frac{1}{4} \cdot R_{\text{carbon}}^2$      | 0.025                                |
| 6                         | 1                          | $15 \cdot R_{\text{carbon}}^2$               | 1.500                                |
| 6                         | 2                          | $\frac{15}{2} \cdot R_{\text{carbon}}^2$     | 0.750                                |
| 6                         | 3                          | $5 \cdot R_{\text{carbon}}^2$                | 0.500                                |
| 6                         | 4                          | $\frac{15}{4} \cdot R_{\text{carbon}}^2$     | 0.375                                |
| 6                         | 5                          | $3 \cdot R_{\text{carbon}}^2$                | 0.300                                |
| 6                         | 6                          | $\frac{5}{2} \cdot R_{\text{carbon}}^2$      | 0.250                                |

a: Number of carbon atoms in molecule or fragment

b: Number of chlorine atoms in molecule or fragment

c: Assuming  $R_{\text{carbon}}=1\%$

In addition, the stable hydrogen isotopes (i.e.  $^1\text{H}$  and  $^2\text{H}$ ) can also contribute to the potential error with the presence of two deuterium atoms in certain molecules and fragments. Similarly, the error can be also determined in a way that three elements, chlorine, carbon and hydrogen, are all involved into the probability computation. However, due to the extremely low natural abundance of deuterium (about 0.0001) (4), this error can be neglected unless the considered compounds has a very large number of hydrogen atoms.



## Literature

1. Freedman, D.; Pisani, R., Purves, R.; Statistics, 4th ed.; W.W. Norton & Company, Inc: New York, U.S., **2008**; pp 222-269.
2. Sakaguchi-Soder, K.; Jager, J.; Grund, H.; Matthaus, F.; Schuth, C., Monitoring and evaluation of dechlorination processes using compound-specific chlorine isotope analysis. *Rapid Commun. Mass Spectrom.* **2007**, *21*, (18), 3077-3084.
3. Aeppli, C.; Holmstrand, H.; Adersson, P.; Gustafsson, Ö., Direct compound-specific stable chlorine isotope analysis of organic compounds with quadrupole GC/MS using standard isotope bracketing. *Anal. Chem.* **2010**, *82*, (1),420-426.
4. Hoefs J.; Stable Isotope Geochemistry, 6th ed.; Springer: Berlin, Germany, **2009**.

## S2. Integrated Carbon and Chlorine Isotope Modeling: Applications to Chlorinated Aliphatic Hydrocarbons Dechlorination

### S2.1 Initial abundances of carbon-chlorine isotopologues

VC and cis-DCE, have chemically equivalent C-Cl bonds. Thus, eq 3.1 (in the manuscript) is used to compute the initial carbon–chlorine isotopologues abundances of those compounds according to the international standards of carbon and chlorine isotope ratios (i.e. VPDB and SMOC [1]). Table S2.1 and S2.2 report the carbon-chlorine VC and cis-DCE isotopologues, the number of  $^{12}\text{C}$ ,  $^{13}\text{C}$ ,  $^{35}\text{Cl}$  and  $^{37}\text{Cl}$ , and the isotopologues' relative abundance.

**Table S2.1.** Initial abundances of VC carbon-chlorine isotopologues.

| VC<br>Isotopologue | Carbon          |                 | Chlorine         |                  | Abundance <sup>a</sup><br>[%] |
|--------------------|-----------------|-----------------|------------------|------------------|-------------------------------|
|                    | $^{12}\text{C}$ | $^{13}\text{C}$ | $^{35}\text{Cl}$ | $^{37}\text{Cl}$ |                               |
| 1                  | 2               | 0               | 1                | 0                | 74.1065                       |
| 2                  | 1               | 1               | 1                | 0                | 1.6651                        |
| 3                  | 2               | 0               | 0                | 1                | 23.6838                       |
| 4                  | 1               | 1               | 0                | 1                | 0.5322                        |
| 5                  | 0               | 2               | 1                | 0                | 0.0094                        |
| 6                  | 0               | 2               | 0                | 1                | 0.0030                        |
| sum                |                 |                 |                  |                  | 100.0000                      |

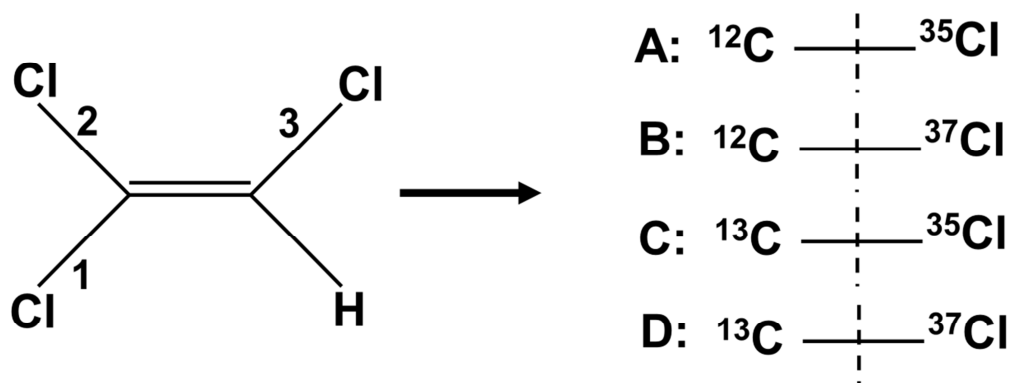
<sup>a</sup> computed according to eq 3.1 in the manuscript

**Table S2.2.** Initial abundances of cis-DCE carbon-chlorine isotopologues.

| cis-DCE<br>Isotopologue | Carbon          |                 | Chlorine         |                  | Abundance <sup>a</sup><br>[%] |
|-------------------------|-----------------|-----------------|------------------|------------------|-------------------------------|
|                         | <sup>12</sup> C | <sup>13</sup> C | <sup>35</sup> Cl | <sup>37</sup> Cl |                               |
| 1                       | 2               | 0               | 2                | 0                | 56.1586                       |
| 2                       | 2               | 0               | 1                | 1                | 35.8957                       |
| 3                       | 2               | 0               | 0                | 2                | 5.7360                        |
| 4                       | 1               | 1               | 2                | 0                | 1.2619                        |
| 5                       | 1               | 1               | 1                | 1                | 0.8066                        |
| 6                       | 1               | 1               | 0                | 2                | 0.1289                        |
| 7                       | 0               | 2               | 2                | 0                | 0.0071                        |
| 8                       | 0               | 2               | 1                | 1                | 0.0045                        |
| 9                       | 0               | 2               | 0                | 2                | 0.0007                        |
| sum                     |                 |                 |                  |                  | 100.0000                      |

<sup>a</sup> computed according to eq 3.1 in the manuscript

Differently from cis-DCE and VC, the three C-Cl bonds of TCE are not chemically equivalent (Figure S1), and the cleavage of different bonds results in different products (i.e. 1→cis-DCE; 2→trans-DCE; 3→1,1-cis-DCE, according to the schematic of Figure S1). Given that the three bonds of TCE are all reactive, the initial abundances of TCE isotopologues have to be computed by eq 3.2 (in the manuscript) and are listed in Table S2.3.

**Figure S2.1.** Cleavage of different isotopic C-Cl bonds during TCE dechlorination reaction.

**Table S2.3.** Initial abundances of TCE carbon-chlorine isotopologues. The bond numbering (1, 2, 3) and isotopic composition (A, B, C, D) refer to the schematic of Figure S2.1.

| TCE<br>Isotopologue | Carbon          |                 | Chlorine         |                  | Abundance <sup>a</sup><br>[%] | bond 1 | bond 2 | bond 3 |
|---------------------|-----------------|-----------------|------------------|------------------|-------------------------------|--------|--------|--------|
|                     | <sup>12</sup> C | <sup>13</sup> C | <sup>35</sup> Cl | <sup>37</sup> Cl |                               |        |        |        |
| 1                   | 2               | 0               | 3                | 0                | 42.5622                       | A      | A      | A      |
| 2                   | 2               | 0               | 2                | 1                | 13.6025                       | A      | A      | B      |
| 3                   | 2               | 0               | 2                | 1                | 13.6025                       | A      | B      | A      |
| 4                   | 2               | 0               | 2                | 1                | 13.6025                       | B      | A      | A      |
| 5                   | 2               | 0               | 1                | 2                | 4.3473                        | A      | B      | B      |
| 6                   | 2               | 0               | 1                | 2                | 4.3473                        | B      | A      | B      |
| 7                   | 2               | 0               | 1                | 2                | 4.3473                        | B      | B      | A      |
| 8                   | 2               | 0               | 0                | 3                | 1.3894                        | B      | B      | B      |
| 9                   | 1               | 1               | 3                | 0                | 0.4758                        | A      | A      | C      |
| 10                  | 1               | 1               | 2                | 1                | 0.1521                        | A      | A      | D      |
| 11                  | 1               | 1               | 2                | 1                | 0.1521                        | A      | B      | C      |
| 12                  | 1               | 1               | 2                | 1                | 0.1521                        | B      | A      | C      |
| 13                  | 1               | 1               | 1                | 2                | 0.0486                        | A      | B      | D      |
| 14                  | 1               | 1               | 1                | 2                | 0.0486                        | B      | A      | D      |
| 15                  | 1               | 1               | 1                | 2                | 0.0486                        | B      | B      | C      |
| 16                  | 1               | 1               | 0                | 3                | 0.0155                        | B      | B      | D      |
| 17                  | 1               | 1               | 3                | 0                | 0.4758                        | C      | C      | A      |
| 18                  | 1               | 1               | 2                | 1                | 0.1521                        | C      | C      | B      |
| 19                  | 1               | 1               | 2                | 1                | 0.1521                        | C      | D      | A      |
| 20                  | 1               | 1               | 2                | 1                | 0.1521                        | D      | C      | A      |
| 21                  | 1               | 1               | 1                | 2                | 0.0486                        | C      | D      | B      |
| 22                  | 1               | 1               | 1                | 2                | 0.0486                        | D      | D      | B      |
| 23                  | 1               | 1               | 1                | 2                | 0.0486                        | D      | D      | A      |
| 24                  | 1               | 1               | 0                | 3                | 0.0155                        | D      | D      | B      |
| 25                  | 0               | 2               | 3                | 0                | 0.0053                        | C      | C      | C      |
| 26                  | 0               | 2               | 2                | 1                | 0.0017                        | C      | C      | D      |
| 27                  | 0               | 2               | 2                | 1                | 0.0017                        | C      | D      | C      |
| 28                  | 0               | 2               | 2                | 1                | 0.0017                        | D      | C      | C      |
| 29                  | 0               | 2               | 1                | 2                | 0.0005                        | C      | D      | D      |
| 30                  | 0               | 2               | 1                | 2                | 0.0005                        | D      | C      | D      |
| 31                  | 0               | 2               | 1                | 2                | 0.0005                        | D      | D      | C      |
| 32                  | 0               | 2               | 0                | 3                | 0.0002                        | D      | D      | D      |
| sum                 |                 |                 |                  |                  | 100.0000                      |        |        |        |

<sup>a</sup> computed according to eq 3.2 in the manuscript

## S2.2 Validation with Data from a Well-Mixed Experimental Setup

We apply our modeling approach to simulate the reductive dechlorination experiments in [2]. We describe the degradation kinetics with a Michaelis-Menten formulation:

$$r = \frac{k_{\max} C}{K_M + C} \quad (\text{S2.1})$$

where  $k_{\max}$  [ $\mu\text{M}\cdot\text{day}^{-1}$ ] is the maximum degradation rate and  $K_M$  [ $\mu\text{M}$ ] is the half-saturation constant. The values of the parameters ( $k_{\max,DCE}=4.8$ ,  $K_{M,DCE}=1.9$  and  $k_{\max,VC}=5.76$ ,  $K_{M,VC}=602$ ) are adopted from a similar batch study [27]. The dual isotope simulations are performed with the integrated C and Cl modeling approach (IM) described above. We used the experimentally determined carbon and chlorine bulk enrichment factors ( $\varepsilon_{C,cisDCE}=-18.5\text{‰}$ ,  $\varepsilon_{Cl,cisDCE}=-1.5\text{‰}$ ;  $\varepsilon_{C,VC}=-25.2\text{‰}$ ,  $\varepsilon_{Cl,VC}=-1.8\text{‰}$ , from [18]) and simulated simultaneously the degradation of all the combined carbon–chlorine isotopologues of cis-dichloroethene and vinyl chloride (9 isotopologues for cis-DCE and 6 isotopologues for VC, see Table S2.1 and Table S2.2). The results of the simulations are shown in Figure S2.2 together with the experimental data published by Abe et al. [2]. The measured C and Cl isotope ratios are mostly in the zone where the dual isotope relation can be well approximated with a constant slope given by the ratio of the bulk chlorine and carbon enrichment factors ( $\sim 0.07$  and  $\sim 0.08$  for VC and cis-DCE, respectively). It can be noticed that both the CM and the IM approaches can capture the observed dual isotope behavior for cis-DCE and VC. The discrepancies between the methods become significant at late reaction times. At the end of the simulation the differences are  $\delta^{13}C=9.8\text{‰}$  and  $\delta^{37}Cl=1.0\text{‰}$  for VC and  $\delta^{13}C=7.2\text{‰}$  and  $\delta^{37}Cl=0.2\text{‰}$  for cis-DCE.

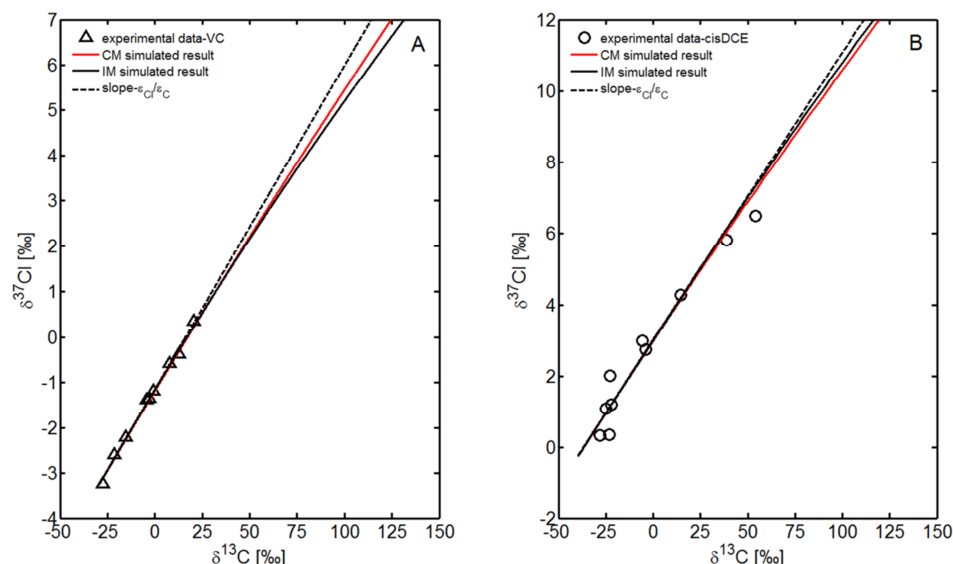


**Figure S2.2.** Simulated carbon and chlorine isotope ratios of VC (A) and cisDCE (B) during dechlorination processes using CM (red line) and IM (dark line). The symbols represent the experimental data published by Abe et al. [2].

### S3.3 Governing equations and parameters used in the mass-transfer limited TCE biodegradation application

We used our model to simulate the carbon and chlorine isotope fraction of TCE in a three-phase system (i.e. air–organic–aqueous). A double-Monod kinetic was used to model the reaction in the aqueous phase, and is given by

$$r = k_{\max} \cdot \frac{[TCE]}{[TCE] + K_{M,TCE}} \cdot \frac{[H_2]}{[H_2] + K_{M,H_2}} \cdot X \quad (\text{S2.2})$$

where  $r$  is the reaction rate,  $k_{\max}$  [ $\mu\text{mol} \cdot \text{cell}^{-1} \cdot \text{h}^{-1}$ ] is the maximum consumption rate,  $K_{M,TCE}$  [ $\mu\text{mol} \cdot \text{L}^{-1}$ ] and  $K_{M,H_2}$  [ $\mu\text{mol} \cdot \text{L}^{-1}$ ] are the half-saturation constants for TCE and  $H_2$ , respectively, and  $X$  [ $\text{cells} \cdot \text{L}^{-1}$ ] is the biomass concentration. The governing equations for the mass-transfer limited TCE biodegradation system described in Aeppli et al. [3] can be written as:

**Aqueous phase**

$$\frac{d[{}^jTCE]_{aq}}{dt} = -\sum_{k=1}^m r_k^j + \kappa_{TCE}^{org-aq} \cdot a_0^{aq} \cdot ([{}^jTCE]_{aq}^{eq} - [{}^jTCE]_{aq}) \quad (S2.3)$$

$$\frac{d[{}^j cisDCE]_{aq}}{dt} = +\sum_{k=1}^m r_k^j + \kappa_{cisDCE}^{org-aq} \cdot a_0^{aq} \cdot ([{}^j cisDCE]_{aq}^{eq} - [{}^j cisDCE]_{aq}) \quad (S2.4)$$

$$\frac{d[H_2]_{aq}}{dt} = -\sum_{k=1}^m r_k^j + \kappa_{H_2}^{org-aq} \cdot a_0^{aq} \cdot ([H_2]_{aq}^{eq} - [H_2]_{aq}) \quad (S2.5)$$

$$\frac{dX}{dt} = +\sum_{k=1}^m r_k^j \cdot Y \quad (S2.6)$$

**Organic phase**

$$\frac{d[{}^jTCE]_{org}}{dt} = -\kappa_{TCE}^{org-aq} \cdot a_0^{org} \cdot ([{}^jTCE]_{aq}^{eq} - [{}^jTCE]_{aq}) - \kappa_{TCE}^{org-gas} \cdot a_0^{org} \cdot ([{}^jTCE]_{gas}^{eq} - [{}^jTCE]_{gas}) \quad (S2.7)$$

$$\frac{d[{}^j cisDCE]_{org}}{dt} = -\kappa_{cisDCE}^{org-aq} \cdot a_0^{org} \cdot ([{}^j cisDCE]_{aq}^{eq} - [{}^j cisDCE]_{aq}) - \kappa_{cisDCE}^{org-gas} \cdot a_0^{org} \cdot ([{}^j cisDCE]_{gas}^{eq} - [{}^j cisDCE]_{gas}) \quad (S2.8)$$

$$\frac{d[H_2]_{org}}{dt} = -\kappa_{H_2}^{org-aq} \cdot a_0^{org} \cdot ([H_2]_{aq}^{eq} - [{}^j H_2]_{aq}) - \kappa_{H_2}^{org-gas} \cdot a_0^{org} \cdot ([H_2]_{gas}^{eq} - [H_2]_{gas}) \quad (S2.9)$$

**Gas phase**

$$\frac{d[{}^jTCE]_{gas}}{dt} = +\kappa_{TCE}^{org-gas} \cdot a_0^{gas} \cdot ([{}^jTCE]_{aq}^{eq} - [{}^jTCE]_{gas}) \quad (S2.10)$$

$$\frac{d[{}^j\text{cisDCE}]_{\text{gas}}}{dt} = +\kappa_{\text{cisDCE}}^{\text{org-gas}} \cdot a_0^{\text{gas}} \cdot ([{}^j\text{cisDCE}]_{\text{gas}}^{\text{eq}} - [{}^j\text{cisDCE}]_{\text{gas}}) \quad (\text{S2.11})$$

$$\frac{d[H_2]_{\text{gas}}}{dt} = +\kappa_{H_2}^{\text{org-gas}} \cdot a_0^{\text{gas}} \cdot ([H_2]_{\text{gas}}^{\text{eq}} - [H_2]_{\text{gas}}) \quad (\text{S2.12})$$

where  $j$  indicates each carbon-chlorine TCE or cis-DCE isotopologues,  $r_k^j$  is the bond-specific reaction rate,  $X$  is the biomass concentration [ $\text{cells}\cdot\text{L}^{-1}$ ],  $Y$  [ $\text{cells}\cdot\mu\text{mol}^{-1}$ ] is the yield factor,  $\kappa$  [ $\text{cm}\cdot\text{h}^{-1}$ ] is the interphase mass-transfer coefficient of TCE or cis-DCE, and  $a_0^{\text{aq}}$  [ $\text{cm}^{-1}$ ] is the interface area per unit volume of the aqueous phase.

The input parameters are taken from Aeppli et al. [3], and are summarized in Table S2.4.

**Table S2.4** Kinetic parameters for the mass-transfer limited TCE biodegradation example [3].

| Parameter  | Values  |
|--|---------|
| $k_{\text{max}}$ [ $\mu\text{mol}\cdot\text{cell}^{-1}\cdot\text{h}^{-1}$ ]          | 6.1e-9  |
| $K_{\text{M,TCE}}$ [ $\mu\text{mol}\cdot\text{L}^{-1}$ ]                             | 70      |
| $K_{\text{M,H}_2}$ [ $\mu\text{mol}\cdot\text{L}^{-1}$ ]                             | 1       |
| $\kappa_{\text{TCE}}^{\text{org-aq}} \cdot a_0^{\text{aq}}$ [ $\text{h}^{-1}$ ]      | 13.8    |
| $\kappa_{\text{cisDCE}}^{\text{org-aq}} \cdot a_0^{\text{aq}}$ [ $\text{h}^{-1}$ ]   | 13.8    |
| $\kappa_{H_2}^{\text{org-aq}} \cdot a_0^{\text{aq}}$ [ $\text{h}^{-1}$ ]             | 1       |
| $\kappa_{\text{TCE}}^{\text{org-gas}} \cdot a_0^{\text{org}}$ [ $\text{h}^{-1}$ ]    | 5       |
| $\kappa_{\text{cisDCE}}^{\text{org-gas}} \cdot a_0^{\text{org}}$ [ $\text{h}^{-1}$ ] | 5       |
| $\kappa_{H_2}^{\text{org-gas}} \cdot a_0^{\text{gas}}$ [ $\text{h}^{-1}$ ]           | 5       |
| $X_0$ [ $\text{cells}\cdot\text{L}^{-1}$ ]   | 1.09e10 |
| $Y$ [ $\mu\text{mol}\cdot\text{L}^{-1}$ ]  | 2.31e+7 |

Solving the system of governing differential equations (eqs S2.3-S2.12) allows describing the evolution of the reactive species in the three-phase system. The concentration profiles, the  $\delta^{37}\text{Cl}$  and  $\delta^{13}\text{C}$  values and the corresponding dual isotope plots in the aqueous phase are shown in the manuscript Figure 3.3 (panels B1-B4). In Figure S2.3 we report the results for the organic phase and the total system.



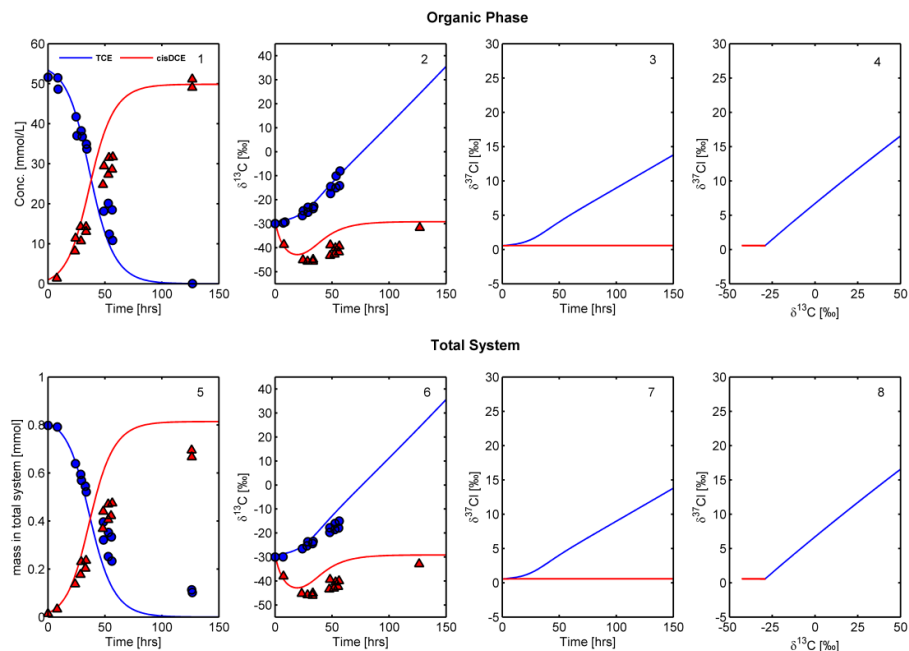


**Figure S2.3.** Simulation results for organic phase (1-4) and total system (5-8) using the IM. Blue and red lines are TCE and cis-DCE concentration, respectively, red lines are cis-DCE concentration, blue circles and red triangles are the experimental data for TCE and cis-DCE from reference [3].

## Literature

- (1) de Laeter, J. R.; Bohlke, J. K.; De Bièvre, P.; Hidaka, H.; Peiser, H. S.; Rosman, K. J. R.; Taylor, P. D. P., Atomic weights of the elements. *Pure Appl. Chem.* **2009**, *81*, (8), 1535-1536.
- (2) Abe, Y.; Aravena, R.; Zopfi, J.; Shouakar-Stash, O.; Cox, E.; Roberts, J. D.; Hunkeler, D., Carbon and chlorine isotope fractionation during aerobic oxidation and reductive dechlorination of vinyl chloride and cis-1,2-dichloroethene. *Environ. Sci. Technol.* **2009**, *43*, (1), 101-107.
- (3) Aeppli, C.; Berg, M.; Cirpka, O. A.; Holliger, C.; Schwarzenbach, R. P.; Hofstetter, T. B., Influence of Mass-Transfer Limitations on Carbon Isotope Fractionation during Microbial Dechlorination of Trichloroethene. *Environ. Sci. Technol.* **2009**, *43*, (23), 8813-8820.

### S3. Mechanistic Approach to Multi-Element Isotope Modeling of Organic Contaminant Degradation

#### S3.1 Relative abundances of position-specific isotopologues

The initial relative abundances are computed for the position specific isotopologues, which are specified for different reaction mechanisms of toluene, MTBE and nitrobenzene. Eq.4.1 in the manuscript is used to compute these values according to the international standards of isotope ratios (de Laeter et al., 2009).

Table S3.1. Initial abundances of toluene position specific isotopologues (C-H)

| Toluene Isotopologue | Carbon          |                 | Hydrogen       |                | Abundance [%] |
|----------------------|-----------------|-----------------|----------------|----------------|---------------|
|                      | <sup>12</sup> C | <sup>13</sup> C | <sup>1</sup> H | <sup>2</sup> H |               |
| 1                    | 1               | 0               | 1              | 0              | 98.8776       |
| 2                    | 1               | 0               | 0              | 1              | 0.0114        |
| 3                    | 0               | 1               | 1              | 0              | 1.1109        |
| 4                    | 0               | 1               | 0              | 1              | 0.0001        |
| sum                  |                 |                 |                |                | 100.0000      |

Table S3.2. Initial abundances of MTBE position specific isotopologues for different reaction pathways (C-H, C-H<sub>3</sub> and C-H<sub>9</sub>)

| MTBE Isotopologue | Carbon          |                 | Hydrogen       |                | Abundance [%] |
|-------------------|-----------------|-----------------|----------------|----------------|---------------|
|                   | <sup>12</sup> C | <sup>13</sup> C | <sup>1</sup> H | <sup>2</sup> H |               |
| 1 <sup>a</sup>    | 1               | 0               | 1              | 0              | 98.8776       |
| 2                 | 1               | 0               | 0              | 1              | 0.0114        |
| 3                 | 0               | 1               | 1              | 0              | 1.1109        |
| 4                 | 0               | 1               | 0              | 1              | 0.0001        |
| sum               |                 |                 |                |                | 100.0000      |
| 1 <sup>b</sup>    | 1               | 0               | 3              | 0              | 98.8549       |
| 2                 | 1               | 0               | 2              | 1              | 3.41e-2       |
| 3                 | 1               | 0               | 1              | 2              | 3.92e-6       |
| 4                 | 1               | 0               | 0              | 3              | 1.50e-10      |
| 5                 | 0               | 1               | 3              | 0              | 1.1106        |
| 6                 | 0               | 1               | 2              | 1              | 3.83e-4       |
| 7                 | 0               | 1               | 1              | 2              | 4.41e-8       |
| 8                 | 0               | 1               | 0              | 3              | 2.00e-12      |
| sum               |                 |                 |                |                | 100.0000      |
| 1 <sup>c</sup>    | 1               | 0               | 9              | 0              | 98.7867       |
| 2                 | 1               | 0               | 8              | 1              | 0.1023        |
| 3                 | 1               | 0               | 7              | 2              | 4.70e-5       |
| 4                 | 1               | 0               | 6              | 3              | 2.62e-8       |
| 5                 | 1               | 0               | 5              | 4              | 2.18e-12      |
| 6                 | 1               | 0               | 4              | 5              | 2.50e-16      |
| 7                 | 1               | 0               | 3              | 6              | 1.92e-20      |
| 8                 | 1               | 0               | 2              | 7              | 9.47e-25      |
| 9                 | 1               | 0               | 1              | 8              | 2.72e-29      |
| 10                | 1               | 0               | 0              | 9              | 3.48e-34      |
| 11                | 0               | 1               | 9              | 0              | 1.1099        |
| 12                | 0               | 1               | 8              | 1              | 1.15e-3       |
| 13                | 0               | 1               | 7              | 2              | 5.29e-7       |
| 14                | 0               | 1               | 6              | 3              | 1.42e-10      |
| 15                | 0               | 1               | 5              | 4              | 2.45e-14      |
| 16                | 0               | 1               | 4              | 5              | 2.81e-18      |
| 17                | 0               | 1               | 3              | 6              | 2.16e-22      |
| 18                | 0               | 1               | 2              | 7              | 1.06e-26      |
| 19                | 0               | 1               | 1              | 8              | 3.06e-31      |
| 20                | 0               | 1               | 0              | 9              | 4.00e-36      |
| sum               |                 |                 |                |                | 100.0000      |

<sup>a</sup>methyl group oxidation; <sup>b</sup>S<sub>N</sub>2-type hydrolysis; <sup>c</sup>S<sub>N</sub>1-type hydrolysis

Table S3.3. Initial abundances of nitrobenzene position specific isotopologues during partial reduction (C-N)

| Nitrobenzene Isotopologue | Carbon          |                 | Nitrogen        |                 | Abundance [%] |
|---------------------------|-----------------|-----------------|-----------------|-----------------|---------------|
|                           | <sup>12</sup> C | <sup>13</sup> C | <sup>14</sup> N | <sup>15</sup> N |               |
| 1                         | 1               | 0               | 1               | 0               | 98.5290       |
| 2                         | 1               | 0               | 0               | 1               | 0.3600        |
| 3                         | 0               | 1               | 1               | 0               | 1.1070        |
| 4                         | 0               | 1               | 0               | 1               | 0.0040        |
| sum                       |                 |                 |                 |                 | 100.0000      |

Table S3.4. Initial abundances of nitrobenzene position-specific isotopologues during oxidation (C-N-H)

| Nitrobenzene Isotopologue | Carbon          |                 | Nitrogen        |                 | Hydrogen       |                | Abundance [%] |
|---------------------------|-----------------|-----------------|-----------------|-----------------|----------------|----------------|---------------|
|                           | <sup>12</sup> C | <sup>13</sup> C | <sup>14</sup> N | <sup>15</sup> N | <sup>1</sup> H | <sup>2</sup> H |               |
| 1                         | 2               | 0               | 1               | 0               | 1              | 0              | 97.4232       |
| 2                         | 1               | 1               | 1               | 0               | 1              | 0              | 2.1891        |
| 3                         | 0               | 2               | 1               | 0               | 1              | 0              | 0.0123        |
| 4                         | 2               | 0               | 0               | 1               | 1              | 0              | 0.3559        |
| 5                         | 1               | 1               | 0               | 1               | 1              | 0              | 0.0080        |
| 6                         | 0               | 2               | 0               | 1               | 1              | 0              | 4.49e-5       |
| 7                         | 2               | 0               | 1               | 0               | 0              | 1              | 0.0112        |
| 8                         | 1               | 1               | 1               | 0               | 0              | 1              | 0.0003        |
| 9                         | 0               | 2               | 1               | 0               | 0              | 1              | 1.41e-6       |
| 10                        | 2               | 0               | 0               | 1               | 0              | 1              | 4.09e-5       |
| 11                        | 1               | 1               | 0               | 1               | 0              | 1              | 9.20e-7       |
| 12                        | 0               | 2               | 0               | 1               | 0              | 1              | 5.00e-9       |
| sum                       |                 |                 |                 |                 |                |                | 100.0000      |

### S3.2 Model evaluation for nitrobenzene degradation

A Michaelis-Menten kinetic formulation was used to simulate the degradation of nitrobenzene (NB):

$$\frac{d[NB]}{dt} = -k_{max} \cdot \frac{[NB]}{[NB] + K_{M,NB}} \cdot X \quad (S3.1)$$

where  $k_{max}$  [ $\mu\text{mol} \cdot \text{cell}^{-1} \cdot \text{h}^{-1}$ ] is the maximum consumption rate,  $K_{M,NB}$  [ $\mu\text{mol} \cdot \text{L}^{-1}$ ] is the half-saturation constant for NB, and  $X$  [ $\text{cells} \cdot \text{L}^{-1}$ ] is the biomass concentration.

The dynamics of the biomass was described including a growth and a linear decay term:

$$\frac{dX}{dt} = Y \cdot k_{max} \cdot \frac{[NB]}{[NB] + K_{M,NB}} \cdot X - b \cdot X \quad (S3.2)$$

where  $Y$  [ $\text{cells} \cdot \mu\text{mol}^{-1}$ ] is the yield factor, and  $b$  [ $\text{T}^{-1}$ ] is the decay rate for microbial growth.

We used Eq. S3.1 and S3.2 to describe the evolution of nitrobenzene concentrations observed in the biodegradation experiments performed by Hofstetter et al. (2008) using two distinct microbial strains: *Pseudomonas pseudoalcaligenes* strain JS45 (nitrobenzene partial reduction) and *Comamonas sp.* strain JS765 (nitrobenzene dioxygenation). An optimization procedure based on a trust-region-reflective method for the minimization of the non-linear least squares problem was adopted to fit the experimental data using the reaction kinetic parameters,  $k_{max}$ ,  $K_{M,NB}$  and the initial biomass  $X_0$  as fitting parameters. The results are reported in Figure S3.1 and S3.2 for the partial reduction and dioxygenation pathways, respectively.

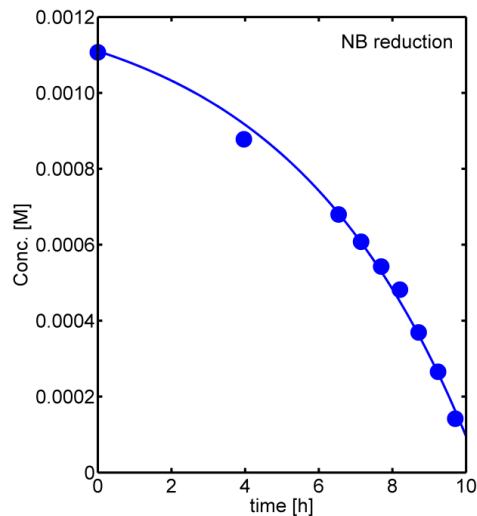


**Fig. S3.1.** Observed (symbols) and simulated (line) nitrobenzene concentrations during biodegradation by *Pseudomonas pseudoalcaligenes* strain JS45 (nitrobenzene partial reduction). This figure corresponds to reaction pathway 1 in the multi-element isotope fractionation plot reported in Fig. 4.4 A of the paper.

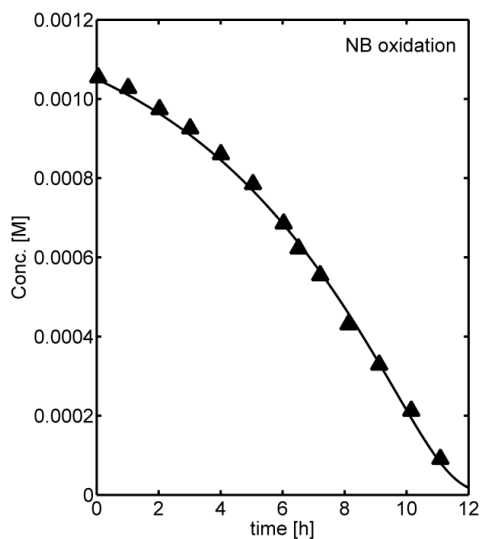


**Fig. S3.2.** Observed (symbols) and simulated (line) nitrobenzene concentrations during biodegradation by *Comamonas sp.* strain JS765 (nitrobenzene dioxygenation). This figure corresponds to reaction pathway 2 in the multi-element isotope fractionation plot reported in Fig. 4.4A of the paper.

Table S3.5. Reaction kinetic parameters for nitrobenzene degradation.

| Parameters   | NB Partial Reduction | NB Dioxygenation |
|--|----------------------|------------------|
| $k_{max}$ [ $\mu\text{mol} \cdot \text{cell}^{-1} \cdot \text{h}^{-1}$ ] | 1.06e-8              | 7.73e-9          |
| $K_{M,NB}$ [ $\mu\text{mol} \cdot \text{L}^{-1}$ ]                       | 73.00                | 89.99            |
| $X_0$ [ $\text{cells} \cdot \text{L}^{-1}$ ]                             | 2.88e+9              | 5.12e+9          |
| $Y^*$ [ $\text{cells} \cdot \mu\text{mol}^{-1}$ ]                        | 2.31e+7              | 2.31e+7          |
| $b^*$ [ $\text{h}^{-1}$ ]  | 0.0045               | 0.0045           |

\* estimated based on literature values

## Literature

- de Laeter, J. R.; Bohlke, J. K.; De Bièvre, P.; Hidaka, H.; Peiser, H. S.; Rosman, K. J. R.; Taylor, P. D. P., Atomic weights of the elements. Pure Appl. Chem. 2009, 81, (8), 1535-1536.
- Hunkeler, D., Van Breukelen, B.M., Elsner, M., 2009. Modeling Chlorine Isotope Trends during Sequential Transformation of Chlorinated Ethenes. Environ. Sci. Technol. 43, 6750-6756.
- Elsner, M., 2010. Stable isotope fractionation to investigate natural transformation mechanisms of organic contaminants: principles, prospects and limitations. J. Environ. Monit. 12, 2005-2031.
- Hofstetter, T.B., Spain, J.C., Nishino, S.F., Bolotin, J., Schwarzenbach, R.P., 2008b. Identifying competing aerobic nitrobenzene biodegradation pathways by compound-specific isotope analysis. Environ. Sci. Technol. 42, 4764-4770.

## S4. Effects of Aqueous Diffusion on Spatial Isotopic Gradients of Organic Contaminants

### S4.1 Experimental protocol

A schematic description of the experimental setup geometry and of the experimental protocol is illustrated in Figure S4.1. The figure shows the sequence of fundamental steps we followed in performing the diffusion experiments, described in the section “Materials and Methods” of the manuscript. These steps include the initial filling of the blank agar medium in the diffusion tubes (B); the filling of the source medium containing the organic contaminants (C); the diffusion phase at  $T=20^{\circ}\text{C}$ , where the contaminants diffuse from the source to the initially pristine medium (D); the slicing of the gel medium and the sampling procedure (E); and the final steps of analytical measurement and data evaluation (F).

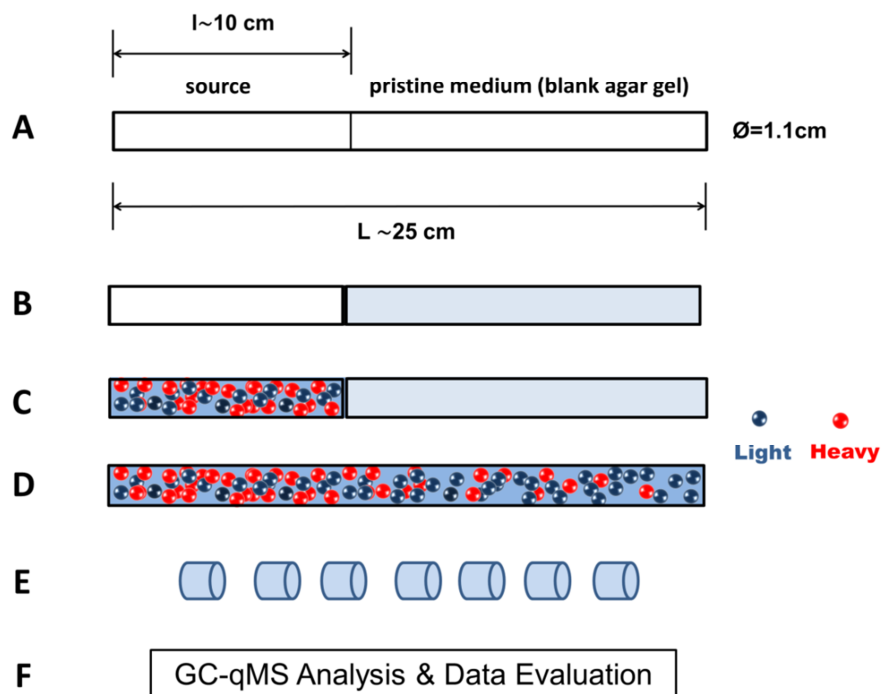


**Figure S4.1.** Schematic illustration of the experimental procedure. A: geometry of the glass tubes ( $L$ : total length;  $l$ : source zone length;  $\text{Ø}$ : inner diameter); B: filling of blank agar solution; C: filling of source agar solution; D: diffusion of organic compounds at a constant temperature of  $20^{\circ}\text{C}$ ; E: slicing and sampling; F: sample analysis using GC-MS and data evaluation using a one-dimensional modeling approach.



## S4.2 Modeling approach and parameter fitting

An inverse modeling procedure was used to estimate the key parameters of this study (i.e., diffusion coefficients,  $D$ , and the exponent,  $\beta$ , of the inverse mass law relation) from the experimental data. We use the one-dimensional diffusion equation (eq 5.2, in the manuscript) as forward model to fit the concentration and isotopic values measured at each sampling point. The inverse modeling approach is based on the minimization of the sum of normalized squared errors (SNSE) of both concentration and isotope data between the experimental observations and the simulation results:

$$SNSE = SNSE_{conc.} + SNSE_{isotope} \quad (S4.1)$$

$$SNSE_{conc.} = \frac{\sum_{i=1}^{n_c} (C_i^{obs} - C_i^{sim})^2}{\sigma_c^2} \quad (S4.2)$$

$$SNSE_{isotope} = \frac{\sum_{i=1}^{n_R} (R_i^{obs} - R_i^{sim})^2}{\sigma_R^2} \quad (S4.3)$$

where  $C^{obs}$  are the observed concentrations,  $C^{sim}$  are the simulated concentration,  $R^{obs}$  are the observed isotope ratios,  $R^{sim}$  are the simulated isotope ratios,  $\sigma_c$  and  $\sigma_R$  are the variance of concentration and isotope ratio data, respectively.  $n_R$  and  $n_c$  are the number of measured concentration and isotopic data, respectively.

The best-fit parameters,  $D$  and  $\beta$ , were obtained for each experimental run by solving the nonlinear least square data fitting problems using the Matlab function `lsqnonlin`. The uncertainties of the estimated parameters were also determined. Such uncertainties were estimated according to the procedure described in [1]:

$$V = \frac{SNSE}{n_c + n_R - n_p} \cdot (J^T A J)^{-1} \quad (S4.4)$$

where  $V$  is the mean square error (MSE) matrix,  $J$  is the Jacobian matrix of first derivatives of the model outcomes with respect to the parameters,  $A$  is a diagonal matrix of the variance of all concentration and isotope data.  $n_p$  is the number of estimated parameters,  $n_R$  and  $n_c$  are the same as defined in eqs S4.2 and S4.3. The standard error for

the estimated parameters ( $D$  and  $\beta$ ) can be calculated from the diagonal elements of the mean square error matrix,  $V$ :  $\pm\sqrt{V_{11}}$  and  $\pm\sqrt{V_{22}}$ , respectively.

### S4.3 Comparison of Experimentally-Determined and Calculated Diffusion Coefficients

The aqueous diffusion coefficients of the selected organic compounds were also calculated with empirical correlations proposed in the literature. The classical formula of Wilke and Chang [2] was used to calculate the diffusion coefficients of toluene, ethylbenzene, cisDCE and TCE:

$$D = \frac{7.4 \times 10^{-8} \cdot (\phi M)^{0.5} \cdot T}{\mu V^{0.6}} \quad (\text{S4.5})$$

where  $D$  [ $\text{cm}^2\text{s}^{-1}$ ] is the diffusion coefficient,  $\phi$  [-] is an empirical parameter equal to 2.6 for water;  $M$  [g/mol] is the molecular weight;  $T$  [K] is the absolute temperature;  $\mu$  [centipoise] is the dynamic viscosity of water;  $V$  [ $\text{cm}^3\text{mol}^{-1}$ ] is the molar volume of the solute.

The diffusion coefficients were also calculated with a more recent correlation proposed, by Worch [4], for organic compounds:

$$D = \frac{3.595 \cdot 10^{-14} \cdot T}{\eta M^{0.53}} \quad (\text{S4.6})$$

where  $D$  [ $\text{m}^2\text{s}^{-1}$ ] is the diffusion coefficient;  $T$  [K] is the absolute temperature;  $M$  [g/mol] is the molecular weight;  $\eta$  [Pa·s] is the dynamic viscosity of water.

The diffusion coefficients in our experimental setup are determined in a gel system with minimal differences from a purely aqueous system. However, to take into account the effect of such small differences and to directly compare the experimental results with the results obtained with eq S4.6 and eq S4.7, we applied the correction proposed by Lauffer [3]:

$$D_{\text{water}} = D_{\text{gel}} \cdot \frac{(1-\varphi)}{(1-\alpha \cdot \varphi)} \quad (\text{S4.7})$$

where  $D_{\text{water}}$  and  $D_{\text{gel}}$  are the diffusion coefficients of the considered solute in water and agar.  $\varphi$  is the effective volume fraction of the gel substance and  $\alpha$  is a coefficient of obstruction. The values of these empirical coefficients (0.05 and 1.67, respectively) were

taken by Lauffer [3] who used a similar gel composition to the one in our diffusion experiments.

Table S4.1 reports the calculated and experimentally-determined aqueous diffusion coefficients; the latter are corrected according to eq S4.7.

**Table S4.1.** Calculated and experimentally-determined aqueous diffusion coefficients.

| Compounds | D [ $\times 10^{-9} \text{ m}^2 \text{ s}^{-1}$ ] |                 |                |
|-----------|---|-----------------|----------------|
|           | Worch   | Wilke and Chang | EXP. Corrected |
| TOL       | 0.957   | 0.901           | 0.834          |
| D-TOL     | 0.915   | 0.857*          | 0.803          |
| ETB       | 0.887   | 0.827           | 0.785          |
| D-ETB     | 0.846   | 0.784*          | 0.753          |
| cisDCE    | 0.931   | 1.105           | 1.148          |
| TCE       | 0.793   | 0.996           | 0.931          |

\*calculated assuming the same density as for the non-labeled compounds

Considering the correction between  $D_{agar}$  and  $D_{water}$  has no effect on the extent of isotope fractionation. In fact, expressing the correction factor in eq S4.7 as a tortuosity factor  $\tau^2 = (1-\phi)/(1-\alpha \cdot \phi)$  (e.g. Eggenkamp and Coleman [4]), the extent of diffusive isotope fractionation can be written as:

$$\alpha_D = \frac{D_{gel}^H}{D_{gel}^L} = \frac{\frac{D_{water}^H}{\tau^2}}{\frac{D_{water}^L}{\tau^2}} = \frac{D_{water}^H}{D_{water}^L} \quad (\text{S4.8})$$

where  $\alpha_D$  is the diffusive fractionation factor.

#### S4.4 Isotopologue-specific properties of cisDCE and TCE at natural isotopic abundance

For a chlorinated organic compound, the relative abundance of an isotopologue containing “k”  $^{37}\text{Cl}$  atoms out of a total of “n” chlorine atoms can be expressed as:

$$I_{(n,k)} = \binom{n}{k} H^k L^{n-k} \quad (\text{S4.9})$$

$$\binom{n}{k} = \frac{(n-k+1) \cdot (n-k+2) \cdots (n-1) \cdot (n)}{k!} \quad (\text{S4.10})$$

where  $I$  is the relative abundance of a certain isotopologue of a chlorinated compound,  $H$  is the abundance of  $^{37}\text{Cl}$ ,  $L$  is the abundance of  $^{35}\text{Cl}$ ,  $n$  is the total number of chlorine atoms in a certain chlorinated compound and  $k$  is the number of  $^{37}\text{Cl}$  atoms in a specified isotopologue. The binomial coefficient (eq S4.10) represents the number of possible ways in which  $k$  atoms of  $^{37}\text{Cl}$  can be distributed over  $n$  positions of chlorine atoms in a molecule. Applying eq S4.9 and eq S4.10 to cisDCE and TCE results in 3 and 4 chlorine isotopologues, respectively, with the calculated abundances reported in Table S4.2.

Furthermore, based on the  $\beta$  values and the average diffusion coefficients obtained in the diffusion experiments (see Table 5.2 in chapter 5), we calculated the isotopologue-specific diffusion coefficients for cisDCE and TCE in each experiment. The properties of cisDCE and TCE isotopologues are summarized in Table S4.2.

**Table S4.2.** Summary of properties for cisDCE and TCE isotopologues.

| Chlorine Isotopologue                           | cisDCE |        |        | TCE    |        |        |        |
|---|--------|--------|--------|--------|--------|--------|--------|
|   | LL     | LH     | HH     | LLL    | LLH    | LHH    | HHH    |
| Molecular Mass                                  | 96     | 98     | 100    | 130    | 132    | 134    | 136    |
| Abundance [%]                                   | 57.4   | 36.7   | 5.9    | 43.5   | 41.7   | 13.4   | 1.4    |
| D [ $\times 10^{-9} \text{m}^2 \text{s}^{-1}$ ] |        |        |        |        |        |        |        |
| Exp. I  | 1.0991 | 1.0968 | 1.0945 |        |        |        |        |
| Exp. J  | 1.1058 | 1.1041 | 1.1024 |        |        |        |        |
| Exp. K  | 1.1210 | 1.1190 | 1.1170 |        |        |        |        |
| Average cisDCE (Exp. I-K)                       | 1.1090 | 1.1070 | 1.1050 |        |        |        |        |
| Exp. L  |        |        |        | 0.8985 | 0.8978 | 0.8972 | 0.8965 |
| Exp. M  |        |        |        | 0.8993 | 0.8989 | 0.8984 | 0.8980 |
| Exp. N  |        |        |        | 0.8965 | 0.8958 | 0.8952 | 0.8946 |
| Average TCE (Exp. L-N)                          |        |        |        | 0.8984 | 0.8978 | 0.8973 | 0.8967 |

## Literature

1. Smith, L. H.; Kitanidis, P. K.; McCarty, P. L., Numerical modeling and uncertainties in rate coefficients for methane utilization and TCE cometabolism by a methane-oxidizing mixed culture. *Biotechnol. Bioeng.* **1997**, *53*, (3), 320-331.
2. Wilke, C. R.; Chang, P.C., *American Institute of Chemical Engineers Journal* **1955**, *1*, 264.
3. Lauffer, M. A., Theory of diffusion in gels. *Biophys Jour* **1961**, *1*, ((3)), 205-213.
4. Eggenkamp, H. G. M.; Coleman, M. L., The effect of aqueous diffusion on the fractionation of chlorine and bromine stable isotopes. *Geochim. Cosmochim. Acta* **2009**, *73*, (12), 3539-3548.



# Curriculum Vitae

## Biao JIN

Date of birth: 1984-02-18, Jilin, China

Centre for Applied Geoscience,  
Eberhard Karls University of Tübingen,  
Sigwartstr. 10, 72076 Tuebingen, Germany

**Phone:** +49) 0176-2973176 (office)

**E-mail:** biao.jin@uni-tuebingen.de

kim\_pure999@hotmail.com

### Education Background

*Oct.2009 to Oct.2013*

#### **Ph. D candidate**

Eberhard Karls University of Tübingen, Germany

*Sept. 2007 to Sept.  
2009*

#### **M.Sc. Applied Environmental Geoscience**

Eberhard Karls University of Tübingen, Germany

*Sept. 2003 to Jun.  
2007*

#### **B.Sc. Hydrology and Water Resources Engineering**

Wuhan University, China

### Awards and Honors

*April. 2013*

#### **2012 Chinese Government Prize for Outstanding Self-Financed Chinese Student Aboard**

Awarded by Chinese Scholarship Council (globally 480 prize holders from all scientific fields )

*Oct. 2009 to Oct. 2012*

#### **IPSWaT Ph.D Scholarship,**

Research proposal funded by German Federa Ministry of Education and Research (BMBF)

*2005 to 2006 semester*

#### **Outstanding Student of Wuhan University Award**

*April. 2003*

**Excellent High School graduates of Jilin Province**

### **Peer-Reviewed Publications**

1. **Jin, B.;** Laskov, C.; Rolle, M.; Haderlein, S. B., Chlorine Isotope Analysis of Organic Contaminants Using GC-qMS: Method Optimization and Comparison of Different Evaluation Schemes. *Environ. Sci. Technol.* **2011**, *45*, (12), 5279-5286.
2. **Jin, B.;** Haderlein, S.B.; Rolle, M., Integrated carbon and chlorine isotope modeling: applications to chlorinated aliphatic hydrocarbons dechlorination. *Environ. Sci. Technol.* **2013**, *47*, 1443-1451.
3. **Jin, B.;** Rolle, M., Mechanistic Approach to Multi-Element Isotope Modeling of Organic Contaminant Degradation. *Chemosphere*. **2013**. *Chemosphere*, *95*, 131-139.
4. **Jin, B.;** Haderlein, S.B.; Rolle, M., Effects of Aqueous Diffusion on Spatial Isotopic Gradients of Organic Contaminants. *Environ. Sci. Technol.* (submitted).

### **Workshop and Conference**

*25th to 30th Aug. 2013*

**Goldschmidt 2013, Florence, Italy**

*2nd to 7th Sept. 2012*

**Jesium2012, Leipzig, Germany**

*14th to 19th Aug. 2011*

**Goldschmidt 2011, Prague, Czech Republic**

*16th to 28th Aug. 2010*

**2nd summer school on flow and transport on porous and fractured media, Corsica, France**

*9th to 12th May 2010*

**Wasser 2010, Bayreuth, Germany**

*9th to 11th Sept. 2009*

**Phreeqc Hydrochemical & Geochemical Modeling Course, Ferrara, Italy**